THE EFFECTS OF LIFE HISTORY STRATEGY AND UNCERTAINTY ON A PROBABILITY-BASED APPROACH TO MANAGING THE RISK OF OVERFISHING

Emily C. Susko

Thesis submitted to the Faculty of the
Virginia Polytechnic Institute and State University
In partial fulfillment of the requirements
for the degree of

Master in Science
in
Fish and Wildlife Conservation

James M. Berkson
Paul B. Conn
Yan Jiao
Donald J. Orth

February 17, 2012
Blacksburg, Virginia

Keywords: Fisheries management, stock assessment, simulation model, risk, uncertainty, life history, vermilion snapper, sandbar shark, gulf menhaden

The Effects of Life History Strategy and Uncertainty
on a Probability-Based Approach to Managing the Risk of Overfishing

Emily C. Susko

ABSTRACT

Recent U.S. legislation applies a precautionary approach to setting catch regulations in federal fisheries management. A transparent approach to complying with federal guidelines involves calculating the catch recommendation that corresponds to a specified probability, *P**, of exceeding the "true" overfishing limit (OFL) located within an estimated distribution.

The *P** methodology aims to manage the risk of overfishing explicitly, but choice of *P** alone does not provide sufficient information on all of the risks associated with a control rule—both the *probability* of overfishing and the *severity* of overfishing. Rather, the ramifications of *P** choices depend on the amount of uncertainty in the stock assessment and on the life history of the species in question. To evaluate these effects on the risks associated with *P** rules, my study simulated fishing three example species under three levels of uncertainty.

Trends identified among example species were consistent with predictions from life history. Periodic strategists, which have highly variable recruitment, experienced probabilities of overfishing which exceeded *P** and which increased in time. Equilibrium strategists showed more predictable risks of overfishing but may have less capacity to recover from depleted biomass levels. Differences in the size of the OFL distribution—representing differences in levels of uncertainty—led to mixed results depending on whether the distribution was biased or whether uncertainty was fully characterized. Lastly, because OFL distributions are themselves estimates and subject to uncertainty in their shape and size, lower *P** values closer to the tails of the estimated distribution produced more variable resulting risks.

TABLE OF CONTENTS

LIST OF TABLES vii
LIST OF FIGURES viii
ACKNOWLEDGEMENTS xi

CHAPTER 1: Incorporating scientific uncertainty into marine stock assessment: a review of the literature

Introduction 1
The Need to Manage Fisheries 2
The Role of Fisheries Science 2
The Dangers of Uncertainty in Fisheries Stock Assessment: A Case Study 5
Risk and Precaution in Fisheries Management 7
A Probabilistic Approach to Precaution and Risk 9
From Probability to Risk Analysis 13
The Effects of Life History 14
The Effects of Uncertainty in the Overfishing Limit (OFL) 16
Management Context: The South Atlantic Fisheries Management Council 17

Summary 18

Literature Cited 19

CHAPTER 2: A simulation model to investigate the impacts of probability-based control rules on stocks of differing life history strategies

Introduction 28

Methods 30
I. Age-Structured Fishery Population Models 30

Mortality Rates *30*
Individual Growth Models *31*
Spawner-Recruit Relationship *32*
Catch and Yield *33*
II. Equilibrium Calculations to Generate Benchmarks 34
Spawning Stock Benchmarks *34*
Life History Parameterization *35*
III. Incorporating Recruitment Stochasticity 36
IV. Life History Parameterization 37
Species Overview *38*
Constant Parameters *39*
Age-Specific Parameters *39*
On Calculating Fecundity *39*
On Rescaling Natural Mortality *40*
Recruitment Variation in Sharks *42*
V. Simulations I: Simulating Uncertainty 42
Uncertainty in Steepness and Natural Mortality *42*
Creating Distributions from Ranges *43*
Sampling and Rescaling *44*
VI. Species-Specific Parameter Distributions 45
Vermilion Snapper *45*
Sandbar Shark *46*
Gulf Menhaden *46*
VII. Simulations II: Simulating *P** Control Rules 47
Initialization *48*
Fishing *48*
Yearly Calculations *49*
VIII. Analysis: Monitoring Performance Measures 50

Results **52**

I. Benchmark Analysis and Population Initializations 52

Vermilion Snapper *52*

Sandbar Shark *52*

Gulf Menhaden *53*

II. Probabilistic Risk of Overfishing 53

Vermilion Snapper *53*

Sandbar Shark *53*

Gulf Menhaden *54*

Analysis *54*

Determining Drivers of Probabilistic Risk *55*

Interpreting Drivers of Probabilistic Risk *57*

Effects of Life History Strategy *57*

Effects of Level of Uncertainty *58*

Effects of P* *Value* *58*

III. Probabilistic Risk Increases in Time 58

Vermilion Snapper *59*

Sandbar Shark *59*

Gulf Menhaden *60*

Analysis *60*

IV. Comprehensive Risk: Consequences to the Natural Resource 61

Vermilion Snapper *62*

Sandbar Shark *63*

Gulf Menhaden *64*

Analysis *65*

Determining Drivers of Comprehensive Risk *65*

Interpreting Drivers of Comprehensive Risk *69*

Effects of Life History *69*

Effects of Level of Uncertainty *70*

Effects of P* *Value* *71*

Exploring Species Resilience *71*

Discussion **72**
I. Life History 72
Current stock status biases results *72*
Recruitment variability increases risk of overfishing in time *75*
Productivity likely determines resilience to fishing pressure *76*
Life History Conclusions *78*
II. Uncertainty 79
Unaccounted uncertainty decreases management accuracy *79*
Sizes of overfishing limit distributions affect potential severity of overfishing *81*
Uncertainty Conclusions *82*
III. Level of Allowable Risk, *P** 83
IV. Summary of Management Implications 85
Probabilistic Risk *85*
Comprehensive Risk *86*

Conclusion **87**

Literature Cited **88**

LIST OF TABLES

Table 1. Age-constant life history parameters. 93

Table 2. Vermilion snapper age-specific life history. 94

Table 3. Sandbar shark age-specific life history. 95

Table 4. Gulf menhaden age-specific life history. 96

Table 5. Life history parameter ranges. 97

Table 6. Vermilion snapper acceptable biological catch (ABC) values. 98

Table 7. Sandbar shark ABC values. 98

Table 8. Gulf menhaden ABC values. 98

Table 9. Percent of vermilion snapper populations overfishing in the first year. 99

Table 10. Percent of sandbar shark populations overfishing in the first year. 99

Table 11. Percent of gulf menhaden populations overfishing in the first year. 99

Table 12. Vermilion snapper crash rates. 100

Table 13. Gulf menhaden crash rates. 100

LIST OF FIGURES

Figure 1.1. Sustainable Yield. 25

Figure 1.2. Maximum Sustainable Yield.....25

Figure 1.3. Original and current methods for defining *P**, the allowable risk of overfishing. 26

Figure 1.4. The influence of scientific uncertainty on the value of ABC. 27

Figure 2.1. Constructed overfishing limit (OFL) distributions for vermilion snapper.....101

Figure 2.2. Constructed OFL distributions for sandbar shark. 102

Figure 2.3. Constructed OFL distributions for gulf menhaden. 103

Figure 2.4. Percent of vermilion snapper populations in each scenario experiencing overfishing in the first year of the control rule's implementation. 104

Figure 2.5. Percent of sandbar shark populations in each scenario experiencing overfishing in the first year of the control rule's implementation.....105

Figure 2.6. Percent of gulf menhaden populations in each scenario experiencing overfishing in the first year of the control rule's implementation. 106

Figure 2.7. Flow Chart 1: Probability of overfishing under ideal starting conditions. 107

Figure 2.8. Flow Chart 2A: Possible fishing mortality rate outcomes for non-overfished populations. 108

Figure 2.9. *Flow Chart 2B*: Possible fishing mortality rate outcomes for overfished populations. 109

Figure 2.10. Current and cumulative percentages of vermilion snapper populations undergoing overfishing in each scenario. 110

Figure 2.11. Current and cumulative percentages of sandbar shark populations undergoing overfishing in each scenario. 111

Figure 2.12. Current and cumulative percentages of gulf menhaden populations undergoing overfishing in each scenario. 112

Figure 2.13. Yearly increase in risk of overfishing, averaged across uncertainty level. 113

Figure 2.14. Current and cumulative percentages of vermilion snapper populations overfished in each scenario. 114

Figure 2.15. Current and cumulative percentages of sandbar shark populations overfished in each scenario. 115

Figure 2.16. Current and cumulative percentages of gulf menhaden populations overfished in each scenario. 116

Figure 2.17. Percent of vermilion snapper populations crashing in the duration of the experiment. 117

Figure 2.18. Percent of gulf menhaden populations crashing in the duration of the experiment. 118

Figure 2.19. Flow Chart 3: Probability of becoming overfished under ideal starting conditions. 119

Figure 2.20. Flow Chart 4A: Pathways by which non-overfished populations may become overfished.....120

Figure 2.21. Flow Chart 4B: Pathways by which overfished populations may recover. 121

ACKNOWLEDGEMENTS

I am greatly indebted to the guidance and support of my advisor, Dr. Jim Berkson. His confidence in my abilities was unwavering, and his feedback on my work challenged me to strive for the highest quality. I could not ask for a better mentor. I am also very grateful to my committee, Dr. Paul Conn, Dr. Yan Jiao, and Dr. Don Orth, each of whom brought unique expertise and helpful insight to my project. I would like to acknowledge the time, advice, and support of many of the researchers at the National Marine Fisheries Service's Beaufort Laboratory: Dr. Kyle Shertzer, Dr. Erik Williams, Dr. Katie Andrews, Dr. Amy Schueller, and, now retired, Dr. Michael Prager and Dr. Doug Vaughan. I would like to thank Lynn Hayes at Virginia Tech for her immeasurable help. I am also indebted the friendship and support of my fellow graduate students: Adyan Rios, Staci Rijal, Katelin Shugart-Schmidt, and Amy Tillman, as well as Yan Li, Josh Hatch, and Matt Vincent. Finally, I would like to thank my friends and family, with whose love and support I have been graciously blessed.

CHAPTER 1: Incorporating scientific uncertainty into marine stock assessment: a review of the literature

Introduction

Sustainable fisheries management poses one of the most challenging natural resource problems of our time. Through much of the last century, fisheries science depended on classical models that promoted ambitious management goals without acknowledging the uncertainties inherent to their calculation. As a result, decades of risk-prone fisheries management have led to worldwide declines, and even collapses, of marine fish populations. A famous example of one such collapse, briefly reviewed here, exemplifies the sources of uncertainty in fisheries science and the consequences of ignoring them.

Recent U.S. legislation requires a more precautionary approach to fisheries management. Scientific recommendations must now incorporate a buffer to explicitly account for uncertainty in assessment, and managers cannot exceed this buffered recommendation in setting catch regulations. What is not specified is how *much* precaution should be taken—or, conversely, how much risk should be permitted. Because this is a value decision, it remains the responsibility of fisheries managers, who set control rules that guide scientists in calculating buffers.

One recent approach to setting control rules uses simple probability theory to calculate the size of the uncertainty buffer that corresponds to a chosen probability, or risk, that recommended catch regulations exceed an estimated safety threshold. This approach allows scientists to account for the uncertainty in their estimates while letting managers decide the allowable level of risk. The following study utilizes simulation models to explore the effects of stock life history and level of scientific uncertainty on the implementation of such an approach, with the goal of providing generalized advice on control rules employing this probabilistic strategy.

The Need to Manage Fisheries

"Fisheries resources, unlike most natural resources, are usually common property, being open to all comers on an equal footing. In consequence, so long as there is an opportunity to obtain more return to a unit of effort than its cost, […] men will be attracted to a fishery…"

- M. Schaefer, 1959

"Freedom in a commons brings ruin to all." – G. Hardin, 1968

Marine fisheries represent the world's last remaining dependence on wild animal resources for major commercial enterprise (Cury and Caryé 2001), and as such, they necessitate management as common property resources. But the challenges of meeting the rising seafood demand accompanying the threefold increase in the human population over the last century have rendered marine fisheries repeated victims of Hardin's "Tragedy of the Commons." A 2005 report by the Food and Agriculture Organization of the United Nations (FAO) ranks a quarter of the world's marine fish stocks as already overexploited or depleted, and more than half of the remaining stocks as "fully exploited" with no room for expansion (FAO 2005). In fact, the total yield from wild stocks worldwide has peaked and may be declining (Hilborn et al. 2003).

Faced with the reality that the seas are indeed exhaustible, societies worldwide have to come to accept that monitoring and controls are needed to determine and maintain sustainable harvest levels. The fields of fisheries science and fisheries management have developed throughout the last century in response.

The Role of Fisheries Science

While many historical fisheries were sustainable, in other cases declines were observed well before the booming population and technological advances of the 20th century. Fishermen in the Scottish herring fishery of the 19th century reported increasing difficulty in maintaining catch sizes of earlier decades, and their fishing fleets were forced to move further offshore as inshore herring stocks were depleted (MacGarven 2001). But science authorities pointed to the fish's staggering individual fecundity (each adult female lays millions of eggs) as proof that the great

fish populations of the seas were "inexhaustible," and that any fluctuations must be in response to environmental conditions. This belief persisted into the twentieth century (MacGarven 2001, Hilborn et al. 2003). World Wars I and II allowed many European and U.S. fisheries an unplanned respite from heavy exploitation, and fishermen returning from the wars found fish populations restored. The results of this "Great Fishing Experiment" helped refute assertions that the effects of human fishing pressure on fish were negligible (Hilborn et al. 2003). Newly industrialized fishing boomed in the post-war era and spurred the development and expansion of fisheries science to advise management decisions (Holt 1998).

In North America, fisheries science began to champion the concept of maximum sustainable yield (Schaefer 1959, Holt 1998). This concept was derived from a basic population model that assumes that a fish population displays logistic, density-dependent growth in the absence of fishing. This logistic growth in biomass can be modeled as a function of total stock biomass, *B,* intrinsic growth rate, *r*, and carrying capacity, *K* (Shertzer et al. 2008b):

Logistic growth $$\frac{dB}{dt} = rB(1 - \frac{B}{K})$$ (Eq. 1)

In fisheries, this change in biomass due to reproduction and individual growth—but not to fishing—is called *latent production,* and the graph of the above equation the *production curve*. Meanwhile, the fish biomass captured by the fishery is termed *yield,* or *catch* (C)*,* and its removal from total stock biomass affects the following year's production. The instantaneous catch rate can be described as a product of stock biomass times an instantaneous *fishing mortality rate*, *F* (Quinn and Deriso 1999):

Catch rate $$\frac{dC}{dt} = FB$$ (Eq. 2)

Thus, the rate of change in biomass *when fishing is present* is calculating by subtracting the catch rate from the logistic growth rate, or latent production, in Eq. 1:

Total change in biomass $$\frac{dB_{Total}}{dt} = rB(1 - \frac{B}{K}) - FB \qquad \text{(Eq. 3)}$$

Sustainable *yield* (SY) occurs whenever the total biomass remains the same from year to year, implying that the total rate of change in biomass is equal to zero. This occurs when the catch rate equals latent (and, from the fisheries perspective, "surplus") production—anywhere along the production curve (Figure 1.1). The "$_{SY}$" subscripts for B and F specify that the following relationships are only true at certain values.

Sustainable yield $$\frac{dB_{Total}}{dt} = 0 \Rightarrow rB_{SY}(1 - \frac{B_{SY}}{K}) = F_{SY}B_{SY} = SY \qquad \text{(Eq. 4)}$$

The *maximum sustainable yield* (MSY) corresponds with the maximum value of the parabola described by the production curve (Figure 1.2). Finding the maximum of the production curve requires considering the rate of change *of production*, which is the second derivate of biomass, and calculating the values at which this second derivative equals zero.

$$\frac{d^2B}{dt^2} = r - \frac{2rB}{K} = 0 \Rightarrow B_{MSY} = \frac{K}{2} \qquad \text{(Eq. 5)}$$

Thus the maximum sustainable yield occurs when biomass is equal to half the stock's carrying capacity (Figure 1.2). Note that the stock biomass at which MSY occurs is labeled B_{MSY}. MSY itself is found by calculating the SY at B_{MSY}:

$$MSY = r(\frac{K}{2})(1 - \frac{1}{K} * \frac{K}{2}) = \frac{rK}{2}(\frac{1}{2}) = \frac{rK}{4} \qquad \text{(Eq. 6a)}$$

Finally, the fishing mortality rate applied to achieve this yield is labeled F_{MSY}:

$$F_{MSY} = \frac{MSY}{B_{MSY}} = \frac{rK}{4} * \frac{2}{K} = \frac{r}{2} \qquad \text{(Eq. 6b)}$$

The relationships described in the graph of the production curve are the classic basis for definitions of cases when the yield at a given biomass is not sustainable. When yield at a given biomass is less than production (points on the graph inside of the parabola), the corresponding fishing mortality rate will be below F_{MSY}, and the total stock biomass should increase the following year despite fishing pressure. This was termed *underfishing*. However, if yield at a given biomass exceeds production (points on the graph outside the parabola), the corresponding fishing mortality rate will exceed F_{MSY}. Fishing at this rate will drive the stock biomass down, as the fish population cannot replenish the removed biomass by the following year. This latter circumstance was the original definition of *overfishing.* The goal of managing for MSY was ideally to adhere to the sustainable yield curve, avoiding either under- or overfishing.

Maximum sustainable yield as a management target was appealing for its comprehensibility and straightforward calculation (Holt 1998, Mace and Sissenwine 2002), and its goal of "fuller utilization of the marine fisheries" was consistent with the contemporary paradigm of conservation as wise resource use (Schaefer 1959). Soon it was incorporated into both national and international fisheries policy (Holt 1998, Mace and Sissenwine 2002). Fisheries scientists used available data to assess the status of individual populations of commercial interest, called *stocks*, and to estimate that stock's MSY. They then presented the results of these *stock assessments* to management as advice for setting catch quotas and gear restrictions. The Magnuson-Stevens Fisheries Management and Conservation Act of 1976 formalized this process by creating eight regional Fishery Management Councils (FMCs). Each FMC is charged with creating *fishery management plans* for the major commercial stocks in their region, based on the recommendations of their respective Scientific and Statistical Committee (SSC).

The Dangers of Uncertainty in Fisheries Stock Assessment: A Case Study

Unfortunately, unwavering faith in the MSY "doctrine" (Larkin 1977) proved to be overoptimistic. For one thing, for years managers viewed MSY as a minimum starting point for negotiating catch levels, and the resulting regulations often exceeded the recommendation by far. But there were other downsides to the MSY-management paradigm. Like any models of reality and predictions of the future, stock assessments are inherently uncertain, with the result that

stock MSYs are difficult to determine precisely and accurately. When they are overestimated, even regulations set strictly according to the advice will unknowingly lead to overfishing.

One of the most famous cases of overfishing exemplifies the tragic consequences of failing to acknowledge the *scientific uncertainty* in stock assessment. The northern cod stock (*Gadus morhua*) off the coast of Newfoundland was the basis of a major fishery for over 500 years; in fact, it was the reason for European settlement of the island (Hilborn et al. 2003). Throughout the 1970's and 1980's it was managed according to state-of-the-art fisheries science, centering around the idea of MSY but choosing supposedly conservative quotas. However, in the early nineties it suffered a catastrophic collapse, and the fishery has been closed completely since 1992, with no signs of recovery nearly twenty years later (Hilborn et al. 2003, MacGarvin 2001). Though other factors were initially blamed for cod's collapse, it has since been acknowledged that the fault lies with prolonged overexploitation. This was allowed in part by the influences of political and economic pressures on management decisions, and it was worsened by compliance issues and underreporting (Walters and Maguire 1996). However, the single greatest enabling factor were the fishing quotas set according to a gross overestimation of the cod stock biomass and MSY (Hutchings and Myers 1994). Such severe errors arose from inadequately accounting for the various sources of uncertainty inherent in any stock assessment (categorized here after Francis and Shotton 1997).

Process uncertainty describes random fluctuations due to natural variation in the system, whether in population parameters (i.e., cod recruitment, fecundity) or environmental conditions (Francis and Shotton 1997, Charles 1998, Mace and Sissenwine 2002). One aspect of stock assessment particularly subject to process uncertainty is the relationship between the sizes of the spawning stock and recruitment, because it is highly influenced by environmental conditions (Mace and Sissenwine 2002). Environmental conditions inevitably fluctuate between favorable and less favorable conditions, and the latter may finally push heavily exploited stocks to the point of collapse (Charles 1998). However, with cod, perhaps *too much* recruitment variation was attributed to process uncertainty. Scientists assumed that no spawner-recruit relationship existed, and some initially blamed the stock's collapse on environmental conditions, rather than overfishing (Walters and Maguire 1996).

Observation uncertainty results from sampling or measurement error or bias. Population estimates that relied on effort data from the commercial cod fisheries failed to account for the bias due to improving technology, while those constructed from independent survey data had standard errors of 30-40% (Hutchings and Myers 1994). As these two sources produced widely different population estimates, stock assessors seeking the "best" estimate calculated an intermediate value rather than explore them as possible alternatives (Hilborn et al 1993).

Model uncertainty encompasses the uncertainty surrounding the structure, conceptual relationships, and assumptions chosen in the modeling process. In the case of cod, for example, assessors did not question the assumption of constant yearly recruitment, because cod are known to be highly fecund (Walters and Maguire 1996). In reality, recruitment was plummeting, as cod do indeed show a strong spawner-recruitment relationship, and the population of spawning cod was declining severely (Hutchings and Myers 1994, Walters and Maguire 1996).

These previous sources accumulate *estimation uncertainty*, which surrounds parameters used in and estimated by population models. Ideally, these are expressed in confidence intervals or probability distributions. However, rather than present these uncertainties, both scientists and managers tended to rely on point estimates of biomass and MSY (MacGarvin 2001, Mace and Sissenwine 2002). Ignoring this estimation uncertainty perpetuated the overestimation of biomass and resulting underestimation of fishing mortality rates until it was too late.

Risk and Precaution in Fisheries Management

For years, uncertainty had been held up as an argument for inaction. Stakeholders resisting management regulation argued that because scientists' models could not reliably predict the stock status, conservative management actions were unjust. Consequently, fisheries stock assessment scientists tended to downplay uncertainty. Scientists reported only point value "best estimates" of MSY, as managers given more realistic confidence intervals tended to favor the most optimistic values (MacGarvin 2001, Mace and Sissenwine 2002). In fact, in the

Newfoundland cod assessments, certainty of stock status was publicly overemphasized to give weight to management restrictions (MacGarvin 2001).

The collapses of cod and other fish stocks called for a paradigm shift in science and management regarding the reality of uncertainty in stock assessment (Charles 1998, Richards and Maguire 1998, Mace and Sissenwine 2002). In ignoring uncertainty, managers erring in favor of the fishing industry were implicitly accepting a relatively high *risk* that overfishing might occur. But the devastating consequences of stock collapses—in the case of Newfoundland, a severe blow to the island's economy and culture, and over $1 billion in annual unemployment payouts (Hilborn et al. 2003)—provided a compelling argument for a reconsideration of risk in fisheries management throughout the decade.

Attention turned toward finding the best method of incorporating the *Precautionary Principle*, a concept which had gained popularity in other fields, especially regarding pollutants or chemicals potentially hazardous to human health, since the 1970's (Harremoes et al 2001). The principle argued for greater precaution—reducing risk—in the face of greater uncertainty. Accordingly, the "burden of proof" of overfishing or otherwise should be lifted off of science (Restrepo et al. 1998). International collaborations (UN Straddling Stocks Agreement 1995, FAO Code of Conduct of Responsible Fisheries 1995) adopted a "precautionary approach," which similarly emphasized that lack of data or scientific information is not a reason to postpone conservation measures (Restrepo et al. 1998, MacGarven 2000, Mace and Sissenwine 2002). While previous management goals had been centered around recommended *target reference points* (TRPs) (catch quotas, fishing mortality rates, or minimum stock biomasses), these agreements introduced the concept of corresponding *limit reference points* (LRPs) representing upper limits of "safe" exploitation which were not to be exceeded.

In the United States, the most recent reauthorization of the Magnuson-Stevens Fishery Conservation and Management Act (2006) seeks to give precautionary management the legal backing necessary to end overfishing and to begin rebuilding the U.S. stocks that are overfished. This addresses two separate (but overlapping) classes of overexploited stocks, defined using the limit reference points for fishing mortality rate F and stock biomass B. Whenever the current

fishing mortality rate exceeds the limit (i.e., when $F > F_{MSY}$, or, more generally, $F > F_{limit}$), then *overfishing is occurring.* Whenever the current stock biomass falls below the desired threshold (when $B < B_{MSY}$, for example, or $B < B_{limit}$) then the stock is *overfished*. Stocks may be both undergoing overfishing and overfished. The MSRA 2006 requires ending both scenarios by "specifying annual catch limits… at a level such that overfishing does not occur in the fishery" (MSRA 2006).

The accompanying National Standard Guidelines for implementing the MSRA outline a method for explicitly incorporating uncertainty into these *annual catch limits* (ACLs.) Under this methodology, once scientific advisors have estimated the *overfishing limit* (OFL) (often, MSY), they must also calculate an *acceptable biological catch* (ABC), a yield value lower than the overfishing limit which provides a buffer for scientific uncertainty and which managers cannot exceed in setting ACLs.

ACL inequality $\quad ACL \leq ABC < OFL \quad$ (Eq. 7)

Quantifying scientific uncertainty is the responsibility of scientists, but determining the appropriate buffer —that is, the degree of precaution to take given this uncertainty—is a value decision that must be made by managers. Management councils set *control rules* dictating how the ABC should be calculated from the estimated OFL. These control rules differ by council, reflecting various approaches to risk mitigation. Some councils use a "decision-theoretic" approach, which applies decision theory to set buffers according to qualitative relative risk aversion (Restrepo and Powers 1999). An alternative method focuses on a frequentist concept of risk, considering the probability of experiencing an undesirable outcome (Restrepo and Powers 1999). This second method, which has recently been incorporated into the control rules of five of the eight regional management councils (Witherell 2010), is the focus of the following study.

A Probabilistic Approach to Precaution and Risk

Following the UN Straddling Stocks agreement in 1995, Caddy and McGarvey (1996) proposed a method of quantifying the risk of overfishing using standard probability theory and the

probability density functions of estimated reference points. Prager et al. (2003) and Shertzer et al. (2008a) extended this method to allow for additional sources of uncertainty and to comply with fisheries policy in the U.S.

Scientific uncertainty can be described in probability distributions surrounding estimated parameters. These distributions, or density functions, describe the range of possible values of the parameter and then weight these possibilities according to the likelihood that they capture the "true" value. The cumulative probability of the true value occurring below a certain point is calculated by finding the area under the probability density function within that range. This cumulative probability is the basic concept underlying the quantitative definition of the risk of overfishing, whose derivation is traced below.

Caddy and McGarvey (1996) were the first to suggest management according to an allowable risk level. Adhering to recent international terminology, they defined the "risk of overfishing" as the probability that a fishery would exceed a limit reference point (LRP) in a given management time frame. Focusing on fishing mortality rate *F,* the authors suggested that F_{MSY}, now widely accepted to be too high for a management target, would make a useful limit. Thus, they describe the *risk of overfishing P* as

$$P = \Pr(F > F_{MSY}) \qquad \text{(Eq. 8)}$$

where *F* is the realized fishing mortality rate for that time frame. Caddy and McGarvey's method uses a point estimate of F_{MSY}, because here, it serves as an upper limit for management goals. They then account for the uncertainty in both the science of measuring and the management of enforcing a fishing mortality rate *F* during a given year by representing this realized *F* value with a probability density function. Given the size and shape of the expected distribution of *F,* fisheries scientists can use numerical solution algorithms to estimate appropriate target *F* values (F_{T}) corresponding to any limit *F* value (F_{MSY}) and specified risk *P*.

$$\Pr(F_T > F_{MSY}) = \int_{F_{MSY}}^{\infty} pdf_{F_T}(F)dF \qquad \text{(Eq. 9)}$$

Caddy and McGarvey provide examples for normally and lognormally distributed F.

Prager et al. (2003) expanded the methods of Caddy and McGarvey for determining the risk of overfishing, denoting it "P^*." First, they relaxed the assumption of certainty in the limit reference point estimate (in this case, F_{MSY}), by assigning F_{MSY} its own probability density function. This was designed to account for scientific uncertainty in estimating the LRP.

$$P^* = \Pr(F_T > F_{MSY}) = \int_0^\infty [1 - cdf_{F_T}(F)] \cdot [pdf_{F_{MSY}}(F)] dF \qquad \text{(Eq. 10)}$$

Secondly, Prager et al. (2003) replaced the target and limit reference points with dimensionless ratios describing the quantities in relation to the current "status quo" (F_{NOW}):

$$R_{lim} = F_{lim} / F_{NOW} \text{ (here, } = F_{MSY} / F_{NOW}) \qquad \text{(Eq. 11)}$$

$$R_T = F_T / F_{NOW} \qquad \text{(Eq. 12)}$$

Prager et al. termed this extended method REPAST, for Ratio-Extended Probability Approach to Setting Targets. They argued that ratios were preferable to scaled quantities for the following reasons: first, management objectives are frequently applied based on these ratios; second, ratios cancel out the sampling error in the scaled quantities, as well as the problem of scale; and third, the use of ratios reduces the possible (though likely negligible) correlation between the distributions of F_{NEXT} and F_{MSY}. Prager et al. also provided an example using biomass target and limit reference points, defining $P^* = \Pr(B < B_{lim})$ (with example $B_{lim} = B_{MSY}$).

In the 2006, when the U.S. Magnuson-Stevens Act mandated an end to overfishing, it defined overfishing in terms of fishing mortality rate (F), a fishery "input" value, while setting the control mechanism (annual catch limits, ACLs) in terms of yield, a fishery "output" value (Shertzer et al. 2008a). Shertzer et al. (2008a) revised REPAST to accommodate the need to achieve appropriate model inputs by controlling model outputs. As before, P^* is defined as the risk of overfishing:

$$P^* = \Pr(F > F_{\lim}) \qquad \text{(Eq. 13)}$$

However, the new method, PASCL, (Probability-based Approach to Setting Catch Limits) allows for management using *annual catch targets* (ACTs) and their associated probability distributions. These ACTs are set below the ACLs to account for management uncertainty, carrying forward the target-limit relationship of the previous regulations. PASCL employs a stochastic projection model to represent a stock assessment, simulating various sources of uncertainty surrounding the estimate of $F_{\lim}$ and removing the need to assume equilibrium for benchmark calculations. Additionally, PASCL extends the management time frame across more than one year, recognizing that with a constant P^*, the actual probability of overfishing in at least one year grows with time T:

$$\Pr(\text{any } F_t > F_{\lim}) = 1 - (1 - P^*)^T \qquad \text{(Eq. 14)}$$

The PASCL method begins by simulating N stochastic replicates of the population of interest. To determine the annual catch target (ACT) that would correspond to an allowable risk of overfishing P^*, PASCL uses an indirect trial-and-error method. It chooses a trial ACT, simulates uncertainty in achieving that target during the ensuing year, and calculates F values corresponding to the "realized" catches for each of the N simulated populations. This constructs a probability distribution of F, which is used to check $P = \Pr(F > F_{MSY})$ against the desired P^*. The result of this comparison determines whether the trial ACT should be applied to that year or whether a new value should be tried. Once PASCL determines an appropriate ACT, it applies it for that year, increases the time step, and begins the process over.

Currently, following the National Standard Guidelines for implementing the reauthorized Magnuson-Stevens Act, many management councils simplify the incorporation of P^* into control rules by casting it not as the probability of the fishing mortality rate F exceeding a limitin a given year, but as the probability of the recommended acceptable biological catch (ABC) exceeding the overfishing limit (OFL) in a given year (Prager and Shertzer 2010).

$$P^* = \Pr(\text{ABC} > \text{OFL}) \qquad \text{(Eq. 15)}$$

It is this definition of *P** (Eq. 15) that will be considered in the following study (Figure 1.3).

From Probability to Risk Analysis

While the *P** literature (Prager et al. 2003, Shertzer et al. 2008a, Prager and Shertzer 2010) provides some basic examples of applying *P** methodology, the authors of these studies point to an opportunity for further analysis. The need to objectively identify and compare the risks associated with different management actions motivates the *risk assessments,* or *risk analyses*, conducted by scientific advisors and analysts across fields (Francis and Shotton 1997, Suter 2007). But a conventional understanding of *risk* takes into account both the probability of an undesired outcome, and the severity of its consequences (Suter 2007). *P**, in quantifying the probability that catch exceeds overfishing thresholds, describes only the first component of the risk of overfishing. Formal risk analysis of control rules using *P**, then, would explore the more "comprehensive" risks associated with each "probabilistic" risk (*P** level) for the stock in question.

Many forms of risk analyses used in fisheries management employ computer simulation studies to evaluate different harvest strategies or management procedures (Francis and Shotton 1997, Butterworth and Punt 1999, Sainsbury et al. 2000, Deroba and Bence 2008). These simulation studies are particularly useful because they allow scientists to conduct experiments on simulated fish populations that would be logistically or legally impossible for real fish populations (Smith 1993, CSIRO 2009). Furthermore, those experiments are unlimited in the range and sample size of population types on which to test these management strategies. By varying certain factors, researchers can explore the effects of population type on the performance of each control rule or management regulation.

As managers increasingly adopt and incorporate methods employing *P** into current fishing regulations, it is imperative both for management efficacy and transparency that they possess a clear understanding of the implications of these choices. The need for a better understanding of *P** control rules motivates my research question: *What are the consequences of managing different stocks at different levels of risk?* Simulation studies are the means by which I can

attempt to answer this question. To evaluate control rules based on P^*, I will project the consequences of harvesting these simulated populations according P^* values that range from risk averse to risk prone. This evaluation will extend managers' understanding of P^* decisions from strictly probabilistic risk to a broader, more inclusive risk.

I hypothesize that two stock characteristics will affect the long-term risks associated with each probabilistic risk P^*. First, I hypothesize that a given level of P^* corresponds to different levels of risk depending on species life history. Second, I hypothesize that a given level of P^* corresponds to different levels of precaution (and, therefore, risk) depending on the scientific uncertainty in the stock assessment. The motivations behind testing these two factors are further detailed below.

The Effects of Life History

The optimal allowable risk levels may depend on the species' life history. Species with different life histories have different capacities to recover from overfishing (Adams 1980, Jennings et al. 1998).

In classical ecology, species life histories are compared along a relative scale from those that favor high growth rate (*r*-selected species) to those that favor high individual survival (*K*-selected species) (MacArthur and Wilson 1967). One on end, *r*-selected species have evolved in response to high or indiscriminant mortality, and individuals maximize surviving offspring by investing in high fecundity and quick maturation. Fish with this life history strategy can sustain high levels of fishing mortality, and they recover their numbers quickly when released from fishing pressure (Adams 1980). The dolphin fish, or mahi mahi, *Coryphaena hippurus*, is an example of an *r*-selected species. Maturing in only 4-5 months and producing tens of thousands of eggs, mahi mahi are considered highly resilient (Palko 1982).

In contrast, *K*-selected species have evolved in response to low or selective mortality, experiencing greater selection pressure from resource limitation and intraspecific competition. Individuals in *K*-selected populations maximize surviving offspring by investing in the fitness of

individual offspring. Fish with this life history tend to have few offspring and later maturation. They cannot withstand heavy fishing mortality, and once overfished, the population will take a much longer time to recover (Adams 1980). An example of strongly *K*-selected is the sandbar shark *Carcharhinus plumbeus*. Because sandbar sharks mature only after 12-16 years, and females produce only 5-12 young at once, they have very low resilience (Compagno 1984).

Winemiller and Rose (1992) refined life history theory to better explain trends within the fishes, identifying three extreme life-history types and placing fish species within a triangular spectrum along three gradients. One of these types corresponds closely to the classical *K*-selected species type, with low fecundity, slow maturation, and high juvenile survivorship. The authors term this the *equilibrium strategy,* for the environmental conditions that tend to favor it: relatively stable resource availability and predictable mortality rates. However, the *r*-selected type is essentially split into two, both with low juvenile survivorship. *Opportunistic* species colonize highly variable and unpredictable conditions by maturing quickly but investing little in each reproductive batch. *Periodic* species face highly variable but fairly predictable conditions which favor more investment in each reproductive batch, achieved through later maturation and high fecundity over multiple years. The bay anchovy *Anchoa mitchilli,* which inhabits tidal habitats and matures in a few months, is an opportunistic strategist (Whitehead et al. 1988, Winemiller and Rose 1992). The bluefin tuna *Thunnus thynnus*, which matures at 3-5 years but produces 10 million eggs, is a periodic strategist (Collette 1999, Winemiller and Rose 1992). The dolphin fish may fall somewhere in between.

Fish species, in their exhaustive diversity, occupy the full range of life history spectrums. Jennings et al. (1998) showed this trend empirically by comparing life history traits and stock declines among closely related species. This variation has direct implications for management. Opportunistic and periodic strategists, for example, display a very unpredictable relationship between stock size and recruitment success, adding uncertainty to population projections (Winemiller 2005). Because the consequences of overfishing the more *K*-selected species (or equilibrium strategists) are likely to be more severe than those for fishes with greater compensation potential, equal probabilistic risks of overfishing P^* will translate into different comprehensive risks of overfishing for different life histories. Managers must account for this

difference when incorporating *P** into control rules: equally low *P** values may appear to be equally risk-averse, but if the stocks' comprehensive risks differ, they will not in fact provide equal levels of precaution for the resources.

The Effects of Uncertainty in the Overfishing Limit

Different allowable risk levels may be appropriate for different amounts of scientific uncertainty in the stock assessment. The amount and quality of data available for different fish stocks vary greatly, and for many stocks are quite poor (Richards and Maguire 1998). Among stocks that meet minimum data requirements, varying levels of scientific uncertainty are reflected in the varying shapes and spreads of their overfishing limit (OFL) distributions. Preferably, these distributions are provided in stock assessments, but when they are not they can be approximated using variances of B and F_{lim} (Prager and Shertzer 2010).

The four sources of scientific uncertainty—process, observation, model, and estimation or parameter uncertainties—are true sources that every stock assessment realistically faces. However, fully quantifying and incorporating each of these sources into each stock assessment is logistically impossible, due to time and resource constraints, and perhaps theoretically impossible, owing to unknowns surrounding the uncertainty itself. In practice, scientists employ a wide variety of methods for calculating uncertainty (Mace and Sissenwine 2002). Depending on the method and the models used, different sources of incorporated uncertainty will influence the spread of the OFL distribution to differing degrees. For example, Jiao et al. (2005) conducted a sensitivity analysis for one common population model and found that for this model the (estimation) uncertainty in natural mortality was the strongest determinant of the uncertainty in the threshold fishing mortality (F) estimate.

Control rules based on the application of *P** are inherently sensitive to the shape of these distributions. A given *P** defines the area underneath the probability distribution curve, but the OFL distribution defines the distance between the estimated OFL and the calculated allowable biological catch (ABC) that bounds this area—that is, the size of the buffer against uncertainty. As a result, a single level of allowable risk (*P**) will require catch reductions of different

magnitudes for fish stocks assessed with different levels of uncertainty. Furthermore, even for the same stock, a single level of P^* may result in different catch reductions from one year of assessment to another, as the quality and availability of data and the sophistication and choice of models change over time. Because managers often prefer to stabilize regulations as much as possible, they must take these factors into account: equal P^* values do not necessarily imply equal impacts on fishermen and the fishery (Figure 1.4).

Management Context: The South Atlantic Fisheries Management Council

Risk evaluations in fisheries management compare the results of their projections using *performance measures*. A wide variety of performance measures exist; Francis and Shotton (1997) count nearly 40 in the literature at the time of their review. Butterworth and Punt (1999) group them into three categories according to the general objectives they rate. Performance in terms of maximizing catch, for example, may be rated by monitoring cumulative catch or average long-term catch over the span of the projection. A more conservative objective of minimizing risk to the resource may be measured in terms of the probability of stock biomass dropping below a threshold. The third common objective the authors identify is that of maximizing industry stability (or, minimizing interannual catch variability), which may be measured by monitoring catch variance through time. Which performance measures are used in an evaluation of control rules depends on the specific management objectives and broader societal goals of the individual fishery (Deroba and Bence 2008).

My study will focus on the stocks and the management objectives relative to one of NOAA Fisheries' eight regional management councils, the South Atlantic Fisheries Management Council (SAFMC). The SAFMC has management authority over 88 species, grouped into eight fisheries, many of which are highly important to the commercial sector (SAFMC 2010). These fisheries include the coastal migratory pelagics (mackerels and cobia); the dolphin fish / wahoo fishery; the golden crab, spiny lobster, and shrimp fisheries; and the snapper/grouper complex, a mixed fishery of 73 species. Determining which of these stocks to use in my simulation studies, and which performance measures will be most relevant, falls within the first objective of this thesis.

Summary

Mounting challenges in fisheries management call for innovative solutions to staving off declines in marine populations without sacrificing the fishing industries on which so many livelihoods depend. Scientists and managers now recognize that these solutions must be grounded in a paradigm of precaution and thus should err in favor of the resource. This precautionary approach is most effectively and fairly implemented when managers have a clear understanding of the *risks* associated with each *action*. A new method of doing so, however, allows managers to understand instead the *actions* associated with each *risk*, where "risk" is considered only in terms of the probability P^* of an unwanted outcome. The following study seeks to characterize this method by predicting the effects of managing according to P^* will have on a range of population types. In doing so, it can contribute both in a theoretical sense to the field of fisheries risk management, and in practical sense to the management authority (the South Atlantic Fisheries Management Council) on whose stocks the analysis will be based.

Literature Cited

Adams, P. 1980. Life history patterns in marine fishes and their consequences for fisheries management. Fishery Bulletin: 78(1): 1-12.

Butterworth, D. S. and M. O. Bergh. 1993. The development of a management procedure for the South African anchovy resource. Pages 83-99 *in* S. J. Smith, J. J. Hunt, and D. Rivard, editors. Risk evaluation and biological reference points for fisheries management. Canadian Special Publication of Fisheries and Aquatic Sciences 120.

Butterworth, D. S. and A. E. Punt. 1999. Experiences in the evaluation and implementation of management procedures. ICES Journal of Marine Science 56: 985-998.

Caddy, J. F. and R. McGarvey. 1996. Targets or limits for management of fisheries? North American Journal of Fisheries Management 16: 479-487.

Collette, B. B. 1999. Mackerels, molecules, and morphology. Pages 149-164 *in* B. Séret and J. Y. Sire, editors. Proceedings of the 5th Indo-Pacific Fish Conference, Noumea, Paris. *In* R. Froese, and D. Pauly, editors. FishBase. www.fishbase.org (May 2010.)

Compagno, L. V. 1984. Sharks of the world: an annotated and illustrated catalogue of the shark species known to date, Part 2: Carcharhiniformes. FAO Fisheries Synopsis 125: 251-665 *in* R. Froese, and D. Pauly, editors. FishBase. www.fishbase.org (April 2010.)

Charles, A. T. 1998. Living with uncertainty in fisheres: analytical methods, management priorities and the Canadian groundfishery experience. Fisheries Research 37: 37-50.

CSIRO. 2009. Management strategy evaluation. CSIRO Marine and Atmospheric Research. http://www.cmar.csiro.au/research/mse/ (April 2010.)

Cury, P. and P. Cayré. 2001. Hunting became a secondary activity 2000 years ago: marine fishing did the same in 2021. Fish and Fisheries 2:162-169.

Deroba, J. J. and J. R. Bence. 2008. A review of harvest policies: understanding relative performance of control rules. Fisheries Research 94: 210-223.

FAO. 1995. Precautionary approach to fisheries. Part 1: Guidelines on the precautionary approach to capture fisheries and species introductions. FAO Fisheries Technical Paper No. 350.

FAO. 2005. Review of the state of world marine fishery resources. FAO Fisheries Technical Paper No. 457. FAO, Rome.

Francis, R. I. C. C. and R. Shotton. 1997. "Risk" in fisheries management: a review. Canadian Journal of Fisheries and Aquatic Sciences 54: 1699-1715.

Hardin, G. 1968. The tragedy of the commons. Science 162: 1243-1248.

Harremoes, P., D. Gee, M. MacGarvin, A. Stirling, J. Keys, B. Wynne, and S. Guedes Vaz. 2001. Late lessons from early warnings: the precautionary principle 1896-2000. Environmental Issue Report No. 22. European Environmental Agency, Copenhagen, Denmark.

Heemstra, P. C., and J. E. Randall. 1993. Groupers of the world (family Serranidae, subfamily Epinephelinae): An annotated and illustrated catalogue of the grouper, rockcod, hind, coral grouper and lyretail species known to date. FAO Fisheries Synopsis 125(16.) *in* R. Froese, and D. Pauly, editors. FishBase. www.fishbase.org (April 2010.)

Hilborn, R., T. A. Branch, B. Ernst, A. Magnusson, C. V. Minte-Vera, M. D. Scheuerell, and J. L. Valero. 2003. State of the world's fisheries. Annual Reviews in Environmental Resources 28: 359-399.

Holt, S. J. 1998. Fifty years on. Reviews in Fish Biology and Fisheries 8: 357-366.

Hutchings, J. A. and R. A. Myers. 1994. What can be learned from the collapse of a renewable resource? Atlantic cod, *Gadus morhua*, of Newfoundland and Labrador. Canadian Journal of Fisheries and Aquatic Sciences 51: 2126-2146.

Jennings, S., J. D. Reynolds, and S. C. Mills. 1998. Life history correlates of responses to fisheries exploitation. Proceedings of the Royal Society B 265: 333-339.

Jiao, Y., Y. Chen, and J. Wroblewski. 2005. An application of the composite risk assessment method in assessing fisheries stock status. Fisheries Research 72: 173-183.

Larkin, P. A. 1977. An epitaph for the concept of maximum sustainable yield. Transactions of the American Fisheries Society 106(1): 1-11.

MacArthur, R. H., and E. O. Wilson. 1967. The theory of island biogeography. Princeton University Press, Princeton, New Jersey.

Mace, P. M., and M. P. Sissenwine. 2002. Coping with uncertainty: evolution of the relationship between science and management. Pages 9-28 *in* J. M. Berkson, L. L. Kline, and D. J. Orth, editors. Incorporating uncertainty into fishery models. Amercian Fisheries Society Symposium 27, Bethesda, Maryland.

MacGarven, M. 2001. Fisheries: taking stock. Pages 17-30 *in* P. Harremoes, D. Gee, M. MacGarvin, A. Stirling, J. Keys, B. Wynne, and S. Guedes Vaz, editors. Late lessons from early warnings: the precautionary principle 1896-2000. Environmental Issue Report No. 22. European Environmental Agency, Copenhagen, Denmark.

MSRA (Magnuson-Stevens Fishery Conservation and Management Reauthorization Act of 2006). 2006. Pub. L. No. 109-479, 120 Stat. 3575.

Palko, B. J., G. L. Beardsley, and W. J. Richards. 1982. Synopsis of the biological data on dolphin-fishes, *Coryphaena hippurus* Linneaus and *Coryphaena equiselis* Linneaus. NOAA Technical Report NMFS Circulation 443: 1-28 *in* R. Froese, and D. Pauly, editors. FishBase. www.fishbase.org (April 2010.)

Prager, M. H., C. E. Porch, K. W. Shertzer, and J. F. Caddy. 2003. Targets and limits for management of fisheries: a simple probability-based approach. North American Journal of Fisheries Management 23: 349-361.

Prager, M. H., and K. W. Shertzer. 2010. Deriving acceptable biological catch from the overfishing limit: implications for assessment models. North American Journal of Fisheries Management 30: 289-294.

Punt, A. E., F. Pribac, B. L. Taylor, and T. I. Walker. 2005. Harvest strategy evaluation for school and gummy shark. Journal of Northwest Atlantic Fishery Science 35: 387-406.

Quinn II, T. J. and R. B. Deriso. 1999. Quantitative fish dynamics. Oxford University Press Inc, New York, New York.

Restrepo, V. R. and J. E. Powers. 1999. Precautionary control rules in US fisheries management: specification and performance. ICES Journal of Marine Science 56: 846-852.

Restrepo, V. R., G. G. Thompson, P. M. Mace, W. L. Gabriel, L. L. Low, A. D. MacCall, R. D. Methot, J. E. Powers, B. L. Taylor, P. R. Wade, and J. F. Witzig. 1998. Technical guidelines on the use of precautionary approaches to implementing National Standard 1 of the Magnuson-Stevens Fishery Conservation and Management Act. NOAA Technical Memorandum NMFS-F/SPO-31.

Richards, L. and J. J. Maguire. 1998. Recent international agreements and the precautionary approach: new directions for fisheries management science. Canadian Journal of Fisheries and Aquatic Sciences 55: 1545-1552.

Sainsbury, K. J., A. E. Punt, and A. D. M. Smith. 2000. Design of operational management strategies for achieving fishery ecosystem objectives. ICES Journal of Marine Science 57: 731-741.

Schaefer, M. B. 1959. Biological and economic aspects of the management of commercial marine fisheries. Transactions of the American Fisheries Society 88: 100-104.

Shertzer, K. W., M. H. Prager, and E. H. Williams. 2008. A probability-based approach to setting annual catch levels. Fishery Bulletin 106: 225-232.

Shertzer, K. W., M. H. Prager, D. S. Vaughan, and E. H. Williams. 2008. Fishery Models. Pages 1582-1593 *in* S. E. Jorgensen and B. Fath, editors. Encyclopedia of ecology. Elsevier, Oxford.

Smith, A. D. M. 1993. Management strategy evaluation—the light on the hill. Pages 249-253 *in* D. A. Hancock, editor. Population dynamics for fisheries management. Australian Society for Fish Biology, Perth.

South Atlantic Fishery Management Council. Fishery management plans/amendments. http://www.safmc.net/ (April 2010.)

Suter, G. W. 2007. Ecological risk assessment, 2nd edition. CRC Press, Taylor and Francis Group, Boca Raton, Florida.

UN. 1995. Agreement for the implementation of the provisions of the United Nations Convention on the Law of the Sea of 10 December 182 relating to the conservation and

management of straddling fish stocks and highly migratory fish stocks. United Nations General Assembly Document A/CONF.164/37, New York.

Walters, C. and J. J. Maguire. 1996. Lessons for stock assessment from the northern cod collapse. Reviews in Fish Biology and Fisheries 6: 125-137.

Whitehead, P. J. P., G. J. Nelson, and T. Wongratana. 1988. Clupeoid fishes of the world (Suborder Clupeoidei): An annotated and illustrated catalogue of the herrings, sardines, pilchards, sprats, shads, anchovies, and wolf-herrings. Part 2: Engraulidae. FAO Fisheries Synopsis 125: 305-579 *in* R. Froese, and D. Pauly, editors. FishBase. www.fishbase.org (May 2010.)

Winemiller, K. O. 2005. Life history strategies, population regulation and implications for fisheries management. Canadian Journal of Fisheries and Aquatic Sciences 62: 872-885.

Winemiller, K. O. and K. A. Rose. 1992. Patterns of life-history diversification in North American fishes: implications for population regulation. Canadian Journal of Fisheries and Aquatic Sciences 49: 2196-2218.

Witherell, D., editor. 2010. Report of a national SSC workshop on establishing a scientific basis for annual catch limits. Second National Meeting of the Regional Fishery Management Councils' Scientific and Statistical Committees. Carribbean Fishery Management Council, St. Thomas.

Figure 1.1. Sustainable Yield: On a graph of yield against stock biomass, sustainable yield at a given stock biomass falls on the parabola described by the production curve.

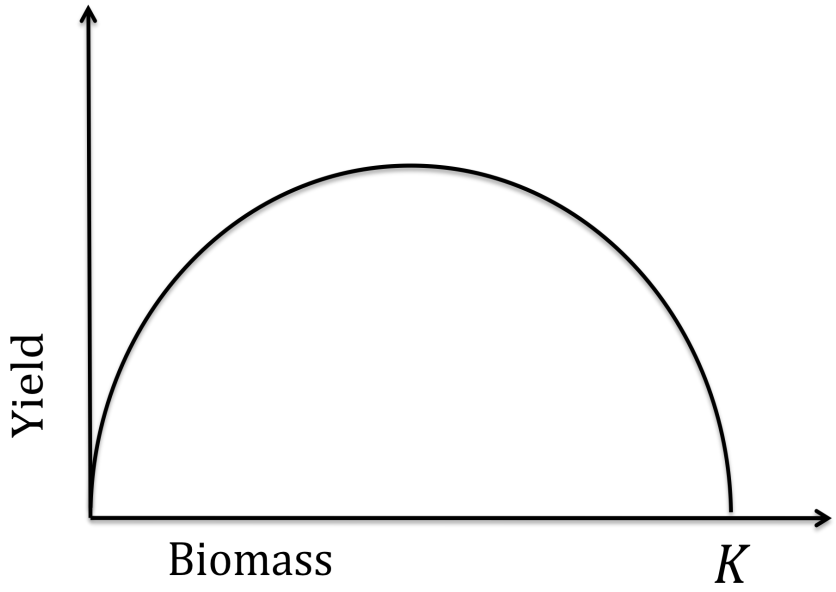

Figure 1.2. Maximum Sustainable Yield: In general, the stock biomass needed to achieve the *maximum sustainable yield* (MSY) is called $B_{\mathbf{MSY}}$. If logistic growth is assumed, MSY occurs when B equals half the carrying capacity.

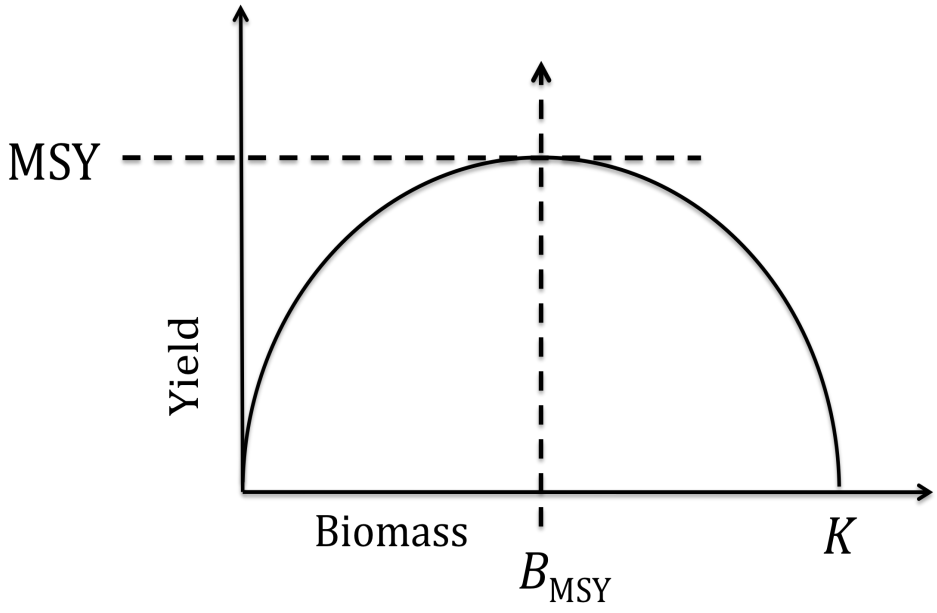

Figure 1.3. Original and current methods for defining P^*, the allowable risk of overfishing. P^*=0.20, as defined by Caddy and McGarvey (1996) above and Prager and Shertzer (2010) below. **A)** A target fishing mortality rate F_{tgt} is set below some limit fishing mortality rate F_{lim} to allow for uncertainty in implementation of regulation. The realized fishing mortality rate F for this time period falls anywhere within a distribution around F_{tgt}, and the probability that $F > F_{lim} = P^*$, the area under the curve to the right of $F_{lim.}$ **B)** The acceptable biological catch ABC is set below the estimated overfishing limit OFL to allow for scientific uncertainty in stock assessment. The *true* OFL, which can never be known exactly, is expected to fall within a distribution around the estimated OFL, and the probability that $OFL_{true} < ABC = P^*$, the area under the curve to the left of ABC. If a P^* value is preset, the ABC can be calculated accordingly.

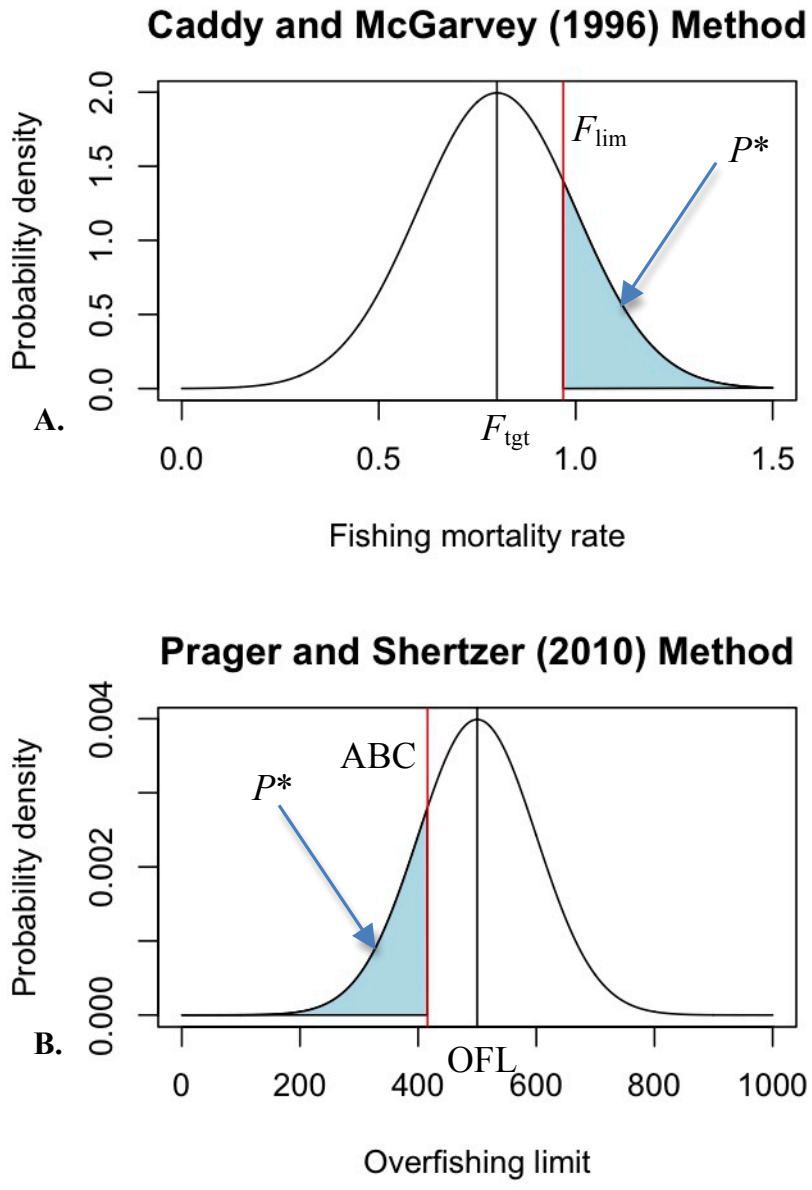

Figure 1.4. The influence of scientific uncertainty on the value of ABC. **A)** A single estimate of the *overfishing limit* (OFL) may have a range of distributions depending on uncertainty in the stock assessment: shown here, distributions with CVs equal to 10% (narrowest), 20% (middle), and 30% (widest). **B)** Depending on the spread of the distribution, a single *P** value will correspond to different *acceptable biological catches* (ABCs) at different reductions from the OFL estimate: shown here, ABCs calculated for *P**=0.20 for the three distributions in (a.) A control rule using *P**=0.20 may result in these three ABCs depending on scientific uncertainty.

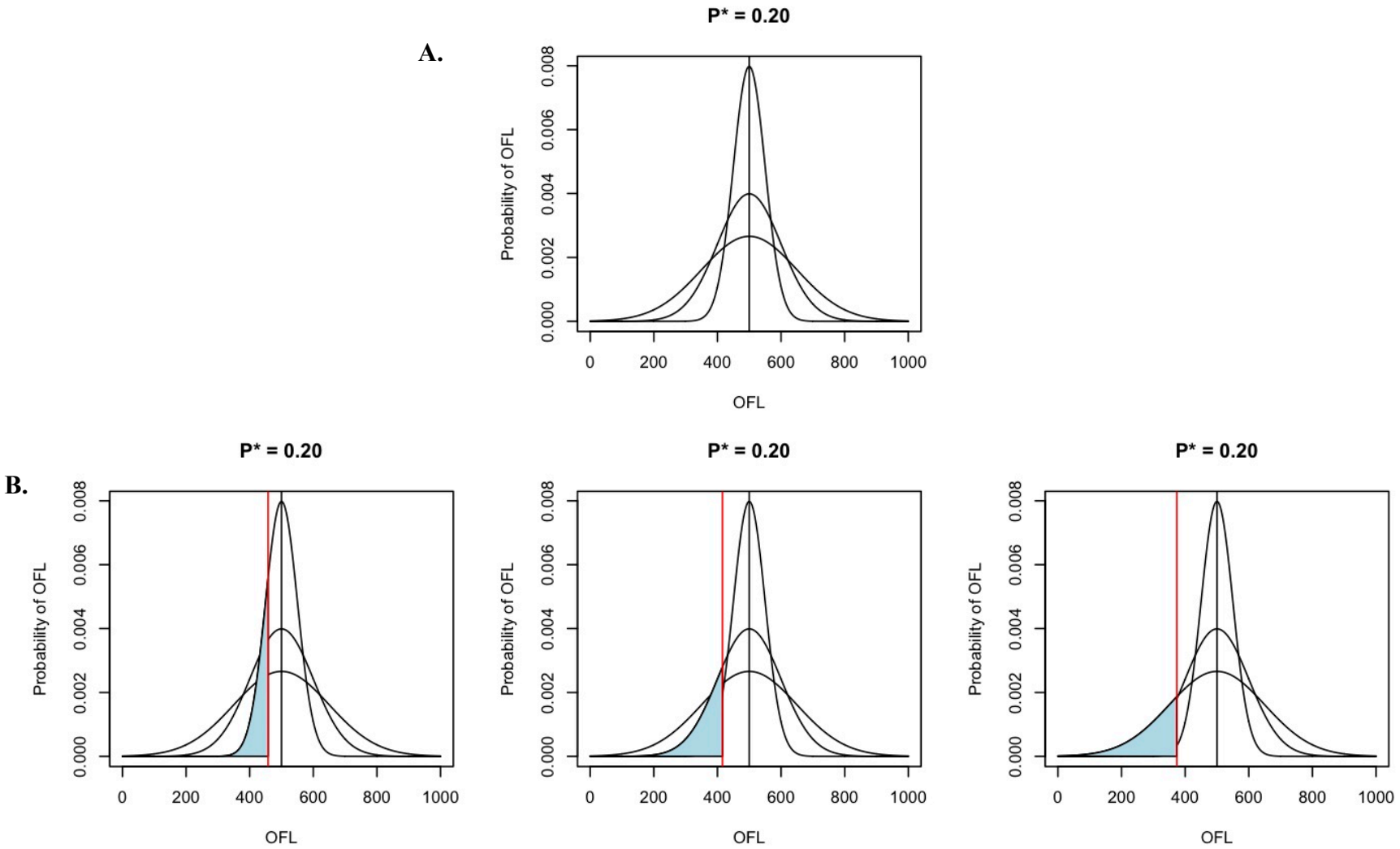

CHAPTER 2: A simulation model to investigate the impacts of probability-based control rules on stocks of differing life history strategies

Introduction

The National Standard 1 Guidelines for implementing the Magnuson-Stevens Fishery Conservation and Management Act involve a series of catch level reductions that explicitly account for different sources of uncertainty (MSRA 2006). According to these guidelines, scientists conduct an assessment to estimate a stock's *overfishing limit*, OFL, but recommend an *acceptable biological catch*, ABC, reduced from the OFL to provide a buffer against scientific uncertainty. Managers cannot exceed the ABC in setting *annual catch limits* (ACLs). Although it is scientists' role to estimate the OFL and to describe the scientific uncertainty surrounding that estimate, risk management is a value decision that must be made by managers. It is therefore managers' role to set *control rules* for calculating the ABC which specify how to appropriately buffer against this uncertainty.

A method based on work by Caddy and McGarvey (1996) and most recently extended by Prager and Shertzer (2010) proposes that managers define an *allowable risk of overfishing*, P^*, where this risk describes the probability that the recommended ABC exceeds the value of OFL. Scientists then apply the control rule to the probability distribution of the OFL estimate to determine the catch level corresponding to the chosen percentile (P^*). This catch level is taken to be the ABC. But the probability of an undesired event is only one definition of risk. Another concerns the severity of the consequences of that event, and this risk is important to consider when choosing and acceptable probability.

Two factors seem likely to influence the risks resulting from P^*-based management. First, because P^* is a percentile of a distribution, the magnitude of the precautionary buffer corresponding to P^* depends on the width of the OFL distribution. This suggests that the amount of uncertainty surrounding the OFL estimate affects the implications of a P^* level for a population and its fishery. Secondly, fish life history theory postulates that growth rates, lifespan,

and other biological characteristics leave some life history strategies more vulnerable than others to long-term consequences of overfishing (King and MacFarlane 2003, Winemiller 2005).

To evaluate the effects of these two factors, I selected three Southern Atlantic commercial fish stocks that display a range of life history strategies and assembled life history parameters for each. I used these parameters to estimate theoretical overfishing limits. Next, I simulated various levels of scientific uncertainty by varying these parameters to generate thousands of unique sample populations. Against this backdrop of uncertainty, I simulated fishing the sample populations under different P^*-based control levels and measured the rates at which populations experience overfishing or fall below a certain biomass threshold.

Ultimately, the goal of this study was to identify patterns in simulated risks across life history characteristics of the species, degrees of scientific uncertainty in the stock assessment, and levels of precaution (P^*) in ABC control rules. In doing so, I aim to provide insight into P^*-based management for modelers and managers in the South Atlantic and throughout the nation.

Methods

I. Age-Structured Fishery Population Models

Like the stock assessment models on which it is based, the following simulation study employs and adapts a suite of equations drawn from classic fisheries modeling theory. That theory is reviewed below in order to provide a reference for the equations used in constructing the simulation models.

As life history strategy is a major factor in this experiment, models that adequately captured differences in life history were required. Age-structured population models provide an important level of detail by allowing key life history parameters to vary with age. In the following study, maturity, fecundity, natural mortality, and selectivity parameters for each species are input as vectors of age-specific values.

Mortality Rates

In a population closed to immigration and emigration, survivorship of fish in a given age class and year determines the number of fish in the subsequent age class the following year (Haddon 2001). The mortality that each cohort experiences during the intervening year is categorized into two sources: fishing mortality and natural mortality.

Fishing mortality, F, is the instantaneous death rate due to capture by humans, in any fishery and by any means. Fishing pressure is usually assumed to vary among years, but to be constant within years and to be uniform across space. However, fishing gears do not catch all sizes (and, therefore, ages) of fish evenly. To account for this, a vector of gear-specific selectivity-at-age values is used to scale fishing mortality to reflect the rate at which fish become available and susceptible to that gear (Shertzer et al. 2008). Selectivity-at-age is often described as function of age, length, or a combination of estimated quantities (Shertzer et al. 2008). Below, it is termed s_a, where the a subscript denotes age.

Natural mortality, M, comprises all the sources of mortality unrelated to fishing. It is extremely difficult to estimate and often considered to describe aggregate mortality, constant across age and time (Megrey 1989, Shertzer et al. 2008). There are several methods for scaling constant estimates by weight or age (Peterson and Wroblewski 1984, Chen and Watanabe 1989, Lorenzen 1996). The following equations use age-specific natural mortality, M_a.

Combining natural and fishing mortality, the total mortality rate, $Z_{y,a}$, in year y for age a can be expressed as:

$$Z_{y,a} = M_a + s_a F_y \qquad \text{(Eq. 1)}$$

This total mortality rate determines the yearly survivorship of each age:

$$N_{y+1,a+1} = N_{y,a} e^{-M_a - s_a F_y} \qquad \text{(Eq. 2a)}$$

Most marine fish do not have determinate lifespans (i.e. a single age after which they experience 100% mortality.) Rather, modelers choose the number of age classes to model and allow survivors to the final age (A) to pool into a "plus group," in which all members are subjected to the same mortality rate. The number of fish in this plus group (ages $A+$) is found by modifying Eq. 2a:

$$N_{y+1,A} = (N_{y,A-1} + N_{y,A}) e^{-M_A - s_A F_y} \qquad \text{(Eq. 2b)}$$

Individual Growth Models

Numbers-at-age can be transformed to biomass-at-age through models describing average individual growth. The von Bertalanffy growth equation is the most common method of modeling the relationship between age and length (Quinn and Deriso 1999, Haddon 2001):

$$L_a = L_\infty (1 - e^{-\kappa(a - a_0)}) \qquad \text{(Eq. 3)}$$

where length at age a is predicted using asymptotic length, L_∞; the growth parameter, κ; and the asymptotic age at length 0, a_0. Next, this length-at-age vector L_a can be converted to a biomass-

at-age vector w_a (w for the vernacular term "weight") by assuming allometric growth (Quinn and Deriso 1999):

$$w_a = \alpha L_a^{\beta} \quad \text{(Eq. 4)}$$

Finally, the matrix of biomass-at-age can by obtained by multiplying equation 4 by equation 2:

$$B_{y,a} = w_a N_{y,a} \quad \text{(Eq. 5)}$$

Spawner-Recruit Relationship

Summing the numbers-at-age matrix or biomass-at-age matrix across age classes provides a yearly report of the stock's total number or total biomass. However, only a portion of the total stock contributes to the next year's *recruitment*, defined as the number of new fish added to the population. While the relationship is difficult to observe empirically, recruitment is usually assumed to depend on the amount of mature spawners (often, only mature females) in the population (Shertzer et al. 2008). The number of spawners, S_y, and the amount of spawning stock biomass, SSB_y, are calculated by scaling N_y and B_y, respectively, by maturity-at-age, μ_a, and a constant sex ratio, ρ. Here, S_y is actually expressed as number of eggs (or pups) by scaling $N_{y,a,}$ by fecundity-at-age, f_a (see Section IV).

$$S_y = \rho \sum_{a=1}^{A} \mu_a f_a N_{y,a} \quad \text{(Eq. 6a)}$$

$$SSB_y = \rho \sum_{a=1}^{A} \mu_a B_{y,a} \quad \text{(Eq. 6b)}$$

A classic choice for modeling the spawner-recruitment relationship in marine populations is the Beverton-Holt model, which assumes resource-limited density-dependent survival and asymptotic recruitment at high spawner levels (Haddon 2001):

$$R_{y+1} = \frac{aS_y}{b + S_y} \quad \text{(Eq. 7)}$$

Here, S_y may either be spawner number (as in eq. 6a) or SSB_y (eq. 6b), depending on the model, while R is the number of recruits produced by those spawners.

There are many formulations of the Beverton-Holt spawner-recruit relationship. One alternative formulation, below, redefines the a and b parameters in equation 7 in terms of three more biologically sensible parameters: steepness, h; unfished (or virgin) equilibrium recruitment, R_0; and unfished spawners-per-recruit, ϕ_0 (Mace and Doonan 1988, Shertzer et al. 2008).

$$R_{y+1} = \frac{0.8R_0hS_y}{0.2\phi_0R_0(1-h)+(h-0.2)S_y} \qquad \text{(Eq. 8)}$$

Steepness, h, is defined as the slope of the stock-recruitment relationship when the spawning stock has been reduced to 20% of its virgin size (Shertzer et al. 2008). Unfished spawners-per-recruit, ϕ_0, a measure of the stock's reproductive potential, is calculated for age-structured populations as follows (SEDAR21):

$$\phi_0 = \rho\sum_{a=1}^{A-1} f_a\mu_a e^{-\sum_{j=1}^{a-1}M_j} + \rho * f_A\mu_A\frac{e^{-\sum_{a=1}^{A-1}M_a}}{1-e^{-M_A}} \qquad \text{(Eq. 9)}$$

where f_a is fecundity-at-age. The second term in this equation accounts for the plus group.

Catch and Yield

Equation 2 described the portion of a cohort that survives to the next year. Subtracting the surviving proportion from 1 describes the portion of that cohort that did *not* survive. The fraction of these non-survivors that died due to fishing (F/Z) comprises the catch. This is named the Baranov catch equation (Quinn and Deriso 1999, Haddon 2001):

$$C_{y,a} = \frac{s_aF_y}{M_a+s_aF_y}N_{y,a}(1-e^{-(M_a+s_aF_y)}) \qquad \text{(Eq. 10)}$$

Multiplying Eq. 10 by the biomass-at-age vector (Eq. 4) and summing across ages predicts yield:

$$Y_y = \sum_{a=1}^{A} w_a C_{y,a} \qquad \text{(Eq. 11)}$$

II. Equilibrium Calculations to Generate Benchmarks

In general, federal fisheries policy relies on biomass, fishing mortality, and yield benchmarks to monitor population status and determine management actions. A substantial variety of benchmarks have been developed and used for different fisheries and management bodies over the past century (Quinn and Deriso 1999). The following study considers a set of benchmarks that can be calculated entirely from the input life history parameters. These derive from spawners-per-recruit analysis, which assumes a population is in equilibrium and calculates benchmarks for equilibrium spawning stock biomass, recruitment, and yield, all in terms of fishing mortality. Repeating these calculations over a range of fishing mortalities allows approximate identification of the *maximum* equilibrium yield, a common reference point.

Spawning Stock Benchmarks

In general, let recruitment, R, and spawners per recruits, S/R, be defined as follows:

$$R \equiv S * f(S) \qquad \text{(Eq. 12a)}$$

$$\frac{S}{R} \equiv g(F) \Rightarrow R \equiv \frac{S}{g(F)} \qquad \text{(Eq. 12b)}$$

where f and g are functions (Quinn and Deriso 1999).

At equilibrium, Eq. 12a can be set equal to Eq. 12b:

$$R_* = S_* * f(S_*) = \frac{S_*}{g(F_*)} \Rightarrow f(S_*) = \frac{1}{g(F_*)} \qquad \text{(Eq. 13)}$$

Then equilibrium spawners (or spawning biomass), S_*, can be solved for as a function of F:

$$S_* = f^{-1}(\frac{1}{g(F_*)}) \quad \text{(Eq. 14)}$$

Substituting into Eq. 12a, equilibrium recruitment, R_*, can also be written as a function of F:

$$R_* = S_* * f(S_*) = f^{-1}(\frac{1}{g(F_*)}) * \frac{1}{g(F_*)} \equiv k(F_*) \quad \text{(Eq. 15)}$$

Life History Parameterization

Defining f and g in terms of the life history parameters of interest allows life history-tailored calculation of management benchmarks. These provide a framework for examining the differences between life history strategies and for testing the effects of scientific uncertainty in certain life history traits.

First, let $g(F) = \phi_F$, *fished* spawners-per-recruit, calculated similarly to ϕ_0 in Eq. 9 except with the addition of fishing mortality:

$$\phi_F = \rho \sum_{a=1}^{A-1} f_a \mu_a e^{-\sum_{j=1}^{a-1}(M_j + s_j F)} + \rho * f_A \mu_A \frac{e^{-\sum_{a=1}^{A-1}(M_a + s_a F)}}{1 - e^{-(M_A + s_A F)}} \quad \text{(Eq. 16)}$$

Next, let $f(S)$ (Eq. 13) be specified using the steepness parameterization of the Beverton-Holt recruitment curve (Eq. 8):

$$f(S_*) = \frac{0.8 R_0 h}{0.2\phi_0 R_0 (1-h) + (h - 0.2) S_*} = \frac{1}{\phi_F} \quad \text{(Eq. 17)}$$

Solving for S_* redefines Eq. 14:

$$S_* = \frac{0.8 R_0 h \phi_F - 0.2\phi_0 R_0 (1-h)}{h - 0.2} = \frac{4 R_0 h \phi_F - \phi_0 R_0 (1-h)}{5h - 1} \quad \text{(Eq. 18)}$$

Substituting Eq. 18 into Eq. 12a specifies the function $k(F)$ in Eq. 15:

$$R_* = S_* * \frac{1}{\phi_F} = \frac{4R_0 h\phi_F - \phi_0 R_0(1-h)}{(5h-1)\phi_F} \quad \text{(Eq. 19)}$$

Equilibrium recruitment and equilibrium spawners can likewise be used to calculate other equilibrium quantities, as well as the yield benchmark.

At equilibrium the population has reached a stable size, so $N_{y+1,a} = N_{y,a}$:

$$N_{*,a+1} = N_{*,a} e^{-M_a - s_a F_*} \quad \text{(Eq. 20)}$$

Finally, substituting Eq. 20 into Eq. 10 (catch), and both of these into Eq. 11 (yield) gives equilibrium yield Y_*:

$$Y_* = \sum_{a=1}^{A} \frac{w_a s_a F_*}{M_a + s_a F_*} N_{*,a}(1 - e^{-(M_a + s_a F_*)}) \quad \text{(Eq. 21)}$$

Maximizing this equilibrium yield is one method of estimating the maximum sustainable yield (MSY) so frequently invoked in fisheries management. Maximum Y_* will be taken to be the overfishing limit (OFL) benchmark for the remainder of this study.

III. Incorporating Recruitment Stochasticity

All equations reviewed to this point have been deterministic. In addition to simulating scientific uncertainty in life history parameters (elaborated on later), this study models the *process uncertainty*, or year-to-year natural variation, in the classically noisy spawner-recruitment relationship. It is common to incorporate this stochastically by assuming lognormal residual error between the expected and observed recruitment (Haddon 2001). This can be achieved by multiplying Eq. 9 by the error term e^{ε}:

$$R_{y+1} = \frac{0.8R_0 h S_y}{0.2\phi_0 R_0(1-h) + (h-0.2)S_y} * e^{\varepsilon} \quad \text{(Eq. 22)}$$

where $\varepsilon \sim N(0, \sigma^2)$.

However, adding lognormal error introduces the potential for large positive spikes in recruitment, which the estimate of equilibrium recruitment (R_*) in Eq. 19 does not take into account. To correct for this, equilibrium benchmark calculations can incorporate a bias correction parameter: $\varsigma = \exp(\sigma^2/2)$ (SEDAR 17). Bias-corrected R_* is shown below.

$$R_* = \frac{\varsigma * 4R_0 h\phi_F - \phi_0 R_0(1-h))}{(5h-1)\phi_F} \qquad \text{(Eq. 23)}$$

IV. Life History Parameterization

The following simulations compare the effects of P^*-based ABC control rules along a 3x3x3 factorial design. The first factor is stock life history strategy. Three stocks from the Southeastern United States representing divergent life history strategies were chosen as example stocks: vermilion snapper (South Atlantic), a periodic strategist; sandbar shark (highly migratory, but traveling through the South Atlantic), an equilibrium strategist; and gulf menhaden (Gulf of Mexico), a relatively opportunistic strategist. (For geographical consistency, Atlantic menhaden was originally a candidate for this study. However, its recruitment is no longer modeled according to the Beverton-Holt relationship (Eq. 8), precluding reasonable adaptation of its dynamics to a generalized model. It was exchanged for its more conventionally modeled southerly congeneric.)

While much of the life history information needed for these models is available in the literature, recruitment-related parameters must be estimated from the data through an assessment. Each of these stocks was previously assessed through the SEDAR process (Southeastern Data, Assessment, and Review), a three-step workshop series designed to increase participation and improve transparency in the assessment process (SEDAR 17 2008). First, the Data Workshop compiles and reviews fisheries landings data, independent survey data, and life history information. Next, the Assessment Workshop develops the assessment model, estimates parameters, and runs population projections. Finally, an independent Review Panel peer-reviews the assessment. The most recent SEDARs for the above stocks were SEDAR 17 in 2008 (vermilion), SEDAR 21 in 2011 (sandbar), and SEDAR 27 in 2011 (menhaden.) While the

following simulation study employs a model that is more simplistic and generalized than any of the individual SEDAR assessment models, it uses their life history parameter inputs, as well as the recruitment parameters estimated in these assessments.

Species Overview

Vermilion snapper (*Rhomboplites aurorubens*) is a medium-sized snapper (L_∞ = 506 mm) that inhabits the middle of the water column (to depths of 150m) (Martinez-Andrade 2003). Like all snappers, it matures quickly (by age 2) but is relatively long-lived (a_{max} = 19 years), with a low growth rate (κ = 0.12) and low natural mortality rate (M = 0.22). It has small eggs and high fecundity. It reproduces several times in a season, and year-to-year reproductive success is highly variable. Vermilion's long lifespan and high fecundity provide it repeated opportunities for reproductive success throughout its lifetime, and its ability to weather bad reproductive years and capitalize on good ones classifies it as a periodic strategist (Martinez-Andrade 2003).

Sandbar shark (*Carcharhinus plumbeus)* live even longer than vermilion (a_{max} = 27 years.) They too are slow-growing (κ = 0.12) and have a low natural mortality (M = 0.14). Unlike vermilion, however, they are very slow to mature, with 50% reaching maturity around age 13. They are much larger (L_∞ = 1812 mm). Sandbar invest heavily in individual offspring and have very few at one time (4-10). Their long lifespan, slow maturation rate, and heavy investment in offspring contribute toward relatively stable population dynamics, classifying sandbar as equilibrium strategists (King and MacFarlane 2003).

Gulf menhaden (*Brevoortia patronus*) are an extremely abundant, relatively fast-growing species (κ = 0.44). Like vermilion, they mature by age 2, produce high numbers of eggs, and spawn multiple times in a season. Unlike vermilion, they are planktivorous, have short life spans (a_{max} = 6 years) and very high natural mortality (M = 1.1). While menhaden do not provide a solid example of an opportunistic species—commercially exploited North American marine fishes are heavily skewed toward periodic lifestyles (Vila-Gispert et al. 2002)—they employ a sufficiently different strategy (low trophic level, quick life cycle, extremely high abundance) to provide an interesting contrast to both vermilion and sandbar.

Constant Parameters

The Data Workshop step of the SEDAR process reviews the literature, as well as previous assessments and expert opinion, to recommend values for key life history parameters. Table 1 reports the Von Bertalanffy growth parameters (L_∞, a_0, κ), length-weight relationships (α,β), sex ratio (ρ), and age-constant natural mortality (M) recommended by the Data Workshop and confirmed and utilized by the Assessment Workshop for each species. Also in Table 1 are maximum age modeled (a_{max}, or A in Eqs. 16, 19) and four quantities estimated by the assessment model, all pertaining to recruitment: steepness (h), virgin recruitment (R_0), recruitment variance (σ_S^2), and the bias correction (ς) calculated from the recruitment variance. (Note: As no constant M for sandbar was reported, the value in Table 1 was derived from the age-specific M_a (see below) by calculating the constant M results in the same survivorship to the maximum age.)

Age-Specific Parameters

The Data Workshop also provides values of the age-specific quantities introduced in Section I: maturity (μ_a), fecundity (f_a), and natural mortality (M_a) from the literature, and selectivity (s_a) from the fisheries data. Tables 2, 3, and 4 list the age-specific parameter vectors for vermilion, sandbar, and menhaden, respectively. If multiple gears or industries fish the same stock, the assessment may have applied more than one selectivity, but for simplicity this study chose either a single fishing gear's selectivity or, when provided, a weighted average of selectivities.

On Calculating Fecundity

Some calculations were required to obtain the fecundity vector for each species, but as these differed by stock, they are detailed below rather than summarized in Section I.

For menhaden, the Von Bertalanffy parameters in Table 1 estimate the *fork* length-at-age (FL_a), the length measured to the inside of the forked tail (Helfman et al. 2009.) The Data Workshop Report (DWR) cites a model by Lewis and Roithmayr (1981) that relates menhaden fork length to the mean number of eggs per female. Adapting their equation to age-specific fork length yields age-specific fecundity:

$$E_a = 0.0000516 * FL_a^{3.8775} \qquad \text{(Eq. 24)}$$

where E_a, the average number of eggs at age, is taken as f_a for menhaden.

For vermilion snapper, the Von Bertalanffy parameters estimate the *total* length-at-age (TL_a), the length measured to the outer tip of the forked tail (Helfman et al. 2009). But because the length-fecundity relationship, like that of menhaden, is based on the fork length, the total lengths-at-age must be converted to the fork lengths-at-age through a linear regression:

$$FL_a = 0.371 + 0.898 * TL_a \qquad \text{(Eq. 25)}$$

The batch fecundity can then be estimated through a relationship given by Cuellar et al. (1996):

$$BF_a = 0.0438 * FL_a^{2.508} \qquad \text{(Eq. 26)}$$

The average eggs per female at age (E_a) can then be calculated by multiplying this batch fecundity by the average number of batches in a year:

$$E_a = 31 * BF_a \qquad \text{(Eq. 27)}$$

where 31 is the average number of batches in a season used in the base case of the assessment model (pers. com. Kyle Shertzer) Again, E_a is taken as f_a for vermilion.

The fecundity-at-age vector for sharks differs from those of vermilion and menhaden because in that it requires an extra consideration. Sharks, unlike the finfish, have very low fecundity, which is neither directly related to biomass, nor allometrically related to length. SEDAR 21 provides a vector of the number of pups per litter. Furthermore, females do not reproduce every year, but rather every 2-3 years, so the number of pups/litter at age is divided by 2.5 to give a vector of average yearly pup production that can be used analogously to vermilion's and menhaden's f_a's.

On Rescaling Natural Mortality

The age-specific natural mortality vectors M_a reported in the SEDARs were derived according to the relationships of Chen and Watanabe (1989) (for sandbar) or Lorenzen (1989) (for vermilion

and menhaden), but then subsequently scaled to match constant M estimates derived from other methods. Because the ability to rescale this mortality curve is key to this project (see Section VII), the species-specific methods used are reviewed below.

The vermilion SEDAR describes a method of rescaling based on matching survivorship to the final age class. Survivorship to a particular age, S_a, is the product of survival rates (e^{-Z}) to all of the preceding ages. In the absence of fishing, survivorship to the last age (S_A) is calculated as

$$S_A = \prod_{a=1}^{A} e^{M_a} = e^{\sum_{a=1}^{A} M_a} \quad \text{(Eq. 28)}$$

If M is constant across ages, the survivorship equation (denoted S_A^c) simplifies to:

$$S_A^c = e^{\sum_{a=1}^{A} M} = e^{A*M} \quad \text{(Eq. 29)}$$

S_A can be scaled to equal S_A^c by multiplying the exponent (the summed mortality) by a scalar, θ. Let

$$e^{\theta * \sum_{a=1}^{A} M_a} = e^{AM} \quad \text{(Eq. 30)}$$

Then

$$\theta = \frac{AM}{\sum_{a=1}^{A} M_a} \quad \text{(Eq. 31)}$$

Thus multiplying the full M_a vector by θ rescales natural mortality.

For sharks, the SEDAR reported only an age-specific M_a, so the constant value listed in Table 1 was calculated by setting $S_A^c = S_A$, which leads to M equaling the average of all M_a:

$$M = \frac{\sum_{a=1}^{A} M_a}{A} \quad \text{(Eq. 32)}$$

For menhaden, the reported M_a was already scaled so that mortality age at 2 equaled the constant M estimated from a tagging study. Thus, to rescale menhaden M_a, it is sufficient to apply the ratio of $\theta = M_{new} / M$.

Recruitment Variation in Sharks

Typical of marine fish stocks, vermilion and menhaden have high year-to-year recruitment variation, so their recruitment relationships can be modeled with lognormal error as in Eq. 22. Sharks, however, as equilibrium strategists, have much more predictable recruitment that does not vary lognormally. Here, to include some degree of stochasticity in the recruitment function, the length of the reproductive cycle (used to calculate f_a) is allowed to vary on a yearly basis according to a normal distribution centered around 2.5 years. This models the uncertainty in the f_a vector, not in the strength of the spawner-recruitment relationship itself.

V. Simulations I: Simulating Uncertainty

The equilibrium calculations outlined in part II can be used to obtain point estimates for OFL and other management reference points. But the ABC control rules simulated in this study require estimates of the uncertainty surrounding those values, best characterized by probability distribution functions, or pdfs. The degree of this uncertainty provides the second factor of this study's experimental design.

As benchmark point estimates are derived entirely from life history parameters (and the assumption of equilibrium), they themselves cannot explicitly incorporate the process uncertainty, measurement uncertainty, or model uncertainty that stem from incorporating real-world data sets or making model decisions. However, highlighting the parameter uncertainty in two key life history traits introduced in the last section—steepness and natural mortality—serves here to simulate scientific uncertainty around the OFL estimate.

Uncertainty in Steepness and Natural Mortality

Both steepness and natural mortality are notoriously difficult to estimate (Conn et al. 2010, Shertzer and Conn 2012). In the case of steepness, high intrinsic variability and measurement

uncertainty in the estimated spawner-recruit values often obscure a causal relation. Steepness describes the behavior of this curve at the lower extreme, but frequently the data do not span a sufficient range of stock sizes to inform its estimation (Rose et al. 2001). Added to these challenges is the possibility that the spawner-recruitment relationship may change over time, perhaps in response to fishing pressure (Shertzer et al. 2008).

Natural mortality can be directly estimated through tagging studies, but the open models often required of unbounded ocean ecosystems require large numbers of returned tags to perform well (Pine et al. 2003). Instead, it is more common to estimate M indirectly through correlative relationships with more measurable life history traits, such as the growth parameters (Pauly 1979) or longevity (Hoenig 1983). While it is acknowledged that all of these methods have limitations (Vetter 1988), M is generally fixed in stock assessments to allow estimation of other parameters.

As the values of each of these parameters significantly influence management benchmarks, they provide interesting sources of scientific uncertainty to investigate.

Creating Distributions from Ranges

None of the SEDARs from which the species' life history parameters are drawn provide pdfs for either steepness or natural mortality. The assessments' sensitivity analyses, however, provide low and high values that can serve as endpoints of relevant intervals. As age-specific M vectors are either related or relatable to a constant M through some method of scaling (Eq. 31), uncertainty is considered only for age-constant M.

In the following study, these point estimates and corresponding ranges (listed in Table 5) are used to construct bounded normal distributions, which weight the assessments' base case estimates more heavily than the values drawn from sensitivity analyses. The standard deviations for h and M, denoted σ_h and σ_M, respectively, are chosen such that ~95% of values sampled from these distributions will fall within the original range. More precisely, they can be calculated from the central point estimate and one endpoint of the range as follows:

$$\sigma_h = \frac{h - h_{low}}{1.96} \quad \text{(Eq. 33a)}$$

$$\sigma_M = \frac{M - M_{low}}{1.96} \quad \text{(Eq. 33b)}$$

In this way, $h \sim N(h, \sigma_h^2)$, $h_{\text{low}} \leq h \leq h_{\text{high}}$, and $M \sim N(M, \sigma_M^2)$, $M_{\text{low}} \leq M \leq M_{\text{high}}$.

The above bounded distributions are considered the "base case uncertainties" in the following analysis. To test the effects of degree of uncertainty, additional distributions were created for each species using larger or smaller coefficients of variation (CV) for each parameter.

$$\sigma_h = h * CV_h \quad \text{(Eq. 34a)}$$

$$\sigma_M = M * CV_M \quad \text{(Eq. 34b)}$$

Thus, a total of nine uncertainty "schemes" (base, high, and low for each of the three species) were constructed for use in the simulations. High and low CV values differed by species and are described below in Section VI.

Sampling and Rescaling

The following sampling and calculations were executed using a program written in the statistical computing language R (R Development Core Team 2010). Each pair of h and M parameter distributions described above were sampled 5000 times, generating 5000 sets of population parameters ("populations" hereafter.) For each population, the sample M was used to rescale the age-specific natural mortality vector (Eqs. 30-33), and that rescaled vector was used to recalculate ϕ_0 (Eq. 9).

Next, spawning stock benchmarks were calculated for a sequence of possible F values (at step size 0.01 for vermilion snapper and gulf menhaden, and 0.001 for sandbar shark). For each trial value of F, the program calculated ϕ_F (Eq. 16), bias-corrected R_* (Eq. 23), $N_{*,a}$ (Eq. 20), SSB_* (using $N_{*,a}$, Eq. 5, and Eq. 6b), and Y_* (Eq. 21). At the end of the loop, the F that produced the greatest Y_* was taken to be F_{MSY}, and all equilibrium quantities corresponding to this F_{MSY} were

stored as the "equilibrium benchmarks." In this way, the program constructed sample distributions of maximum Y_* (to be used as OFL) and of the corresponding F_{MSY} and SSB_{MSY}.

VI. Species-Specific Parameter Distributions

The species-specific application of the general methods described in Section V are detailed below.

Vermilion Snapper

The base case distributions for h and M for vermilion were constructed to fall within the ranges listed in Table 5. Because the tested range for steepness was asymmetric (0.47-0.73, surrounding h=0.56), the standard deviation calculation described in Eq. 33a was modified using average distance from the central estimate to each endpoint:

$$\sigma_h = \frac{h_{up} - h_{low}}{2 * 1.96} \qquad \text{(Eq. 37)}$$

According to Eq. 34a, the resulting distribution had a CV_h of ~12%. The range for natural mortality was symmetric (M = 0.22 ± 0.04), so Eq. 33b was appropriate to calculate its standard deviation, σ_M, and Eq. 34b its CV_M of ~14%. Test distributions for each parameter were constructed by sampling the corresponding normal distributions 5000 times, redrawing the samples that fell outside the listed range. The final base case distributions were thus truncated normal distributions.

Wider and narrower distributions of h and M, used to construct wider and narrower distributions of OFL, were both created assuming normal distributions and, for simplicity, equal coefficients of variation: CVs of 8% for the narrow distributions ("low uncertainty") and CVs of 20% for the wider distributions ("high uncertainty".) The high uncertainty scenario relaxed the bounds for both h and M, leaving only a logical upper bound of 0.95 for h.

Sandbar Shark

The reported *h* and *M* parameters for sandbar were estimated more precisely than those of vermilion. Like vermilion, the range provided for *h* was also asymmetric (0.25-0.40, surrounding *h*=0.29). However, the lower bound was so close to the central estimate that the above modification (Eq. 37) would result in an undesirable shift of the distribution's median away from the original *h*. Therefore, the distribution for *h* followed the original Eq. 33a, simply subject to uneven bounds. The resulting CV_h was ~7%. Similarly, the range listed for natural mortality (0.12-0.15, surrounding *M*=0.14) was assumed symmetric, and the resulting approximately normal distribution had a CV_M of ~5%. Test distributions were sampled and re-sampled as described above.

Again, for simplicity, identical CVs were used for the artificially widened and narrowed parameter distributions: a CV of 3% for the "low uncertainty" scenario, and a CV of 10% for the "high uncertainty" scenario. The bounds were relaxed for the wide distribution.

Gulf Menhaden

Each of the reported ranges for menhaden's *h* and *M* were approximately symmetric and suitable for assuming (bounded) normal distributions, but differed in relative precision. The range for steepness (0.45-0.97, surrounding *h*=0.69) resulted in a distribution with a CV of ~17%. The range for natural mortality was notably smaller (0.91-1.27, surrounding *M*=1.10) and resulted in a distribution with a CV of only ~8%.

Because of this difference, assigning the same increased or diminished CV to both *h* and *M* for menhaden would over- or under-emphasize the uncertainty in one of the parameters. Therefore the sizes of the normal distributions assumed for these parameters were modified independently. The "low uncertainty" scenario assigned a CV of 10% for steepness and a CV of 5% for natural mortality, while the "high uncertainty" scenario assigned CVs of 20% and 12%, respectively.

VII. Simulations II: Simulating *P** Control Rules

A second program, also carried out in R, introduced the final experimental factor: the level of allowable risk, *P**, chosen for setting the ABC harvest control rules. Three levels of *P** were tested for each of the nine OFL distributions: P*=0.5, representing no buffer against uncertainty; P*=0.3, representing an intermediate buffer; and P*=0.1, representing an extremely cautious buffer. This created a total of 27 scenarios.

The following simulations consider scenarios in which neither the scientists nor the managers knew the true value of the stock's life history parameters. The scientists were able to estimate the stock's OFL with that scenario's level of uncertainty. The managers then chose a *P** level, which represented the risk they were willing to take in following the catch recommendation. Once the managers made this decision, the scientists calculated ABC as a function of their OFL distribution and the managers' *P**:

$$ABC = f(pdf(OFL), P^*) \qquad \text{(Eq. 35)}$$

where *P** denotes the percentile of the OFL distribution at which the value of ABC is located.

Next, the managers gave the fishers permission to catch ABC. In order to focus only on the effects of scientific uncertainty, these scenarios ignore management uncertainty, assuming instead that a) the managers did not further reduce the catch quota to an annual catch target (ACT, where ACT < ABC), and b) fishermen could catch *exactly* the allowed amount (which, in reality, is impossible.)

Once the ABC control rule was set, the program simulated the possible outcomes of this scenario by generating 5000 sets of parameters that *could* have been the stock's true values. These were pulled from the same uncertainty scheme as that scenario's OFL distribution so that each population's true OFL actually lay within the scenario's distribution. The program then projected the consequences of the fishers' (unrealistically precise) fishing for each sample population. Below, the calculations for each sampled population are outlined.

Initialization

While the simulated scientists and managers remained unaware of the stock's true OFL, the program did not. For each sample population, equilibrium benchmark calculations were conducted as in the previous section (Section V).

Initially, each population was started at its own equilibrium numbers-at-age, $N_{*,a}$, which determined its initial biomass-at-age, $B_{1,a}$ and spawning stock biomass, SSB_1. Then, as before, the program rescaled M_a and recalculated the ϕ_0 parameter. It soon became obvious that stochastic recruitment plays a major role in determining the effects of P^*-based ABC control rules. When simulations started at an exact population size, these effects were not visible until several years into the experiment, when the first cohort of stochastic recruits matured (entered the spawning stock biomass) and became susceptible to fishing mortality.

Instating an initialization period removed this deterministic "lag." During this period, sample populations, subject to stochastic recruitment, were fished at constant fishing mortality rates equal to their own values of F_{MSY} for a number of years sufficient for the first randomized cohort to be reflected in both SSB and catch.

The length of the initialization period depended on the slower of each species' maturity and selectivity rates. Vermilion snapper require about two years to mature and three years to begin to be selected. Therefore, vermilion initialized for four years. Sandbar shark, by the far the slowest-growing species, require 19 years to reach (98%) maturity and 12 years to reach (98%) selectivity. Sandbar were initialized for 20 years. Finally, menhaden require exactly two years to mature and two years to become fully selected, so they were initialized for three years.

Fishing

Once the fishing experiment began, the program feigned ignorance at the population's true properties and fished it according to the single ABC control rule. Simulated fishing started on initialized populations in year 5 for vermilion, year 21 for sandbar, and year 4 for menhaden. Vermilion were experimentally fished for six years, sandbar for ten, and menhaden for seven.

The Baranov catch equation (Eq. 10) requires the value of F_y to calculate that year's catch-at-age. However, the ABC control rule regulates yield (Eq. 11), not fishing mortality rate. Therefore, to determine the fishing mortality rate needed to catch ABC, the program used the R function nlminb (Bates and Sarkar 2010) to optimize F by the least squares method, i.e., by minimizing the squared difference between yield and ABC. (F was bounded between 0 and 30.) The optimized F was used as F_1 and applied to catch equation to determine catch-at-age and yield for the first year.

Yearly Calculations

The program projected the populations through subsequent years by entering them into a yearly loop of calculations. First, it was assumed that fish had a chance to spawn before they were caught, so recruitment was calculated from the previous year's spawning stock biomass, SSB_{y-1}. This recruitment incorporated yearly process error, e^{ε}, (as in Eq. 22) by drawing a random error $\varepsilon \sim N(0,\sigma_S^2)$, where σ_S^2 is species-specific recruitment variance. Next, numbers-at-age for ages 1+ were calculated using the previous year's fishing mortality rate, F_{y-1} (Eqs. 2a,b). Numbers-at-age were converted to biomass-at-age (Eq. 5). Then total biomass, B_y, total numbers, N_y, spawning stock biomass, SSB_y, and spawner number, S_y, were calculated.

Before fishing started at the end of year y, the program checked the biomass level. If too little biomass remained to remove ABC, the program stopped fishing this population for the rest of the time; the population had "crashed." Otherwise, the program simulated fishing by once again optimizing the yield equation to determine F_y and then calculating catch-at-age and yield for that year.

VIII. Analysis: Monitoring Performance Measures

The effects of each of the three experimental factors (life history strategy, level of uncertainty in the OFL distribution, and allowable risk level P^*) on the results of management according to P^* control rules were monitored according to two metrics for judging stock status that are fundamental to marine fisheries management: fishing mortality rate, relative to a mortality threshold, and biomass (here, *SSB*) relative to a biomass threshold.

The first metric is based on the magnitude of the current fishing mortality rate, F, relative to a population's threshold fishing mortality, F_{limit} (here, $F_{limit} = F_{MSY}$.) The following simulations optimized F each year to catch ABC—the lower a population's *SSB*, the greater the fishing pressure required to land the same catch. If a population fell below its SSB_{MSY}, and the scenario's ABC was greater than (or equal to) that population's OFL, the program needed to apply $F > F_{MSY}$ to maintain ABC. However, the addition of a strong year class of recruits to the fishery could boost *SSB* sufficiently for F to fall back below F_{MSY}.

Overfishing, then, is generally defined as $F > F_{MSY}$. For management purposes, however, the allowable risk of overfishing, P^*, is defined as the probability that ABC exceeds a population's true OFL, a definition that uses catch rather than fishing mortality. Whether catching ABC > OFL_{true} actually leads to overfishing depends on the stock's biomass level. Thus P^* can be interpreted as a *prediction* of the probability that overfishing occurs as a result of meeting the catch quota. The accuracy with which a P^* predicts the risk of overfishing can then be judged by comparing it to the observed $Pr(F > F_{MSY})$. This observed probability of overfishing is measured as the proportion of simulated populations experiencing overfishing at each time step. Then the proportion of populations that experience overfishing at least once by that year describes the cumulative risk of overfishing in time.

The second metric is based on the size of the current biomass (or spawning stock biomass) relative to a population's threshold biomass. In practice, managers set this threshold to some value below SSB_{MSY} to allow for inherent variation in stock size. For the purposes of

understanding this experimental system, however, a more strict definition of overfished ($SSB < SSB_{MSY}$) was used to track population stock status relative to the starting point.

Recruitment variation during the initialization period caused some proportion of the samples populations in each scenario to drop below their individual values of SSB_{MSY} by the starting year of the experiment. Once the experiment began, populations with true OFLs less than the scenario's ABC were expected to decrease in biomass over time as they were continually fished at rates they could not sustain. The probability of a population becoming overfished due to the ABC control rules' implementation was not observable until the second year of the experiment, because each year's *SSB* depended on the previous year's fishing mortality rate. Like the overfishing trends, trends in the probability of becoming overfished were tracked as both percentages overfished at each time step and cumulative percentages overfished in at least one year of the experiment.

Results

I. Benchmark Analysis and Population Initialization

For each species, a set of benchmarks was calculated using the constant base case parameter values. Parameters *h* and *M* were allowed to vary according to the distributions described in the methods. These distributions were input into the first simulation program (Methods Section V) to construct three OFL distributions, from which values of ABC were calculated at three test levels of *P**. The sample populations for each species' nine scenarios were then initialized using the second simulation program (Methods Section VII) before the start of the true experiment. The initialization step started populations at SSB_{MSY} but simulated yearly recruitment variability, which inevitably let some population biomasses fall and lose the ability to withstand constant F_{MSY}. Thus some percentage of each scenario's populations became overfished even before the experiment began. The results of these set-up processes are summarized below.

Vermilion Snapper

The base case benchmarks for vermilion (calculated from constant *h* and *M* values) were $F_{MSY} = 0.38$, $SSB_{MSY} = 2.24 \times 10^6$ kg, and OFL (MSY) = 5.02×10^5 kg. Figure 2.1 shows the three OFL distributions constructed for vermilion scenarios. The ABC values for vermilion, calculated from each OFL distribution for *P**=0.1, 0.3, and 0.5, ranged from $3.91 \times 10^5 – 5.07 \times 10^5$ kg (Table 6.) Following initialization, ~60% of vermilion populations in each scenario began the experiment overfished (mean = 59.83%, s.d. = 0.80).

Sandbar Shark

The base case benchmarks for sandbar were $F_{MSY} = 0.02$, $SSB_{MSY} = 9.22 \times 10^6$ kg, and OFL (MSY) = 5.62×10^5 kg. Figure 2.2 shows the three OFL distributions constructed for the sandbar shark scenarios. Sandbar ABC values ranged from $3.32 \times 10^5 – 5.66 \times 10^5$ kg and are shown in Table 7. Following initialization, ~15% of sandbar populations in each scenario began the experiment overfished (mean = 14.59%, s.d. = 0.32).

Gulf Menhaden

The base case benchmarks for menhaden were F_{MSY} = 1.23, SSB_{MSY} = 5.28 x 10^8 kg, and OFL (MSY) = 1.18 x 10^9 kg. Figure 2.3 shows the three OFL distributions constructed for the gulf menhaden scenarios. Menhaden, famously abundant, had ABC values several orders of magnitude larger than those of vermilion and sandbar, ranging from 7.00 x 10^8 – 1.19 x 10^9 kg (Table 8). Following initialization, ~50% of menhaden populations in each scenario began the experiment overfished (mean=49.14%, s.d.=0.67).

II. Probabilistic Risk of Overfishing

As described in the Methods (Section VIII), because removing ABC > OFL_{true} does not necessarily lead to overfishing, *P** is best interpreted as the *expected* probabilistic risk of overfishing. These simulation studies estimate the *observed* probabilistic risk of overfishing by tracking the percentages (of 5000 sample populations) that truly experience overfishing. The resulting discrepancies between the expected and observed risks differed across life history types, across levels of uncertainty, and even across levels of expected risk.

Vermilion Snapper

Figure 2.4 shows the percentage of vermilion snapper populations in each scenario that experienced overfishing in the first year of the control rule's implementation. In every scenario, *P** underestimated this percentage. At *P**=0.1 and *P**=0.3 expected risk levels, the observed percentage overfishing was greatest for the lowest uncertainty and least for the highest uncertainty. (At *P**=0.5 these percentages were very close, and that of the highest uncertainty surpassed that of the lowest by less than a percentage point.) The reasons behind these seemingly paradoxical trends will be addressed later. The differences also varied among risk levels: the observed percent exceeded *P**=0.5 by ~4-7%, *P**=0.3 by ~9-13%, and *P**=0.1 by ~10-20% (Table 9).

Sandbar Shark

Figure 2.5 shows the percentage of sandbar shark populations in each scenario that experienced overfishing in the first year of the control rule's implementation. In each of the sandbar

scenarios, P^* slightly overestimated this percentage. Like vermilion, the differences between P^* and the observed percentage were greatest for scenarios with low uncertainty. Opposite from vermilion, however, the differences were greater for larger P^* values (P^*=0.5: ~3-8%, P^*=0.3: ~2-6%, and P^*=0.1: < 1-3%) (Table 10). Overall, the differences between P^* and the observed percentage were of a much smaller magnitude than were those for vermilion.

Gulf Menhaden

Figure 2.6 shows the percentage of gulf menhaden populations in each scenario that experienced overfishing in the first year of the control rule's implementation. In each of these scenarios, P^* predicted almost exactly the percentage of populations that would undergo overfishing the first year. P^*=0.5 slightly (almost negligibly) overestimated these values, P^*=0.1 slightly underestimated them, and P^*=0.3 varied in the direction of error, but these differences were always less than 2% in either direction (Table 11).

Analysis

In this study, all OFL benchmarks are based on the assumption of equilibrium conditions. Indeed, if all stocks started at equilibrium *SSB*, the observed percentages of populations overfishing would equal the expected (P^*). However, randomized starting points resulting from the initialization process provide opportunities for these percentages to deviate.

How can these deviations be explained? It helps to recognize that the simulation output—the observed probability of overfishing occurring—is in fact a combination of probabilities of several different conditions occurring together. It is possible, and useful, to identify the conditions these component probabilities represent, even without explicitly measuring their values. The experimental factors may affect these individual components independently.

These conditions can be identified through informal deductive reasoning. A starting place would be to divide the populations into two cases: populations starting the year below SSB_{MSY} ("overfished") and populations starting the year at or above SSB_{MSY} ("non-overfished"). Then for each case, it is possible to trace along a pathway the additional conditions necessary for a catch level to lead to overfishing. Labeling the probabilities of these conditions will aid in describing

the influences of various experimental factors on the probabilistic risks associated with P^*-based management.

Determining Drivers of Probabilistic Risk

As stated above, if all populations started the experiment at their own SSB_{MSY}, then P^* = Pr(ABC > OFL) would exactly predict the proportion that experience overfishing as a result of the control rule's implementation (see Flow Chart 1, Figure 2.7). To describe this mathematically, let $\boldsymbol{E}$ be the percentage of populations expected to undergo overfishing, and $\boldsymbol{O}$ be the percentage of populations observed as undergoing overfishing. Then for the deterministic starting point case,

$$\boldsymbol{E} = \boldsymbol{O} = P^* \qquad \text{(Eq. R1)}$$

In this study, however, the populations were initialized first, with the result that some proportion (α) began the experiment already overfished (i.e. $SSB < SSB_{MSY}$). The remaining proportion (1 – α) were categorized as "non-overfished" (i.e. $SSB \geq SSB_{MSY}$). Because the initialization period randomly determines which populations start above SSB_{MSY} and which start below, P^* predicts both the percentages of overfished ($\boldsymbol{E}_{Over}$) and of non-overfished populations ($\boldsymbol{E}_{Non}$) that will experience overfishing in the first year of the experiment as a result of the control rule:

$$\boldsymbol{E} = \boldsymbol{E}_{Over} + \boldsymbol{E}_{Non} = \alpha P^* + (1-\alpha)P^* = P^* \qquad \text{(Eq. R2)}$$

However, whether harvesting ABC > OFL_{true} truly leads to overfishing ($F > F_{MSY}$) depends on two factors: 1) where the population's SSB currently lies relative to SSB_{MSY}; and 2) the extent by which ABC exceeds the population's OFL_{true}. Populations that are *not* already overfished may not require overfishing even to catch ABC > OFL_{true} if the biomass surplus is sufficiently high ($SSB >> SSB_{MSY}$) or the excess catch is not too great (i.e., (ABC – OFL_{true}) is small.) The phenomenon of populations meeting one of these criteria is termed "unexpected underfishing." Flow Chart 2A illustrates the possible outcomes for relative fishing mortality rate for non-overfished populations (Figure 2.8).

Thus the observed percentage of non-overfished populations undergoing overfishing as a result of the control rule, termed $\boldsymbol{O}_{\text{Non}}$, will be

$$\boldsymbol{O}_{\text{Non}} = P^* - \gamma P^* \qquad \text{(Eq. R3)}$$

where γ denotes the probability of "unexpected underfishing" and $-(1-\alpha)\gamma P^*$ represents a potential decrease to the *total* observed percentage overfishing, $\boldsymbol{O}$ (see Eq. 5).

Similarly, whether harvesting ABC < OFL_{true} truly *avoids* overfishing ($F > F_{\text{MSY}}$) depends on two factors: 1) where the population's *SSB* currently lies relative to SSB_{MSY}; and 2) the extent by which ABC undershoots the population's OFL_{true}. Already overfished populations may require overfishing to yield even ABC < OFL_{true} if the *SSB* is sufficiently low ($SSB << SSB_{\text{MSY}}$) or if the difference (OFL_{true} – ABC) is sufficiently small. The phenomenon of populations meeting one of these criteria is termed "unexpected overfishing." Flow Chart 2B illustrates the possible outcomes for relative fishing mortality rate for already-overfished populations (Figure 2.9).

Thus the observed percentage of already-overfished undergoing overfishing as a result of the control rule, $\boldsymbol{O}_{\text{Over}}$, will be

$$\boldsymbol{O}_{\text{Over}} = P^* + \beta(1 - P^*) \qquad \text{(Eq. R4)}$$

where β denotes the probability of "unexpected overfishing" and $\alpha\beta(1 - P^*)$ represents a potential increase to the *total* observed percentage overfishing, $\boldsymbol{O}$ (see Eq. 5).

The total percentage of all populations that experience overfishing as a result of the control rule, *O*, combines Eq. R3 and Eq. R4, scaling them by the probability of starting overfished (α) or of starting at or above SSB_{MSY}, "non-overfished," $(1 - \alpha)$.

$$\boldsymbol{O} = \alpha\boldsymbol{O}_{\text{Over}} + (1 - \alpha)\boldsymbol{O}_{\text{Non}}$$
$$\boldsymbol{O} = \alpha P^* + \beta\alpha(1 - P^*) + (1 - \alpha)P^* - \gamma(1 - \alpha)P^* \qquad \text{(Eq. R5)}$$

The net effect of the positive β-term and the negative γ-term determines whether P^* over- or underestimates the percentage of populations undergoing overfishing the first year of the experiment. It must be stressed that $\boldsymbol{E}$ and $\boldsymbol{O}$, from Eqs. R2 and R5, describe the expected and observed proportions overfishing *for the first year only*. After the first year, overfishing still occurs according to the mechanisms outlined above and illustrated in the flow chart. However, the assumptions that the Pr(ABC > OFL) for non-overfished populations (called P_{Non} for subsequent years) equals Pr(ABC > OFL) for overfished populations (analogously, P_{Over}), and that $P_{Non} = P_{Over} = P^*$, no longer hold. Rather, P_{Non} decreases in time, and P_{Over} increases, as fishing rules sort populations into overfished/non-overfished categories more deterministically.

Interpreting the Drivers of Probabilistic Risk

Equation R5 expresses the observed percentage overfishing in terms of four variables (α, β, γ, and P^*) that represent probabilities of individual conditions. The relative values of these variables must drive the patterns observed in the probabilistic risk of overfishing for each species. As these patterns existed among species, level of uncertainty, and level of expected risk P^*, it is likely that these experimental factors affect the probabilities of the conditions that lead to overfishing.

Effects of Life History Strategy

The value of the first of these variables, α, the proportion of populations already overfished, differs widely among life histories, due to differences in species-specific recruitment stochasticity (Section I). This variable can have a strong influence on the total observed percentage, $\boldsymbol{O}$, because it occurs in every term (Eq. 5). Vermilion snapper's relatively large α values (~0.60) heavily weighted the β-term (unexpected overfishing), driving up the rates of overfishing with the result that the values of P^* consistently underestimated $\boldsymbol{O}$ ($\boldsymbol{E} < \boldsymbol{O}$) (Figure 2.4). Meanwhile, sandbar's low α values (~0.15) heavily weighted the γ-term (via the (1 – α) multiplier), driving down the rates of overfishing with the result that values of P^* *over*estimated $\boldsymbol{O}$ ($\boldsymbol{E} > \boldsymbol{O}$) (Figure 2.5). Menhaden's α values were nearly 0.50, so it is not surprising that the β- and γ-terms for menhaden largely balanced each other out, allowing $\boldsymbol{E}$ to predict $\boldsymbol{O}$ very closely (Figure 2.6).

Effects of Level of Uncertainty

The second factor, level of uncertainty, seems to influence the values of β or γ themselves. Parameters β and γ describe unexpected overfishing or unexpected overfishing, respectively—the probabilities that a relative catch level will *not* lead to its expected relative fishing mortality rate (Eq. 5). These unexpected outcomes can occur when the distance between OFL_{true} and ABC is small, and potentially overridden by the current status of the biomass. For example, an ABC that only slightly exceeds a population's OFL_{true} will not cause overfishing if that population has surplus biomass. The probability of this distance being small increases when the range of possible OFL_{true} is restricted (i.e., narrow.) Thus, a lower uncertainty level increases β or γ, magnifying the net effect of the β or γ term. For vermilion, this increased magnitude meant that lower uncertainty levels led to greater underestimation of $\boldsymbol{O}$ by P^* (Figure 2.4); for sharks it meant greater overestimation (Figure 2.5).

Effects of P* *value*

Finally, the value of P^* itself directly affects the percentages overfishing (Eq. R5), and the degree by which P^* under- or overestimates $\boldsymbol{O}$. Overestimation ($\boldsymbol{E} > \boldsymbol{O}$) was greatest for P^*=0.5 because the γ-term is related to P^* directly; underestimation ($\boldsymbol{E} < \boldsymbol{O}$) was greatest at P^*=0.1 because the β-term is related to P^* inversely (Figures 2.4-2.6).

III. Probabilistic Risk Increases in Time

The previous section analyzed the immediate accuracy of the P^* control rule. However, with each subsequent year, the risk of overfishing *in at least one year* increases at rates that differ among scenarios, particularly among species. As this is an important performance measure for managers, the simulation study tracks this risk as the *cumulative* observed probability of overfishing.

For purposes of understanding the model dynamics, it also helps to keep track of the *current* observed probabilities of overfishing each year. Each year's percentage of sample populations experiencing overfishing can be represented by an additional application of the probabilities outlined in Flow Charts 2A-2B (Figures 2.8-2.9). If the current percentage remains steady in

time, or even declines, while the cumulative percentage climbs, this is an indication of *turnover*; new populations become subject to overfishing while others return to lower levels of fishing mortality.

Vermilion Snapper

Figure 2.10 traces the current percentages (bold lines) and cumulative percentages (faint lines) of populations experiencing overfishing for each of the nine vermilion snapper scenarios, grouped by P^*. The pattern of probabilistic risks observed in the first year of the control rule implementation (Section II) set the stage for subsequent years, whether measured as current or as cumulative percentages of populations overfishing. For $P^*=0.5$, the trajectories of these percentages nearly converged, changing the precise order among levels of uncertainty but not by much.

For vermilion populations, the probabilistic risks of overfishing in at least one year increase steeply in time for all levels of uncertainty and all levels of P^*. Meanwhile, the current percentages of overfishing increase initially, then tend to flatten out after the second year of the experiment, or even decline slightly. This divergence of trajectories indicates relatively high turnover of the populations that are experiencing overfishing at a given time. This high turnover is likely related to vermilion snapper's high recruitment variability.

Sandbar Shark

In contrast to those of vermilion snapper, the probabilities of overfishing sandbar sharks remain relatively constant in time. Bold trajectories in Figure 2.11 show that percentages of populations currently undergoing overfishing actually declined slightly in time, which represents a small amount of recovery. The greatest relative declines occurred for the low uncertainty scenarios and for scenarios with $P^*=0.5$.

That the faint lines in Figure 2.11, the cumulative probabilities of overfishing, almost all stay constant at the first year's value indicates that there is little to no turnover of overfishing shark populations. Thus the first year's control rule determines almost immediately which populations

will experience overfishing and which will not, and the low recruitment stochasticity provides little opportunity for this to change.

Gulf Menhaden

The bold trajectories in Figure 2.12 show the percentage of menhaden populations currently undergoing overfishing in each year. These percentages started almost exactly at P^* and remained there for most of the experiment, dropping in later years for higher P^* and higher uncertainty. Unlike the sandbar trajectories, the cumulative probabilities of overfishing increased even as the current probabilities stayed constant, indicating turnover in populations experiencing overfishing. This increase occurred more slowly than that of vermilion, however. This intermediate increase in probabilistic risk corresponds loosely to menhaden's intermediate recruitment variability.

Analysis

Assuming independence among years, the theoretical probability of overfishing occurring at least once in a sequence of n years under a given P^* is equal to:

$$P_n = 1 - (1 - P^*)^n \qquad \text{(Eq. R6)}$$

The theoretical trajectories of P_n are nearly linear for lower P^* values, and increase in concavity with higher P^* values. However, none of the observed trajectories of P_n match the magnitude of those predicted. Rather, the observed increases are much lower, and they differ even at equal P^* levels. The greatest contrast in rates of increasing probabilistic risk was visible among species, rather than among levels of uncertainty surrounding the OFL estimate. Figure 2.13 compares these increases for the four years following the initial control rule implementation, averaging across levels of uncertainty and grouping by level of P^*.

That these percentages are lower is unsurprising. The benefit of the simulation study is that it takes the previous year's conditions into account as it simulates the current year's risk, removing the need to assume independence among years. The explanatory model in Section II shows that the probability of experiencing overfishing is dependent on the stock status at the start of the

year, which is influenced by the fishing mortality rate the previous year. High recruitment stochasticity increases the variability in spawning stock biomass, which creates greater opportunities for changes in stock status, increasing the (relative) independence among years. Thus the example species with the highest recruitment variability, vermilion snapper, sees the highest turnover and highest increase in probabilistic risk. Those trends are followed by gulf menhaden, the example species with intermediate recruitment variability. Finally, sandbar shark, with the lowest recruitment variability, sees little turnover and no increase in cumulative risk. The connections between recruitment stochasticity and stock status will be explored further in the following section.

IV. Comprehensive Risk: Consequences to the Natural Resource

Sections II-III examined the simulation results pertaining to "probabilistic risk" of overfishing, both as an immediate result of *P**-based management (Section I) and in subsequent years under the same control rule (Section II). But this simulation study also provides predictions of additional consequences of overfishing, whose probabilities are termed here "comprehensive risk."

This comprehensive risk can be monitored through some of the management performance measures introduced in Chapter 1. The nature of this study precludes interesting comparisons of yield loss or catch variability, as the experimental design maintains yearly catch exactly equal to ABC as long as possible. However, the simulations are useful for examining the risk of the fish stock's biomass falling below a certain threshold. As with the probabilities of overfishing presented in the previous section, the results for the probabilities of *becoming overfished* are presented both in cumulative and current percentages of overfished sample populations in time. These trends are observable starting the second year of the experiment, results of the first year's fishing mortalities.

The risk of diminished biomass resulting from hypothetically perfect implementation of an ABC control rule provides a vital metric for managers faced with choosing an appropriate risk level for a given stock. But understanding the factors influencing a stock's capacity to recover from

this diminished biomass is also crucial. In this study, a decline in the percentage of populations currently overfished indicates net recovery of sample populations back to spawning stock biomass levels above SSB_{MSY}. In fact, the percentage recovering in a given year can be calculated explicitly by adding the net decline to the corresponding increase in the cumulative percentage. That is, for a single year,

$$\% \text{ recovered} = \Delta(\% \text{ cumulative}) - \Delta(\% \text{ current}) \qquad \text{(Eq. R7)}$$

where Δ measures the difference in percentages between the current year and the previous year. (In years of net recovery, the sign of Δ(% current) is negative.)

The following comparisons focus on the risk of biomass falling below SSB_{MSY}, but because SSB_{MSY} is an estimated quantity describing a theoretical equilibrium, it makes a poor basis for imposing immediate consequences to the fishing industry. In practice, the "overfished" status, often some proportion of SSB_{MSY}, is determined stock-by-stock (NMFS 2011). However, considering another, lower biomass threshold simulates the relatively minor risk of catastrophic collapse. In these simulations, it was possible for a sample population to "crash" during the time frame of the projections if *SSB* fell below ABC, such that the remaining biomass was less than the catch the program was attempting to remove. In this case, the program was forced to halt fishing, setting F=0. Accounting for these catastrophic collapses helps complete the understanding of the study's model dynamics. Because crashed populations subsequently experienced F=0, they were no longer counted in the percentages currently experiencing overfishing (defined as $F > F_{MSY}$). This is responsible for a portion of the declines observed in the current percentages of populations overfishing presented in Section III.

Vermilion Snapper

The bold trajectories in Figure 2.14 show the current percentages of overfished populations. These percentages generally decline in time according to a clear pattern, indicating net recovery. Among levels of uncertainty, scenarios with the widest OFL distribution showed the quickest declines in percentage overfished (the fastest rate of recovery) while scenarios with the narrowest OFL distribution showed slowest rates of recovery. Patterns also emerged among

levels of P^*. The net recoveries were greatest for the lowest P^* (five-year declines in percentage overfished up to 12%), less for P^*=0.3 (~ 2-3%), and minimal for P^*=0.5 (~1-2%).

The fainter trajectories in Figure 2.14, which start year 2, track the percentage of vermilion populations falling below SSB_{MSY} at least once by that year. The patterns in these cumulative percentages mirror those of the cumulative risks of overfishing presented for vermilion in Section III.

A small percentage of the populations (~1-4%) in each scenario "crashed," forcing the program to halt fishing. The crash rate for each scenario is listed in Table 12. Rates were highest, as expected, for the riskiest fishing pressure (P^*=0.5), but showed an inconsistent pattern among levels of uncertainty (Figure 2.17).

Sandbar Shark

Yearly percentages of populations overfished are represented by the bold lines in Figure 2.15. For P^*=0.1, as for the vermilion scenarios, current percentages of populations overfished dipped in time, indicating net recovery. At first, the high uncertainty scenarios recovered most quickly, but after three years the decline in this percentage slowed and was surpassed by those of the base and low uncertainty scenarios.

At higher levels of expected risk, however, sandbar sharks showed net increase in diminished biomass, rather than net recovery. For P^*=0.3, all three rates dropped initially, but those for the high and base uncertainties began to increase again after two and four years, respectively. For P^*=0.5, only the lowest uncertainty scenario declined in time, and even then only slightly. Overfished percentages for the base and high uncertainty scenarios increased over the nine-year time period (by about 7% and 13%, respectively).

The faint lines in Figure 2.15 show the cumulative percentage of populations overfished. For P^*=0.1, the percentage increased slowly in time, showing the same pattern among uncertainty levels as vermilion (lower uncertainty levels leading to greater percentages overfished.) However, for P^*=0.3 and P^*=0.5, as the trends for percentage currently overfished reversed, so

did the trends for cumulative percentage overfished. All three trajectories increased in time, with high uncertainty presenting the highest risk of becoming overfished at some point in the experiment and low uncertainty the lowest.

Out of all nine scenarios (9 x 5000 = 45000 populations), only one sandbar population "crashed" (i.e., SSB < ABC and fishing was halted.)

Gulf Menhaden

For menhaden, the current percentages overfished in a given year, represented by the bold trajectories in Figure 2.16, quickly declined toward P^*, then maintained approximately that percentage for the duration of the experiment. The low uncertainty scenario was the slowest to decline to P^*=0.1, followed by the base scenario, but the differences were small (a few percentage points.) The steady current percentages indicate neither net recovery nor net increase in rate of biomass loss.

Shown in Figure 2.16, cumulative risk of menhaden populations becoming overfished at least one year in the experiment increased in time for each scenario. For each P^*, the lowest uncertainty showed the highest risk, the base uncertainty the next, and the highest uncertainty, the lowest. These relative patterns of these trajectories are similar to those of the probabilistic risks of overfishing presented for menhaden in Section III, but the rates of increase are much higher in these new trajectories. These quickly increasing cumulative percentages, contrasted with the steady current percentages, indicate high turnover rates for menhaden populations.

Menhaden populations are so resilient that they can sustain catch levels greater than their values of SSB_{MSY}. This inequality (SSB < ABC) would render them all immediately "crashed" by the definition used for vermilion and sandbar. Instead, a modified crash definition checked total biomass B, rather than SSB, against ABC. The crash rates for each scenario, employing this new criterion, are listed in Table 13. They were highest by far for both the riskiest fishing pressure (P^*=0.5) and for the highest amount of uncertainty, showing a more interpretable pattern than did the crash rates for vermilion (Figure 2.18).

Analysis

The explanatory models presented in Section II describe the conditions under which populations will experience overfishing in the simulations experiments. These models illustrated the role that the status of a stock's biomass plays in determining the fishing mortality that results from a given catch level—and, thus, in determining the risk that the ABC leads to overfishing. However, that fishing mortality plays a role in determining the following year's biomass. Just as the explanatory models in Section II considered the conditions that affect the observed risk that overfishing occurs, the following models consider the conditions that affect the observed risk of populations declining to an overfished status.

Determining Drivers of Comprehensive Risk

The following models build on those presented in Section II. But an increased number of conditions are necessary to determine the risk outcome. As these complicate both the models and their flow chart visualizations, it helps to start by revisiting the simplified, ideal case in which 100% of the sample populations start the experiment exactly at SSB_{MSY}. Flow Chart 1 demonstrated that exactly P^* percent of those populations, those fished at ABC > OFL_{true}, would experience overfishing (Figure 2.7). Flow Chart 3 expands Flow Chart 1 to show that, in this ideal case, all of the populations that experience overfishing would decline below SSB_{MSY} by next year (Figure 2.19). Thus P^* would exactly predict not only the observed risk of overfishing, $\boldsymbol{O}$, but also the risk of the population becoming overfished, $\boldsymbol{Q}$:

$$\boldsymbol{O} = \boldsymbol{Q} = P^* \qquad \text{(Eq. R8)}$$

However, as shown in Section II, once the assumption of a perfect, equilibrium starting point is removed, the condition of the stock's biomass level, as well the spread of the OFL distribution, increases or decreases the observed risks of overfishing. These factors also influence the effect of the resulting fishing mortality rate on the stock's status. Thus, just as $\boldsymbol{O}$ rarely equals P^* exactly, especially with repeated application of the control rule, $\boldsymbol{Q}$ rarely equals $\boldsymbol{O}$.

Describing $\boldsymbol{Q}$ mathematically requires building on the equations developed for $\boldsymbol{O}$. For every pathway from starting stock status (whether overfished, α, or non-overfished, 1 – α) to relative

fishing mortality rate (whether overfishing, $F > F_{MSY}$, or underfishing, $F < F_{MSY}$), there are two pathways to subsequent stock status. Below, the equations that describe the first pathways must be multiplied by a new parameter to express their probability of leading to a particular stock status outcome. Condensed versions of Flow Charts 2A-2B are embedded in new Flow Charts 4A-4B to depict these additional pathways visually (Figures 2.20, 2.21).

Flow Chart 4A expands upon Flow Chart 2A to illustrate the pathways by which *non-overfished populations become overfished* (Figure 2.20). Conservative fishing mortality rates tend to prevent non-overfished populations from becoming overfished, but if recruitment is sufficiently variable, that tendency may be overridden by the arrival of a particularly poor recruitment class to the *SSB* the following year. Conversely, while overfishing will wear down surplus biomass, it does so at different rates depending on the severity. The sum of the probabilities of these phenomena—recruitment overruling a positive feedback loop and overfishing depleting surplus biomass—describes the probability $\boldsymbol{Q}_{Non}$ of *non-overfished populations becoming overfished*.

As explained in Section II, non-overfished populations follow two pathways to fishing mortality rates that result in underfishing. The first, "expected underfishing," stems from the fraction of populations $(1 - P_{Non})$ for which $ABC < OFL_{true}$. This pathway creates the primary feedback loop that maintains non-overfished populations above SSB_{MSY}. A secondary feedback loop is due to "unexpected underfishing," cases in which $ABC > OFL_{true}$ does *not* lead to overfishing. This is the γ-term (γP_{Non}) introduced in Eq. R3. The probabilities that these pathways nonetheless result in an overfished stock status are found by multiplying the probabilities of their occurrence by the rates, δ_1 and δ_2, of overrides due to catastrophically low recruitment:

$$\boldsymbol{Q}_{Non\,(1)} = (1 - P_{Non})\delta_1 + \gamma P_{Non}\delta_2 \qquad \text{(Eq. R9)}$$

where P_{Non} equals the current probability that $ABC > OFL_{true}$ for non-overfished populations.

Equation R3, $\boldsymbol{O}_{Non}$, describes the pathway leading to overfishing for non-overfished populations. The probability that overfishing drives down biomass to an overfished status is termed ζ, the

"rate of loss of surplus." Simplifying Eq. R3 to a single term and multiplying by ζ gives this last component of $\boldsymbol{Q}_{\text{Non}}$:

$$\boldsymbol{Q}_{\text{Non (2)}} = \boldsymbol{O}_{\text{Non}}\zeta = (1 - \gamma)P_{\text{Non}}\zeta \qquad \text{(Eq. R10)}$$

where ζ incorporates δ as well. Then the total proportion $\boldsymbol{Q}_{\text{Non}}$ of non-overfished populations that are overfished the next year, equal to the sum of $\boldsymbol{Q}_{\text{Non (1)}}$ and $\boldsymbol{Q}_{\text{Non (2)}}$, can be expressed as

$$\boldsymbol{Q}_{\text{Non}} = (1 - P_{\text{Non}})\delta_1 + \gamma P_{\text{Non}}\delta_2 + (1 - \gamma)P_{\text{Non}}\zeta \qquad \text{(Eq. R11)}$$

As in Eq. 5, scaling $\boldsymbol{Q}_{\text{Non}}$ by the probability of starting non-overfished, $(1 - \alpha)$, describes the percentage of all sample populations following these pathways.

Meanwhile, mechanisms by which *overfished populations recover* are analogous. Flow Chart 4B expands upon Flow Chart 2B to illustrate these (Figure 2.21). Again, feedback loops occur when overfishing an already-overfished population prevents the biomass from recovering above SSB_{MSY}. But these feedbacks can be overridden by particularly strong recruitment years. In contrast, underfishing may imply light enough fishing pressure to allow recovery, but as before this depends on the rate. The total probability of *overfished populations recovering* equals the sum of the probabilities of either method of recovering (light fishing pressure or strong recruitment.) To distinguish that the following models track the probability of non-overfished outcomes rather than of overfished outcomes, this probability is termed $\boldsymbol{R}$ (where $\boldsymbol{R} = 1 - \boldsymbol{Q}_{\text{Over}}$).

Overfished populations follow two pathways to fishing mortality rates that represent overfishing. Their contribution to $\boldsymbol{R}$ comes from the ability of extremely strong recruitment to "rescue" an overfished population despite "expected overfishing" (P_{Over}, populations for which ABC > OFL_{true}) or "unexpected overfishing" (the β-term, $\beta(1 - P_{\text{Over}})$, introduced in Eq. 4). The probabilities of these rescues are constructed analogously to the extreme recruitment events in $\boldsymbol{Q}_{\text{Non (1)}}$ (Eq. R9) by multiplying the probabilities of the overfishing pathways by the rates of unusually high recruitment, δ_1' and δ_2':

$$\boldsymbol{R}_1 = P_{\text{Over}}\delta_1' + \beta(1 - P_{\text{Over}})\delta_2' \qquad \text{(Eq. R12)}$$

where P_{Over} equals the current probability that ABC > OFL_{true} for overfished populations.

Underfishing an overfished population may allow the population to eventually recover. Underfishing occurs when ABC < OFL_{true}, $(1 - P_{\text{Over}})$, and when no exceptional circumstances lead to overfishing unexpectedly $(1 - \beta)$. Multiplying the probability of this pathway by a rate of recovery, η, describes the second component of $\boldsymbol{R}$:

$$\boldsymbol{R}_2 = (1 - \beta)(1 - P_{\text{Over}})\eta \qquad \text{(Eq. R13)}$$

where η, the rate of recovery incorporates δ' as well.

Then the total probability that overfished populations recover by the following year can be expressed as the sum of $\boldsymbol{R}_1$ and $\boldsymbol{R}_2$:

$$\boldsymbol{R} = P_{\text{Over}}\delta_1' + \beta(1 - P_{\text{Over}})\delta_2' + (1 - \beta)(1 - P_{\text{Over}})\eta \qquad \text{(Eq. R14)}$$

Again, the percentages of *all* sample populations following these pathways is found by scaling $\boldsymbol{R}$ by α.

Finally, $\boldsymbol{Q}$, the probability of populations becoming overfished, changes in time according to the difference in these opposing trends of biomass decline and recovery. It grows as more populations drop below SSB_{MSY} ($\boldsymbol{Q}_{\text{Non}}$, Eq. R11) but shrinks as some of those populations grow back above SSB_{MSY} ($\boldsymbol{R}$, Eq. R14). Because $\boldsymbol{Q}$ is itself a percentage of all sample populations, the change in $\boldsymbol{Q}$ for a given year is expressed as the difference in scaled $\boldsymbol{Q}_{\text{Non}}$ and $\boldsymbol{R}$:

$$\Delta\boldsymbol{Q} = (1 - \alpha)\boldsymbol{Q}_{\text{Non}} - \alpha\boldsymbol{R} \qquad \text{(Eq. R15)}$$

Thus the comprehensive risk of overfishing, when defined as the risk of populations becoming overfished in time, can be described by combining the probabilities of various conditions leading

to either recovery or loss of surplus biomass. Though the accompanying equations are more complex than those for the probabilistic risk of overfishing, they still provide a useful tool in interpreting the observed results.

Interpreting Drivers of Comprehensive Risk

As in the first explanatory model, the variables in the above equations reflect the influences of the experimental factors. However, other than α, none of these variables were explicitly estimated in the study. Rather, they are useful for describing conceptually the relationships between the treatments of each experimental factor and the observed trends in risk or recovery.

Effects of Life History

The value of α relative to P^* strongly influences the direction of yearly change in percentage of populations overfished ($\boldsymbol{Q}$). It is reasonable that high values of α (like those of vermilion) increase the likelihood of net recovery, because high values of α indicate that more populations start the experiment overfished than the ABC control rule would dictate. As a result, some of these overfished populations are able to recover because fishing pressure actually lessens for them when the control rule experiment begins (Figures 2.14A-C, 2.15A). Conversely, low values of α (like those of sandbar) increase the likelihood of a net increase in populations overfished. In these cases, populations that were healthy (above SSB_{MSY}) during initialization become subject to harder fishing pressure under the control rule and lose their surplus biomass (Figure 2.15B-C). Finally, mid-range α values (such as menhaden's) indicate relatively even percentages of overfished and non-overfished populations. Rates of becoming overfished approximately equal rates of recovery, leading the percentage overfished trajectories to quickly approach the expected *overfishing* rate, P^*, and then remain relatively constant in time (Figure 2.16).

While species-specific recruitment stochasticity plays a major role in determining the value of α (Section I), it should also influence the magnitudes of the parameters δ and δ', which are the rates at which extreme recruitment events override stock status feedback loops (Eq. R11, Eq. R14). For symmetric recruitment variability, as in the case of sandbar, these rates are likely equal to one another. However, asymmetric lognormal recruitment error, applied to the recruitment functions for vermilion and menhaden, should present greater potential for unusually

high recruitment (Eq. R12) than for unusually low recruitment (Eq. R9), and it is likely that in these scenarios $\delta' > \delta$.

In general, species-specific recruitment variability adds an additional source of uncertainty to catch levels' effects on a stock's biomass—one that is not specifically accounted for in the OFL distributions. Those distributions are constructed based on *parameter uncertainties*, while the yearly recruitment variability is a source of *process uncertainty.* Process uncertainty increases the risk of overfishing occurring (Section III), but it also increases the opportunities for overfished populations recover through strong recruitment classes (above). In this study, the strongest effects of life history on both probabilistic and comprehensive risks of overfishing seem to be due to differences in process uncertainty.

Effects of Level of Uncertainty

As in Section II, the level of uncertainty surrounding the OFL estimate changes the magnitudes of β and γ. A wider OFL distribution increases the chance that ABC is far below the OFL_{true} (dramatically underfishing) or far above the OFL_{true} (dramatically overfishing) and therefore sufficiently high to decimate a healthy population or sufficiently low to rescue a diminished population. Thus, a higher uncertainty level leads to a lower β or γ value, but an increased rate of recovery (η-term) or of surplus loss (ζ-term), due to the $(1 - \beta)$ and $(1 - \gamma)$ multipliers, respectively. Results for all three species demonstrate this pattern. When net recovery occurred ($-\Delta\boldsymbol{Q}$), it occurred most quickly for the highest uncertainty scenarios (Figures 2.14A-B, 2.15A, 2.16A-B). Similarly, when some sandbar scenarios became increasingly overfished ($+\Delta\boldsymbol{Q}$), those increases in percentages overfished happened most quickly for the highest uncertainty scenarios (Figures 2.15B-C).

Thus, level of parameter uncertainty, by affecting the distribution of differences between ABC and OFL_{true}, has inverse effects on probabilistic risk of overfishing and comprehensive risk of overfishing. A greater probability of a small $|ABC - OFL_{true}|$, which leads to "unexpected" overfishing or underfishing (Section II), implies a reduced probability of a large $|ABC - OFL_{true}|$, which leads to "dramatic" overfishing or underfishing (above). The former increases the risk of overfishing occurring, while the latter reduces the risk of a population becoming overfished.

Effects of P* *Value*

Level of *P** also directly impacts the trends in populations recovering or becoming overfished. Even though the expected probabilities of overfishing (i.e., $Pr(ABC > OFL_{true})$) change in time for each classification of populations (P_{Non} decreases; P_{Over} increases), the magnitude of the original *P** determines the relative magnitudes of both P_{Non} and P_{Over}. Higher values of *P** increase P_{Non}, and this parameter, in turn, directly increases the ζ-term (rate of surplus loss) (Eq. R10). Meanwhile, lower *P** values imply lower P_{Over}, and inversely increase η-terms (rates of recovery) (Eq. R13).

The trends predicted by the equations are visible in the species' results. For sandbar, the only species that experiences net loss of surplus biomass, scenarios with *P**=0.50 most quickly fall overfished (Figure 2.15C). For all three species, the rates of recovery are fastest for scenarios with *P**=0.10 (see Figures 2.14A, 2.15A, and 2.16A). These patterns are intuitive. It makes sense that riskier harvest strategies increase the chance that a population surplus will be fished down below the biomass threshold. Conversely, more risk-averse harvest policies should increase the chances that populations will be fished lightly enough to allow recovery.

Exploring Species Resilience

The remaining parameters in these terms, ζ and η, are challenging to interpret, but may relate to species life history. The influences of two of the experimental factors—uncertainty level and risk level—seem adequately captured by the β/γ parameter and *P*'. But α reflects stock status more than it reflects life history, and the recruitment variability that determined this stock status is far from the only difference between the three species' life history strategies. For example, menhaden have the highest individual growth rate and the highest natural mortality rate, indicating a fast turnover of individuals in the population. Vermilion and sandbar have lower (and identical) growth rates, and much lower rates of natural mortality, sharks having the lowest. Attributing the magnitude of ζ/η to specific life history parameters is outside the scope of this study, but perhaps these parameters can be broadly linked to a species' resilience.

Discussion

Species life history, level of scientific uncertainty in the stock assessment, and level of allowable risk *P** itself influence the way a given *P** value translates to realized probabilities. Simulating scenarios that vary these factors predicts their effects on both probabilistic and comprehensive risks of overfishing.

These simulations are not intended to provide realistic projections of risks for the current populations of South Atlantic vermilion snapper, South Atlantic sandbar shark, or Gulf of Mexico gulf menhaden. Rather, these three stocks were chosen as examples in a theoretical comparison, removed from the current or historical states of their fisheries. The simulation models used here are simplifications and generalizations of the highly-specified models used in each stock's most recent assessment. They were neither calibrated with catch time series nor initialized at the most recent estimate of the stock's biomass.

As a result, some of the apparent results are artifacts of the simulations model's assumptions or design. They do not reflect the true effects of variation among the experimental factors. However, they do relate to real challenges faced in stock assessment and in risk management and can therefore serve as cautions. Then the remaining results can address the goal of the study by providing useful management advice on the influences of life history and uncertainty, particularly in identifying considerations to take in selecting *P** to set control rules.

I. Life History

Current stock status biases results

In order to vary the first experimental factor, life history strategy, a fairly generalized population model was parameterized with species-specific values of key life history traits. However, some of the patterns observed among the example stocks' results were due not to variations in these parameter values but rather to variations in current stock status (Results Section I). As stock status is not truly an inherent property of the example stocks, its effects on risk must be separated out from those actually due to life history strategy.

In each scenario, the sample populations started the control rule experiment at different relative biomass levels, and therefore at different stock statuses. The proportion of sample populations starting overfished (below their individual values of SSB_{MSY}) was constant throughout the nine scenarios for each species, but varied between species. This interspecies variation was an unintended consequence of the initialization method. In simulating an initial fishing period subject to species-specific recruitment variation (Methods Section VII), the method created species-specific probabilities of a population falling overfished by the first year of the experiment (Results Section I).

Because stock status affects the translation of catch level to fishing mortality rate, the probability of starting at an overfished status affects the overall probability that an ABC leads to overfishing. The distribution of starting stock statuses determines whether P^* over- or underestimates the probability of overfishing in the first year following the control rule's implementation (Eq. R5; Results Section II). It also determines whether the probability of stocks becoming overfished increases or decreases in time (but not the rate of increase.) (Eqs. R10, R13, R14; Results Section III).

Two of the species-specific probabilities resulting from the initialization period deviate from an even (50%) chance of sample populations starting overfished. For vermilion snapper, that percentage was approximately 60%. As a result, the observed probability of overfishing exceeded the expectation (P^*) (Results Section II). Also as a result, the simulated stocks saw net recovery as the experiment progressed (Results Section IV). The transition from initialization fishing (constant F_{MSY}) to experimental fishing (optimized F) actually lightens fishing pressure for some portion of the stocks, so the high probability of starting overfished actually created a higher potential for their eventual recovery.

Meanwhile, only about 15% of the populations in each sandbar shark scenario were overfished at the start of the experiment. Consequently, the observed probability of overfishing was less than the expectation (P^*) (Results Section II). Analogously to vermilion snapper, sandbar sharks' low

proportion of already-overfished stocks created the potential for the control rule to drive more populations overfished with repeated application of the control rule (Results Section IV).

In contrast to vermilion snapper and sandbar shark, the probabilities of gulf menhaden populations starting overfished really did equal about 50%, and, correspondingly, the observed probability of overfishing generally equaled P^*. Menhaden's percentage of populations overfished also nearly equaled P^* and stayed fairly constant in time.

In retrospect, these confounding effects of starting stock status distribution could have been canceled by scaling the total biomass of each initialized population to a value of *SSB* drawn randomly from some standardized distribution surrounding that population's SSB_{MSY}. In this way, each scenario's populations would have the same probability of starting above or below SSB_{MSY}, regardless of the species' recruitment characteristics. However, even without this correction, the observed patterns can be informative.

Ideally, stock assessments provide managers with an estimate of relative stock biomass before decisions are made, and stocks estimated to be already overfished may merit management actions outside the realm of P^*-based control rules. But in this study, the simulated managers implement ABC without regard to current stock status, essentially assuming that spawning stock biomass is unknown. While these cases are not ideal, they are not unrealistic. The resources do not exist to assess the population status of every stock every year, so estimates of a population's biomass level may be unavailable or outdated. In assuming no prior knowledge, the study essentially assumes that a stock's starting biomass has an equal probability of being above or below SSB_{MSY}. Unequal probabilities violate that assumption and introduce bias to the results of realized probabilistic and comprehensive risks of overfishing.

The two example species demonstrating starting-point bias, vermilion snapper and sandbar shark, can provide managers insight into cases in which a stock's current biomass has been overestimated or underestimated, respectively. The simulated vermilion snapper scenarios apply management decisions designed assuming equilibrium biomass to sample populations relatively likely to be starting below equilibrium biomass. As a result, observed risk of overfishing

occurring was higher than expected. The simulated sandbar shark scenarios demonstrated the opposite case (managing populations likely to be above equilibrium biomass), to opposite results (lower-than-expected observed risk of overfishing.) Finally, menhaden scenarios, with nearly equal probabilities, offer an experimental control in which starting-point bias was essentially absent. Although the effects of starting-point bias on the risk of overfishing were relatively small in this simulation study —generally a few percentage points—managers should nonetheless be aware of their potential.

Once again, the trends presented above due to starting-point bias cannot be attributed to inherent differences in life history strategy. However, the explanatory model indicates that other trends in risk are due to actual differences in life history parameters, and these can prove informative to management.

Recruitment variability increases risk of overfishing in time

One truly characteristic difference among the example stocks was the degree of variability in the spawner-recruitment relationship. Vermilion snapper and gulf menhaden populations were simulated allowing differing magnitudes of lognormal error in the recruitment function (Methods Section III), while sandbar shark populations were simulated with normal error applied to one parameter of recruitment, length of reproductive cycle (Methods Sections IV). This recruitment variability introduces a source of process uncertainty (Results Section IV).

Process uncertainty decreases the accuracy of the original, equilibrium-based OFL estimate with each subsequent year of simulated recruitment. Thus for vermilion populations, subject to the highest recruitment variability, the cumulative probability of overfishing increased in time most rapidly. Menhaden populations, subject to relatively lower recruitment variability, experienced less rapid increases in cumulative probabilistic risk. Sandbar populations, with the lowest recruitment variability, showed almost no increase in risk of overfishing in time. Process uncertainty in the sandbar simulations was so low that the equilibrium-based OFL estimates remained fairly accurate throughout the simulated time period, allowing the realized risk of overfishing occurring to stay nearly constant.

These patterns are consistent with the predictions of Winemiller (2005). According to Winemiller, periodic species (such as vermilion and menhaden) show weak density dependence and therefore the least predictable stock-recruitment relationships. Equilibrium strategists (such as sandbar shark) show strong density dependence and more predictable relationships between stock and recruitment. Equilibrium strategists' decreased uncertainty should improve the accuracy of their population projections.

Shertzer et al. (2010) caution that the probability of overfishing occurring at least once increases in time. The results of this study build on that caution by suggesting that this increase may be relatively more rapid for species with high recruitment variability. This is an important consideration for stocks that cannot be assessed on a yearly basis. A P^*-based control rule for an equilibrium strategist or another species with relatively steady recruitment may be usable for several years, while one for a periodic strategist will more quickly fail to reflect the original desired risk of overfishing.

Productivity likely determines resilience to fishing pressure and capacity to recover

A second inherent life history characteristic is productivity, which is often taken as an indicator of resilience. The National Standard 1 Guidelines for the implementation of the Magnuson-Stevens Reauthorization define productivity as "the capacity to produce MSY and to recover if the population is depleted." Metrics used to judge productivity include steepness, maximum age, maximum length, age at maturity, individual growth rate, and fecundity, among others (Musick 1999, Patrick et al. 2009).

These metrics can be used to qualitatively assess and compare the example stocks' productivities. Of the examples, sandbar sharks have the longest lifespan, slowest rate of maturity, largest maximum length, and lowest fecundity, all indicative of the low productivity characteristic of large coastal sharks (Patrick et al. 2009) and equilibrium strategists in general. Vermilion snapper have a much quicker rate of maturity, shorter maximum length, and higher fecundity than sandbar sharks, indicating relatively higher productivity. Finally, menhaden are

the most productive of the example species. They have the shortest lifespan and highest rate of natural mortality, which create a relatively rapid rate of population turnover, an indication of high productivity.

One way to compare species resilience may be to examine rates of recovery. Declines the current percentages of overfished populations (in Figures 2.14 – 2.16) indicate *net* recovery, but these are highly influenced by initial conditions and difficult to compare across species. Another metric considered was the probability of individual overfished populations recovering, but this metric obscured an important distinction—the extent to which each population is overfished. Recovering from 99% of SSB_{MSY} does not require the same growth rate or productivity as recovering from 80% of SSB_{MSY}. While, on average, sandbar sharks had the highest individual probabilities of overfished populations recovering, these overfished populations had almost never fallen below even 95% of SSB_{MSY}, so "recovery" was achieved by even slight gains in biomass (not shown.) Future analyses could examine recovery from some standardized low point, described as a percentage of SSB_{MSY}, back above SSB_{MSY}, strengthening the requirements for "recovery." While more formal exploration of this metric lies outside the scope of this project, preliminary examination (using the 95% starting level) suggests that gulf menhaden populations are more likely to make this defined relative recovery than are vermilion snapper populations, consistent with the predictions from productivity assessments.

Often productivity is used as a component in describing a stock's vulnerability to overfishing, which can be a helpful consideration in setting appropriate levels of allowable risk P^*.

Cheung et al. (2007) combined many of the above productivity metrics with ecological characteristics to judge the "intrinsic vulnerability" of various marine stocks on a scale from 1 (least vulnerable) to 100 (most). Gulf menhaden and vermilion snapper were two of the assessed stocks in this study, with intrinsic vulnerability scores of 47 and 59, respectively. While sandbar shark was not assessed, blacktip shark, another large coastal shark in the same genus as sandbar, received a score of 77. As intrinsic vulnerability is roughly the inverse of productivity, this ranking is consistent with the above informal assessments.

Productivity-susceptibility analysis combines productivity assessments with assessments of susceptibility to fishing gear to score vulnerability on a scale from 1 (least vulnerable) to 3 (most). Patrick et al. (2009) applied the PSA methodology to a number of U.S. stocks, including sandbar shark, giving it a relatively high vulnerability rating (2.4.) This study also found that the assessed schooling coastal pelagic fishes (similar to menhaden) merit medium to high productivity ratings, but that their high susceptibilities to fishing gear, due to their easily-located schools, increase their vulnerability.

Both productivity and vulnerability inform the comprehensive risk of overfishing associated with a given P^*. If species such as sandbar shark do indeed have low capacity to recover from low biomass levels, they may merit more cautious initial P^* values, while more resilient species like menhaden would be able to afford higher initial P^* values.

Life History Conclusions

The contrasting implications of these two intrinsic life history characteristics—average lifetime productivity and recruitment variability, which drives variation in productivity—highlight the need for an in-depth consideration of the multiple risks associated with a single probability of overfishing. Making life history-based recommendations based on only one of these will ignore the qualitatively different risk due to the other.

The results of this study suggest that the equilibrium life history type shows the most predictable probabilistic risks over time but suffers the highest comprehensive risks to the resource due to its low inherent productivity. Because the periodic life history strategy is more variable, but more productive, its probabilistic risks increase in time but its comprehensive risks are lower, as recovery potential is higher. Vermilion snapper and gulf menhaden exemplify gradients within this strategy; vermilion snapper's higher recruitment variability leads to more rapid increases in probabilistic risk, while gulf menhaden's higher productivity grants it the highest recovery capacity.

These examples suggest a trade-off between the benefits of relatively predictable probabilistic risk and those of relatively lower comprehensive risk. Making responsible decisions in the face

of such trade-offs requires clear management objectives, ideally based on stakeholder input and values. Perhaps periodic strategists can sustain more risk-prone management (catch levels corresponding to higher P^* values) but require more frequent stock assessments for monitoring and correction, while equilibrium strategists merit more risk-averse control rules (applying lower P^* values) that can be applied for longer periods of time. However, life history strategy is not the only factor affecting risk and should not be the sole basis for allowable risk.

II. Uncertainty

Unaccounted uncertainty decreases management accuracy

The study's design aimed to control the second experimental factor, level of scientific uncertainty in the stock assessment, by adjusting the probability distributions of key life history parameters, which in turn adjust the distributions of the OFL estimates. Lower uncertainty levels were originally expected to correspond to lower risks of overfishing by improving management accuracy. However, most scenarios did not show this correspondence. Instead, for vermilion and menhaden scenarios with $P^* < 0.5$, the narrowest OFL distributions corresponded to the *highest* risks of overfishing. This trend was visible in both the cumulative probabilities of experiencing overfishing (Results Section III) and of becoming overfished (Results Section IV). Meanwhile, the base OFL distributions resulted in the next highest probabilities, followed by those resulting from the widest distributions. Why were the expectations reversed?

In fact, the observed patterns are the result of interactions between the parameter uncertainty simulated in constructing the equilibrium-based OFL distributions, and the process uncertainty introduced afterwards in allowing stochastic recruitment. Thus the results were influenced by *two* sources of uncertainty, but only the first, parameter uncertainty, was accounted for in the OFL distributions. The unaccounted uncertainty decreased the accuracy of the OFL estimates, with the result that improving the precision of those estimates merely shrunk the precautionary buffer afforded by a given ABC, such that "low" uncertainty levels in fact implied riskier harvest strategies. This phenomenon is apparent for vermilion and menhaden scenarios because these species were simulated with high recruitment variability, and therefore substantial process

uncertainty. (Sandbar sharks, with very low recruitment variability, more closely resembled the original expectations.) The affect of unaccounted uncertainty is also most apparent at lower P^* levels, because these correspond to differentiated precautionary buffers. (If the distributions are centered around the same OFL estimate, ABCs derived according to $P^*=0.5$ should be nearly equal across levels of uncertainty.)

Could this have been corrected? Not within the study's current design. The first simulation model (Methods Section V) generated OFL distributions by repeating equilibrium-based benchmark calculations while varying parameter values. This method of simulating uncertainty was simple, easily adapted to different life histories, and useful for a preliminary exploration of the implications of P^* at various uncertainty levels. But by constantly assuming equilibrium, this approach allowed no avenue for incorporating variation in the spawner-recruit relationship into the spread of the OFL distribution. To incorporate the missing variation, the study would need an entirely new approach—one that involves simulating fisheries catch data and then estimating OFL and its uncertainty empirically through a simulated stock assessment.

This need for more thorough simulation of uncertainty has motivated the development of Management Strategy Evaluations (MSEs) (Butterworth and Punt 1999, Peterman 2004). Like this study, an MSEs includes an operating model to simulate a stock's "true" population dynamics under natural process uncertainty both in life history parameters and in recruitment patterns. However, an MSE also simulates sampling and assessment of this true population, incorporating observation uncertainty, estimation uncertainty, and model uncertainty. It then applies management actions based on the simulated stock assessment, potentially simulating implementation uncertainty as well. In this way, an MSE considers a broad range of feedback effects. Ambitious attempts to estimate so many forms of uncertainty have led to criticisms of MSEs overselling knowledge and risking "a false sense of rigour" by specifying probability distributions whose shape and spread are not truly known (Rochet and Rice 2009). However, MSEs, like the models used in study, are best used for assessing the relative risks among scenarios or management procedures, not for estimating absolute risk (Butterworth et al. 2010).

Due to their detail and complexity, conducting an MSE for each example stock was outside the scope of this study. The limitations of this study's relative simple design, particularly the inability of its simulated OFL distributions to account for a simulated source of uncertainty, temper the interpretation of the observed results. However, this does provide a crucial caution. Accounting quantitatively for every source of uncertainty is incredibly difficult, if not impossible, and the endeavor to do so in fisheries stock assessment is relatively young (Patterson et al. 2001). Thus the threat of missing or inadequately quantifying one or many sources is very real, even in state-of-the-art stock assessments and comprehensive management strategy evaluations.

Both managers and modelers must keep in mind that the belief that an ABC corresponds to a predictable level of risk is only as accurate as the OFL distribution from which it is calculated. Stocks with better data availability or longer time series are likely to have more accurate assessments, more complex modeling methods, and more thorough estimates of scientific uncertainty (Chen et al. 2003). Paradoxically, poor data limit the ability to estimate uncertainty and may result in more precise, if potentially less accurate, OFL estimates (Carmichael 2010). Proposals for addressing this paradox include penalizing the P^* by some set percentage based on the stock's data quality (Carmichael 2010). This seems in line with one of the tenants of the precautionary approach; i.e., increasing precaution in the face of increased uncertainty (Rochet and Rice 2009). Anticipating undescribed uncertainty can help prepare against unexpectedly high risks associated with P^* values.

Sizes of OFL distributions affect potential severity of overfishing

Despite the above caveat to the results of this study, the explanatory models can provide insight into theoretical systems in which all sources of uncertainty are accounted.

In its simplest interpretation, P^* is the probability that an ABC is greater than the true value of a stock's OFL. However, it is intuitive that removing an ABC slightly greater than OFL_{true} does not carry the same consequences for the stock as removing an ABC that is significantly greater than OFL_{true}. Small excesses may not lead to overfishing if some surplus biomass remains

(Methods Secion VIII, Results Section II). Toward the other extreme, large excesses may quickly decimate a previously healthy population. This distinction casts a *P** value decision in new terms, because it emphasizes that *P** controls the risk that ABC exceeds OFL_{true} *enough to cause undesired consequences*. From a practical standpoint, it is really this probability that managers must consider. Is a potential excess likely to cause overfishing? Would it drive the population's biomass below a chosen threshold?

The explanatory model identifies the influence of the size of the OFL distribution on the probability of this "consequential" overfishing. A narrow OFL distribution, in restricting the spread of potential OFL values, implies that the magnitudes of potential excesses are more likely to be small, perhaps negligible. A wider OFL distribution spreads the potential OFL values further and increases the potential for large, detrimental differences between ABC and OFL_{true}. Thus as long as the OFL distribution accurately describes scientific uncertainty, higher uncertainty levels *can* imply greater risks of overfishing: both greater probabilities that excess catches outweigh any surplus biomass and lead to overfishing, and greater probabilities that overfishing drives the biomass down below some threshold.

In this study, the simulated scenarios for sandbar shark best demonstrate these trends (Results Sections III, IV). Because their simulated recruitment variability is so minor, sandbar sharks' OFL distributions come closest to describing all of the system's uncertainty and meeting the theoretical requirements for the explanatory model.

Admittedly, the effects of distribution spread are difficult to trace far, because they are conditional on other factors. In this study, the current state of biomass determines whether the comprehensive risks demonstrate a trend of net recovery or net decline. The effects of distribution size are also confounded by the fact that wider distributions, while implying a higher risk of consequential overfishing, also imply a higher risk of extreme *underfishing* that could potentially allow rapid recovery.

Uncertainty Conclusions

Both the consequences of unaccounted uncertainty on relative risks levels, and the consequences

of real uncertainty on the potential severity of overfishing, complicate the implications of managers' choices of *P** for a given stock. Applications of *P**-based control rules are only truly comparable when the relative uncertainty between assessments is preserved in the sizes of the OFL distributions. But the wide range of data availability and stock assessment methods precludes this from happening naturally. Suggested solutions include *ad hoc* increases of CVs for data-poor stocks, perhaps to some minimum level based on data-rich OFL distributions (Carmichael 2010). However, combining deliberate CV inflations on the part of assessment scientists with reductions in *P** on the part of the managers risks double-counting data uncertainty.

It has been pointed out that if *P** is truly to be a value decision, it must be made without regard to the OFL distribution so that managers are truly choosing the allowable risk and not the catch level (Carmichael 2010). However, this strict interpretation may place too much confidence in the shape and spread of the OFL distribution, particularly in the tails, when these uncertainty distributions are bound to be uncertain themselves (Rochet and Rice 2009). Additionally, as this study demonstrates, many conditions apply to the assumption that a *P**-based control rule leads to a risk of overfishing equal to *P**. Thus, it seems important for managers to consider at least qualitatively the degree of uncertainty the stock faces. When relative uncertainty among assessments cannot been preserved, reducing *P** in for stocks with relatively less or lower quality data seems appropriate. Meanwhile, determining the allowable probability of severe or consequential overfishing given a better-informed OFL distribution requires drawing on the previous section's life history considerations.

III. Level of Allowable Risk, *P**

Finally, the study adjusted the third factor, the value of *P**, to simulate changes in managers' decisions concerning the allowable risk of overfishing. As described above, the conditions of the first two factors determine how well the *P**-based catch level achieves that desired risk. Within this simulation study, *P** dictated the probability of overfishing more closely when the effects of starting-point bias were minimal (as they were for menhaden scenarios) and when all sources of

uncertainty were taken into account (as they nearly were for sandbar shark scenarios, which had minimal process uncertainty.)

While *P** clearly controls the expected probability of overfishing occurring, it cannot directly predict the expected probability that overfishing causes declines in biomass. That probability is highly dependent on the state of the stock's current biomass. However, it is clear that higher *P** values increased the chances of becoming overfished in time, while low *P** values decreased those trends and improved the probability of net recovery (Results Section IV).

The results of this study demonstrate that the difference between the risks conferred by different values of *P** depends on the life history of the stock, the accuracy of the OFL estimate, and particularly on the spread of the OFL distribution. Because it tested only three levels of *P**, this study must refrain from making fine-scale recommendations among close *P** choices. However, due to the numerous sources of uncertainty and the challenges of accurately describing these uncertainties, the results of any simulation study should not be used "as if small differences in analytical results are meaningful biologically and in management" (Rochet and Rice 2009, Butterworth et al. 2010). Indeed, the observed patterns and the accompanying explanatory models shed light on trends that operate in the real world but are unable to quantitatively measure those trends' significance therein.

Level of *P** was an experimental factor in that it varied among scenarios, but it differs conceptually from the other experimental factors considered, because it represents the management decision itself rather than external factors that influence the results of the decision. Nonetheless, a few general observations can be made about trends due to *P** itself. Because *P** is a percentage applied to probability distribution, higher values of *P** occur more closely to the distribution's median while lower values of *P** occur further toward the distribution's tail. By design, because these central values are presumably more probable, they are also more stable. Greater differentiation among potential outcomes occurs at lower levels of *P**, because tail probabilities are less likely, less well-known, and highly influenced by individual assumptions and modeling choices (Rochet and Rice 2009, Rothschild and Jiao 2011). Thus, managers considering low *P** values for a particular stock should be aware that it is among the lowest

values that small differences in *P** choice would be most likely to correspond to significant differences in either probabilistic or comprehensive risk.

IV. Summary of Management Implications

The *P** methodology for setting catch recommendations aims to manage the risk of overfishing explicitly, but choice of *P** alone does not provide sufficient information on the real risks associated with a control rule. First, various unknowns, whether unanticipated or miscalculated, can influence how accurately a *P**-based control rule translates into the actual probability that fishing mortality exceeds its threshold. Secondly, different factors influence the potential severity of this overfishing and the probability that it leads to declines in the stock's biomass. Managers deliberating the appropriate *P** for an individual stock must be aware of the circumstances that inflate either the probabilistic or comprehensive risks of overfishing.

Probabilistic Risk

Managers must not assume that *P** determines the probabilistic risk of overfishing exactly. Rather, they must recognize that attempting to control risk by choosing a percentile (*P**) of a probability distribution of OFLs places a high amount of confidence in the stock assessment's estimation of uncertainty. If this estimation is incorrect or insufficient, the OFL distribution will misrepresent the actual probabilities of each catch value, particularly values that lie toward distributions' tails. As a result, the true percentile of an ABC, and therefore the true risk that it results in overfishing, will differ from *P**. Given that it is impossible for scientists to completely describe all sources of uncertainty, these discrepancies seem likely to occur.

Two sources in particular provide examples of the ways unaccounted uncertainty can influence probabilistic risk. The first concerns uncertainty in the biomass estimates from which OFL is derived. Failure of an OFL distribution to adequately reflect biomass uncertainty will affect the accuracy of *P**. For example, if a stock's biomass has been overestimated, the real probability of overfishing will exceed *P**. Unfortunately, overestimation is impossible to detect except in retrospect and cannot be assumed to plague only data-deficient stocks, as demonstrated by the extreme overestimation of the Newfoundland cod stock's biomass prior to its collapse.

The second source stems from the potential effects of random variation in the natural world—particularly recruitment variability. The *P** methodology assumes that the OFL distribution has sufficiently accounted for the uncertainty in the yearly relationship between recruitment and the stock's population of spawners. But this can be especially challenging for stocks with high recruitment variability and poorly understood spawner-recruit relationships. Periodic strategists, which release multiple, large batches of eggs with highly variable survival rates, are prone to these issues. If unaccounted, high recruitment fluctuation will quickly decrease the accuracy of an OFL estimate in time, increasing the probability that overfishing occurs in at least one year. Accommodating such an increase requires choosing relatively cautious initial *P** values or conducting more frequent assessment updates.

Finally, because *any* missing source of uncertainty has the potential to increase probabilistic risk, managers must take particular caution in selecting *P** for stocks with fewer or lower-quality data. A paucity of reliable data will limit modelers' capacity to estimate uncertainty and may lead to OFL distributions that are misleadingly narrow. Because relatively precise distributions imply relatively narrow catch reductions at a given *P**, 'improving' precision without improving accuracy actually *increases* the risk overfishing, because it decreases the precautionary buffer. This apparent paradox highlights that the *P** methodology is most consistent when relative uncertainty is preserved across assessments—i.e., if stocks with less information have wider OFL distributions.

Comprehensive Risk

In contrast to probabilistic risk, comprehensive risks associated with the severity of potential overfishing differ even when uncertainty has been captured perfectly. First, greater actual uncertainty in OFL distributions implies the potential for greater differences between the true overfishing limit and the applied catch level, and large deviations can rapidly impact the stock's biomass. Intense overfishing will quickly drive down biomass, while sufficient underfishing will allow growth. Faced with stocks with highly uncertain OFL estimates, including relatively data-poor stocks with distributions adjusted *ad-hoc* to reflect high data uncertainty, managers must keep in mind that the lower-probability overfishing events may be of more extreme magnitudes.

Secondly, the severity of overfishing depends on the productivity of a species and its resilience to fishing pressure. Highly productive species are more likely to recover from occasional drops in biomass level, even under sustained levels of catch, while stocks with lower productivity are less likely to overcome declines. Broadly, life history theory can advise managers in setting P^* based on productivity; periodic strategists tend to be highly productive, while equilibrium strategists, with long gestation times and small batch sizes, have low productivity. While these are loose categorizations and productivity varies widely within strategies, trends do suggest that equilibrium strategists and other low productivity stocks merit relatively cautious P^* values because the consequences of overfishing them in one year are likely slow to reverse.

Conclusion

This study evaluated the effects of three factors to determine their implications for P^*-based management. The trends identified among example species were consistent with predictions from life history theory. Meanwhile, differences in the size of the OFL distribution—meant to represent differences in levels of uncertainty—led to unexpected results when the distribution was biased or when uncertainty was not fully characterized. Lastly, because OFL distributions are themselves estimates and subject to uncertainty in their shape and size, lower P^* values closer to the tails of the estimated distribution produced more variable resulting risks.

Because the simulations in this study were based on parameterizations of a relatively generalized model, rather than on three individual stock assessment models, the individual projections of risk are not in themselves realistic. However, despite its relative simplicity, the modeling process was crucial in identifying potential sources and evaluating the effects of missing uncertainty. Ideally, in-depth evaluation of the risks for a particular stock will aid in identifying potential missing uncertainty and predicting the impacts of occasional overfishing on the stock's biomass, so that managers can choose an appropriate P^* value with a more complete idea of its implications. Until these evaluations are available, it is hoped that the general patterns presented above can inform management decisions and provide caution regarding the difficulty in truly controlling or predicting the risk of overfishing.

Literature Cited

Bates, D. and D. Sarkar, and the R Development Core Team. 2010. nlminb: optimization using PORT routines. R package *stats* version 2.11.1.

Butterworth, D. S. and A. E. Punt. 1999. Experiences in the evaluation and implementation of management procedures. ICES Journal of Marine Science 56: 985-998.

Butterworth, D. S., N. Bentley, J. A. A. De Oliveira, G. P. Donovan, L. T. Kell, A. M. Parma, A. E. Punt, K. J. Sainsbury, A. D. M. Smith, and T. K. Stokes. 2010. Purported flaws in management strategy evaluation: basic problems or misinterpretations? ICES Journal of Marine Science 67: 567-574.

Caddy, J. F. and R. McGarvey. 1996. Targets or limits for management of fisheries? North American Journal of Fisheries Management 16: 479-487.

Carmichael, J., editor. 2010. Characterizing and presenting assessment uncertainty. Report from SEDAR Procedural Workshop IV, Charlotte.

Chen, Y., L. Chen, and K. I. Stergiou. 2003. Impacts of data quantity on fisheries stock assessment. Aquatic Sciences 65: 1-7.

Chen, S. B. and S. Watanabe. 1989. Age dependence of natural mortality coefficient in fish population dynamics. Nippon Suisan Gak. 55: 205-208.

Cheung, W. W. L., R. Watson, T. Morato, T. J. Pitcher, and D. Pauly. 2007. Intrinsic vulnerability in global fish catch. Marine Ecology Progress Series 333: 1-12.

Conn, P. B., E. H. Williams, and K. W. Shertzer. 2010. When can we reliably estimate the productivity of fish stocks? Canadian Journal of Fisheries and Aquatic Sciences 67: 511-523.

Haddon, M. 2001. Modelling and quantitative methods in fisheries (1st ed.). Chapman and Hall/CRC, U.S.A.

Helfman, G., B. B. Collette, D. E. Facey, and B. W. Bowen. 2009. The diversity of fishes: biology, evolution, and ecology (2nd ed.). Wiley-Blackwell, West Sussex.

Hoenig, J. M. 1983. Empirical use of longevity data to estimate mortality rates. Fishery Bulletin US 82: 898-903.

King, J. R. and G. A. MacFarlane. 2003. Marine fish life history strategies: applications to fishery management. Fisheries Management and Ecology 10: 249-264.

Lewis, R. M., and C. M. Roithmayr. 1981. Spawning and sexual maturity of Gulf menhaden, *Brevoortia patronus*. Fisheries Bulletin 78: 947-951.

Lorenzen, K. 1996. The relationship between body weight and natural mortality in juvenile and adult fish: a comparison of natural ecosystems and aquaculture. Journal of Fish Biology 49: 627-647.

Mace, P. M. and I. J. Doonan. 1988. A generalised bioeconomic simulation model for fish population dynamics. New Zealand Fisheries Assessment Research Document 88/4. 51 pp.

Martinez-Andrade, F. 2003. A comparison of life histories and ecological aspects among snappers (Pisces: Lutjanidae). Ph.D. Dissertation, Louisiana State University.

Megrey, B. A. 1989. Review and comparison of age-structured stock assessment models from theoretical and applied points of view. American Fisheries Society Symposium 6: 8-48.

MSRA (Magnuson-Stevens Fishery Conservation and Management Reauthorization Act of 2006). 2006. Pub. L. No. 109-479, 120 Stat. 3575.

Musick, J.A. 1999. Criteria to define extinction risk in marine fishes. Fisheries 24(12): 6-14.

NMFS. 2011. Annual report to Congress on the status of U.S. Fisheries – 2010. U.S. Department of Commerce, NOAA, National Marine Fisheries Service, Silver Spring, MD. 21 pp.

Patrick, W. S., P. Spencer, O. Ormseth, J. Cope, J. Field, D. Kobayashi, T. Gedamke, E. Cortés, K. Bigelow, W. Overholtz, J. Link, and P. Lawson. 2009. Use of productivity and susceptibility indices to determine the vulnerability of a stock: with example applications to six U.S. fisheries. Vulnerability Evaluation Working Group Report.

Patterson, K., R. Cook, C. Darby, S. Gavaris, L. Kell, P. Lewy, B. Mesnil, A. Punt, V. Restrepo, D. W. Skagen, and G. Stefánsson. 2001. Estimating uncertainty in fish stock assessment and forecasting. Fish and Fisheries 2: 125-157.

Pauly, D. 1979. On the interrelationships between natural mortality, growth parameters, and mean environmental temperature in 175 fish stocks. ICES Journal of Marine Science 39: 175-192.

Peterman, R. M. 2004. Possible solutions to some challenges facing fisheries scientists and managers. ICES Journal of Marine Science 61: 1331-1343.

Peterson, J. and J. S. Wroblewski. 1984. Mortality rate of fishes in the pelagic ecosystem. Canadian Journal of Fisheries and Aquatic Sciences 41: 1117-1120.

Pine, W. E., K. H. Pollock, J. E. Hightower, T. J. Kwak, and J. A. Rice. 2003. A review of tagging methods for estimating fish population size and components of mortality. Fisheries 28(10): 10-23.

Prager, M. H., and K. W. Shertzer. 2010. Deriving acceptable biological catch from the overfishing limit: implications for assessment models. North American Journal of Fisheries Management 30: 289-294.

Quinn II, T. J. and R. B. Deriso. 1999. Quantitative fish dynamics. Oxford University Press Inc, New York, New York.

R Development Core Team. 2010. R: A language and environment for statistical computer. R Foundation for Statistical Computing, Vienna, Austria. http://www.R-project.org.

Rochet, M-J. and J. C. Rice. 2009. Simulation-based management strategy evaluation: ignorance disguised as mathematics? ICES Journal of Marine Science 66: 754-762.

Rose, K. A., J. H. Cowan, Jr., K. O. Winemiller, R. A. Myers, and R. Hilborn. 2001. Fish and Fisheries 2: 293-327.

Rothschild, B. J. and Y. Jiao. 2011. Characterizing uncertainty in fish stock assessments: the case of the Southern New England-Mid-Atlantic winter flounder. Transactions of the American Fisheries Society 140(3): 557-569.

SEDAR 17. 2008. South Atlantic vermilion snapper. SEDAR 17 Stock Assessment Report. Available on the World Wide Web at: www.sefsc.noaa.gov/sedar/.

SEDAR 21. 2011. HMS sandbar shark. SEDAR 21 Stock Assessment Report. Available on the World Wide Web at: www.sefsc.noaa.gov/sedar/.

SEDAR 27. 2011. Gulf of Mexico menhaden. SEDAR 27 Stock Assessment Report. Available on the World Wide Web at: www.sefsc.noaa.gov/sedar/.

Shertzer, K. W. & P. B. Conn. 2012. Spawner-recruit relationships of demersal marine fishes: prior distribution of steepness. Bulletin of Marine Science 88(1): 39-50.

Shertzer, K. W., M. H. Prager, and E. H. Williams. 2008. A probability-based approach to setting annual catch levels. Fishery Bulletin 106: 225-232.

Shertzer, K. W., M. H. Prager, and E. H. Williams. 2010. Probabilistic approaches to setting acceptable biological catch and annual catch targets for multiple years: reconciling methodology with National Standard Guidelines. Marine and Coastal Fisheries: Dynamics, Management, and Ecosystem Science 2: 451-458.

Vetter, E. F. 1988. Estimation of natural mortality in fish stocks: a review. Fishery Bulletin 86(1): 25-43.

Vila-Gispert, A., R. Moreno-Amich, and E. García-Berthou. 2002. Gradients of life-history variation: an intercontinental comparison of fishes. Reviews in Fish Biology and Fisheries 12: 417-427.

Winemiller, K. O. 2005. Life history strategies, population regulation and implications for fisheries management. Canadian Journal of Fisheries and Aquatic Sciences 62: 872-885.

Table 1. Age-constant life history parameters.

			Vermilion Snapper		Sandbar Shark		Gulf Menhaden	
Parameter	**Symbol**	**Units**	**Value**	Source: **SEDAR17**	**Value**	Source: **SEDAR21**	**Value**	Source: **SEDAR27**
max age	a_{max}	yr	19	*DWR 2.3*	27	*AWR Table 2.4*	6	*pers.com. A.S.*
Von Bert length	L_∞	mm	506	*DWR Table 2.6.1*	1811.5	*AWR Table 2.4*	237.8	*gmenhad-064.rdat*
Von Bert growth	κ	1/yr	0.12	"	0.12	"	0.444	"
Von Bert age	a_0	yr	-3.5	"	-2.33	"	-0.878	"
lt-wt scalar	α		2.10E-05	*DWR Table 2.8.1*	1.09E-05	"	1.55E-05	*pers.com. A.S.*
lt-wt exponent	β		2.907	"	3.0124	"	3.18	*pers.com. A.S.*
steepness	h		0.56	*AWR 3.1.2.8*	0.29	*AWR Table 3.14*	0.69	*gmenhad-064.rdat*
virgin recruitment	R_0	#fish	4325709	"	5.63E+05	*AWR Table 3.1*	2.07E+11	"
recruitment variance	σ_S^2		0.745	*pers.com. K.S.*			0.124	*pers.com. A.S.*
bias correction	ς		1.32	"			1.00743	"
natural mortality	M	1/yr	0.22	*DWR 2.3*	0.135597407	*calculated**	1.1	*DWR 3.6.1*
sex ratio	ρ		0.72	*DWR 2.7.4*	0.5	*AWR Table 2.4*	0.5	*DWR 3.5*

note: DWR = Data Workshop Report, AWR = Assessment Workshop Report
A. S. = Amy Schueller, K. S. = Kyle Shertzer

Table 2. Vermilion snapper age-specific life history parameters.

	Maturity[1]	Fecundity[2]	Mortality[3]	Selectivity[4]
		(millions)		
Age	μ_a	f_a	M_a	s_a
1	0.8	0.70	0.341	0
2	1.0	1.02	0.304	0
3	1.0	1.35	0.278	0.5334
4	1.0	1.70	0.258	1
5	1.0	2.05	0.243	1
6	1.0	2.39	0.231	1
7	1.0	2.73	0.222	1
8	1.0	3.04	0.214	1
9	1.0	3.34	0.208	1
10	1.0	3.62	0.202	1
11	1.0	3.88	0.198	1
12	1.0	4.12	0.194	1
13	1.0	4.33	0.191	1
14	1.0	4.53	0.188	1
15	1.0	4.71	0.185	1
16	1.0	4.88	0.183	1
17	1.0	5.03	0.181	1
18	1.0	5.16	0.180	1
19	1.0	5.28	0.178	1

Source: SEDAR 17

[1]DWR 2.7.3

[2]DWR 2.7.2

[3]AWR Table 2.1; scaled to Hoenig estimate

[4]AWR Table 3.7; combined commercial fisheries

Table 3. Sandbar shark age-specific life history parameters.

	Maturity[1]	Fecundity[1,2]	Mortality[1]	Selectivity[3]
		(no. pups)		
Age	μ_a	f_a	M_a	s_a
1	0.00	0.85	0.154	0.001
2	0.00	0.90	0.154	0.003
3	0.00	0.95	0.154	0.007
4	0.00	1.01	0.154	0.018
5	0.00	1.06	0.154	0.047
6	0.01	1.11	0.154	0.119
7	0.02	1.16	0.154	0.269
8	0.03	1.21	0.153	0.500
9	0.06	1.26	0.148	0.731
10	0.12	1.32	0.131	0.881
11	0.20	1.37	0.131	0.953
12	0.33	1.42	0.131	0.982
13	0.48	1.47	0.131	0.993
14	0.64	1.52	0.131	0.998
15	0.78	1.58	0.131	0.999
16	0.87	1.63	0.129	1.000
17	0.93	1.68	0.128	1.000
18	0.96	1.73	0.127	1.000
19	0.98	1.78	0.126	1.000
20	0.99	1.83	0.125	1.000
21	0.99	1.89	0.124	1.000
22	1.00	1.94	0.124	1.000
23	1.00	1.99	0.123	1.000
24	1.00	2.04	0.122	1.000
25	1.00	2.09	0.122	1.000
26	1.00	2.15	0.122	1.000
27	1.00	2.20	0.121	1.000

Source: SEDAR 21

[1]AWR Table 2.4

[2]Fecundity vector / 2.5

[3]AWR Table 2.2; parameters for logistic curve

Table 4. Gulf menhaden age-specific life history parameters.

	Maturity[1]	Fecundity[1,2]	Mortality[3]	Selectivity[4]
		(thousands)		
Age	μ_a	f_a	M_a	s_a
1	0	9.26	1.31	0.45
2	1	23.79	1.1	1
3	1	39.34	1	1
4	1	52.64	0.94	1
5	1	62.77	0.91	1
6	1	69.99	0.89	1

Source: SEDAR 27

[1]DWR 3.5

[2]based on constant Von Bertalanffy parameters

[3]DWR Table 3.15

[4]from gmenhad-064.dat file; average commercial/gill for 2010

Table 5. Life history parameter ranges.

		Steepness, *h*			**Natural Mortality, *M***		
Species	**SEDAR**	central est.	range	*source*	central est.	range	*source*
Vermilion	SEDAR17	0.56	0.47-0.73	AWR 3.1.1.3	0.22	0.16-0.28	DWR 2.3
Sandbar	SEDAR21	0.29	0.25-0.40	DWR 2.8	0.14	0.12-0.15	AWR Table 3.10
Menhaden	SEDAR27	0.69	0.45-0.97	*pers. com. A.S.*	1.10	0.91-1.27	DWR Table 3.15

Tables 6-8. ABC values (in kilograms) for vermilion snapper, sandbar shark, and gulf menhaden at each level of uncertainty, under each *P** control rule.

Table 6. Vermilion Snapper ABC Values (kg)			
		Uncertainty	
*P**	*Low*	*Base*	*High*
0.1	466791	445055	391224
0.3	486519	478034	451492
0.5	501338	506753	499850

Table 7. Sandbar Shark ABC Values (kg)			
		Uncertainty	
*P**	*Low*	*Base*	*High*
0.1	490581	423444	331538
0.3	531979	504195	464696
0.5	560585	565767	554250

Table 8. Gulf Menhaden ABC Values (kg)			
		Uncertainty	
*P**	*Low*	*Base*	*High*
0.1	9.372E+08	8.488E+08	7.000E+08
0.3	1.077E+09	1.031E+09	9.540E+08
0.5	1.171E+09	1.188E+09	1.160E+09

Tables 9-11. Percentages of vermilion snapper, sandbar shark, and gulf menhaden populations experiencing overfishing in the first year of the control rule's implementation.

Table 9. % Vermilion Overfishing First Year			
		Uncertainty	
*P**	*Low*	*Base*	*High*
0.1	38.5%	26.9%	20.5%
0.3	48.9%	41.0%	39.0%
0.5	56.5%	54.7%	56.8%

Table 10. % Sandbar Overfishing First Year			
		Uncertainty	
*P**	*Low*	*Base*	*High*
0.1	7.3%	8.4%	9.7%
0.3	23.7%	27.1%	27.9%
0.5	42.5%	45.5%	46.8%

Table 11. % Menhaden Overfishing First Year			
		Uncertainty	
*P**	*Low*	*Base*	*High*
0.1	11.5%	10.6%	10.7%
0.3	30.7%	29.5%	30.5%
0.5	48.2%	49.5%	49.0%

Tables 12-13. Percentages of vermilion snapper and gulf menhaden populations crashing in the duration of the experiment.

Table 12. Vermilion Crash Rates			
		Uncertainty	
*P**	*Low*	*Base*	*High*
0.1	1.20%	1.56%	0.92%
0.3	1.26%	2.50%	2.38%
0.5	1.86%	3.40%	2.42%

Table 13. Menhaden Crash Rates			
		Uncertainty	
*P**	*Low*	*Base*	*High*
0.1	0.00%	0.04%	0.60%
0.3	0.24%	1.12%	4.64%
0.5	1.12%	6.12%	14.58%

Figure 2.1. Constructed OFL distributions for vermilion snapper. Red lines represent smoothed probability density functions. **A)** Low Uncertainty applies a CV of 8% to both steepness, *h*, and natural mortality, *M*. **B)** Base Uncertainty applies a CV of 12% to *h* and of 14% to *M*. **C)** High Uncertainty applies a CV of 20% to both parameters.

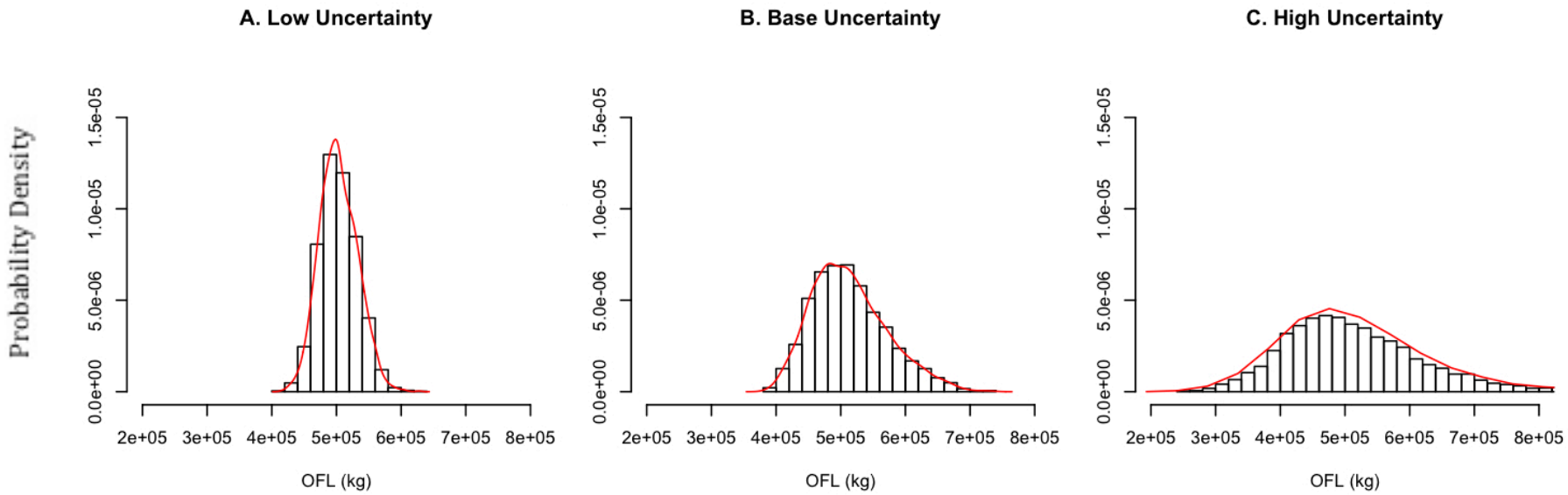

Figure 2.2. Constructed OFL distributions for sandbar shark. Red lines represent smoothed probability density functions. **A)** Low Uncertainty applies a CV of 3% to both steepness, *h*, and natural mortality, *M*. **B)** Base Uncertainty applies a CV of 7% to *h* and of 5% to *M*. **C)** High Uncertainty applies a CV of 10% to both parameters.

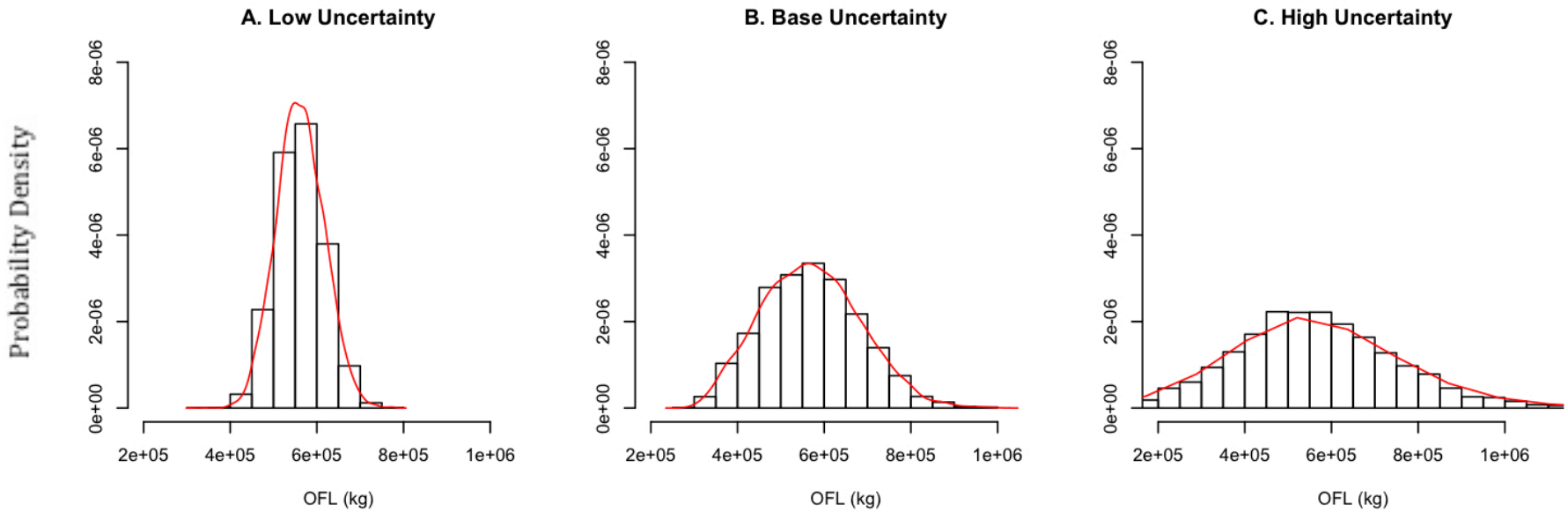

Figure 2.3. Constructed OFL distributions for gulf menhaden. Red lines represent smoothed probability density functions. **A)** Low Uncertainty applies a CV of 10% to steepness, *h*, and of 5% to natural mortality, *M*. **B)** Base Uncertainty applies a CV of 17% to *h* and of 8% to *M*. **C)** High Uncertainty applies a CV of 20% to *h* and a CV of 12% to *M*.

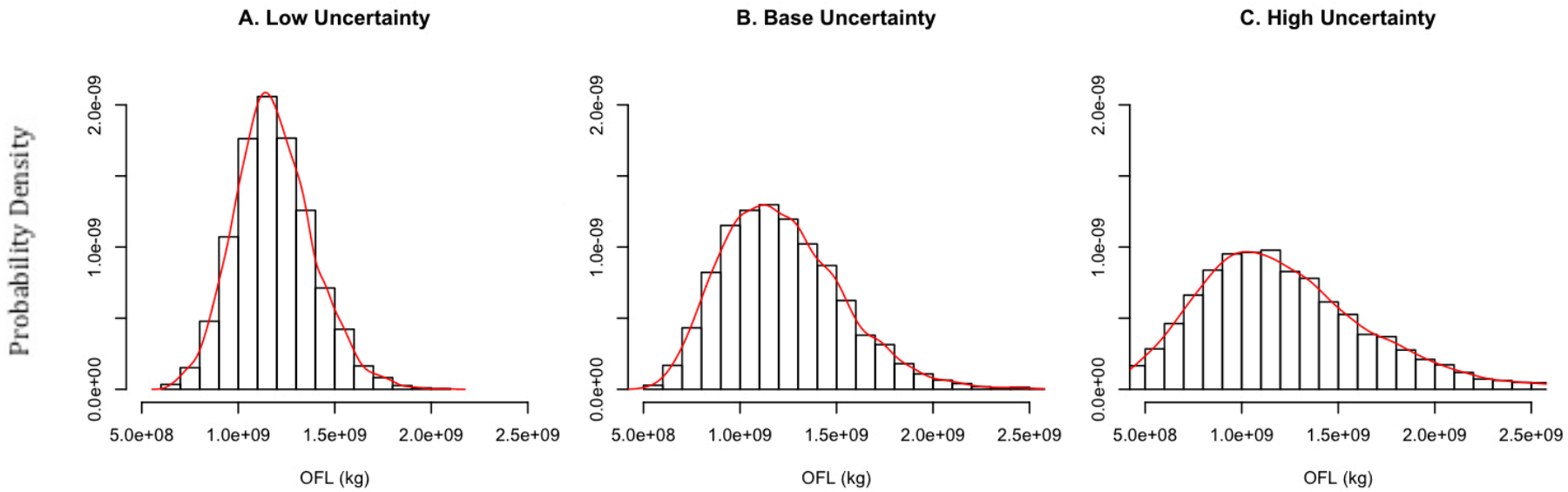

Figure 2.4. Percent of vermilion snapper populations in each scenario experiencing overfishing in the first year of the control rule's implementation. Percentages are plotted against *P** level and colored according to level of uncertainty. The expected percentages, equal to *P**, are traced in black as a reference.

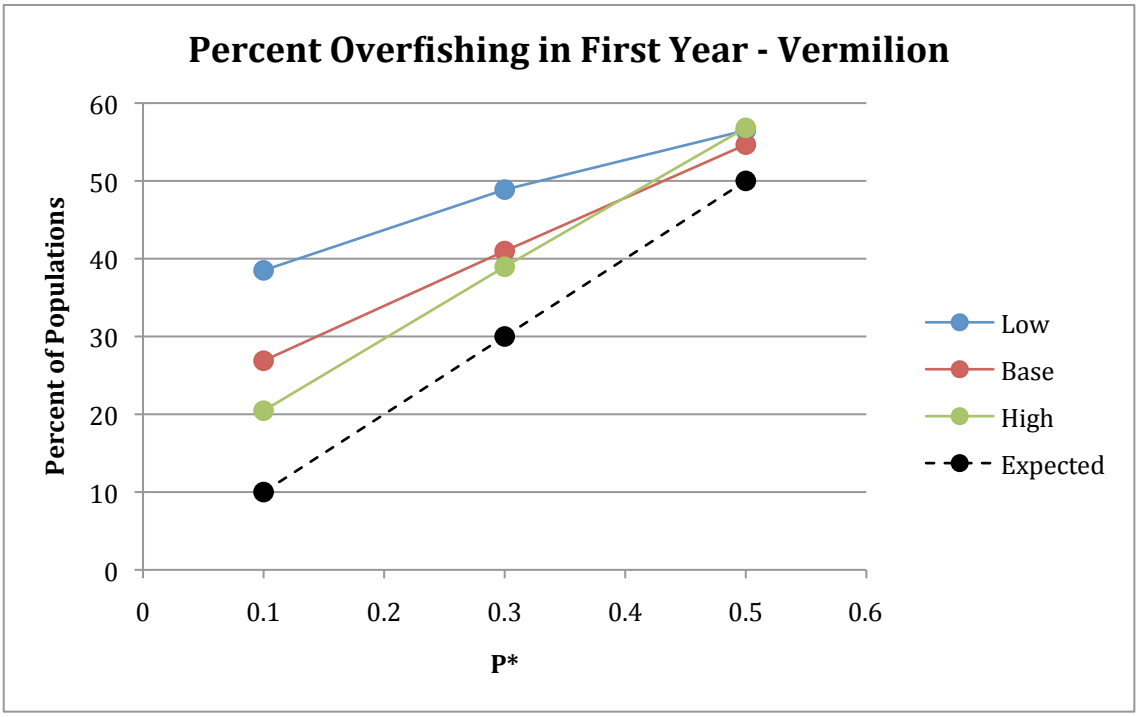

Figure 2.5. Percent of sandbar shark populations in each scenario experiencing overfishing in the first year of the control rule's implementation. Percentages are plotted against *P** level and colored according to level of uncertainty. The expected percentages, equal to *P**, are traced in black as a reference.

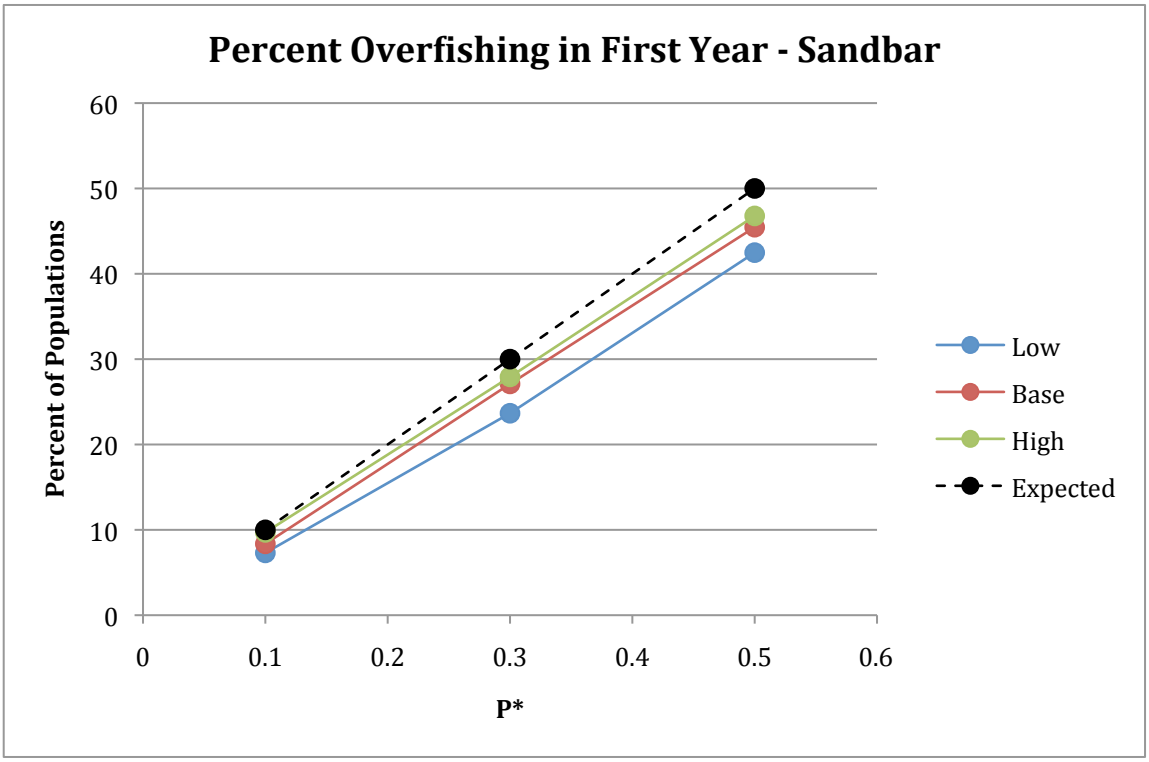

Figure 2.6. Percent of gulf menhaden populations in each scenario experiencing overfishing in the first year of the control rule's implementation. Percentages are plotted against *P** level and colored according to level of uncertainty. The expected percentages, equal to *P**, are traced in black as a reference.

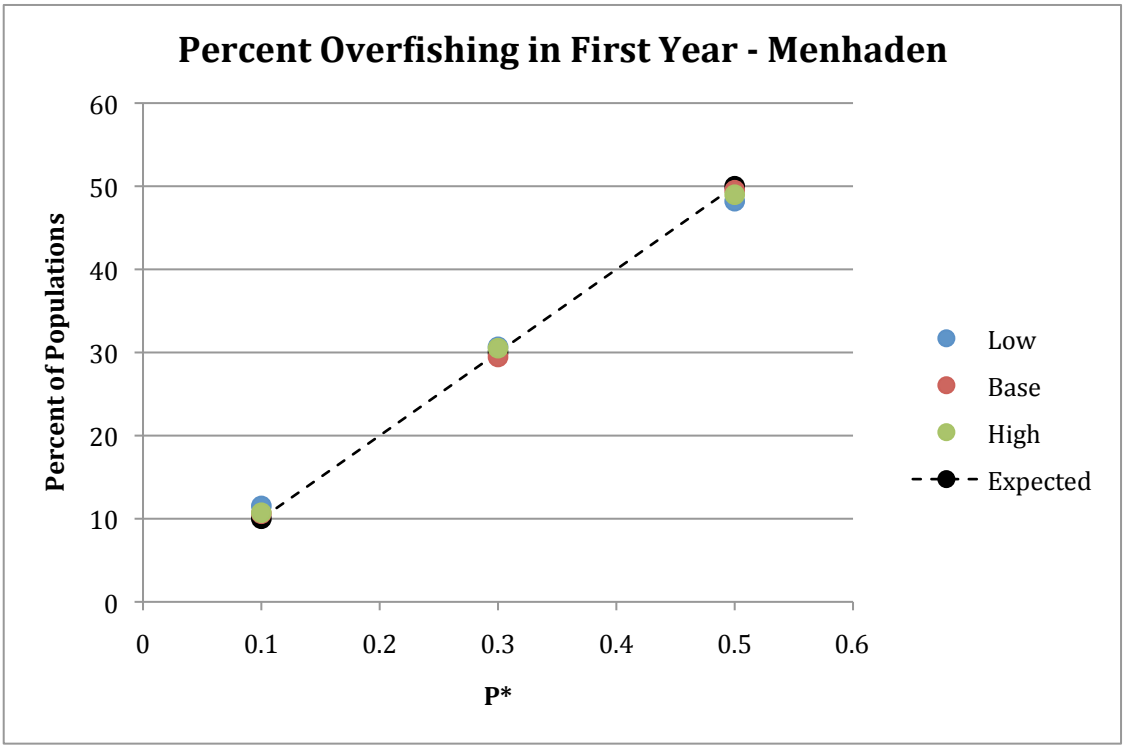

Figure 2.7. FLOW CHART 1: Ideal starting conditions lead to deterministic results (Eq. R1). (Pathways that lead to overfishing are highlighted in red.)

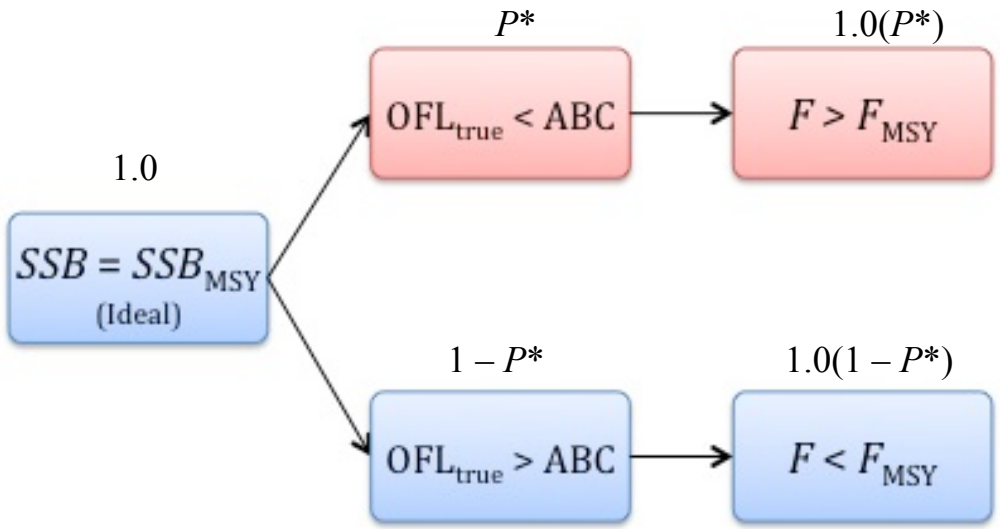

Figure 2.8. FLOW CHART 2A: Possible outcomes for non-overfished populations (Eq. R3). (Pathways that lead to overfishing are highlighted in red.)

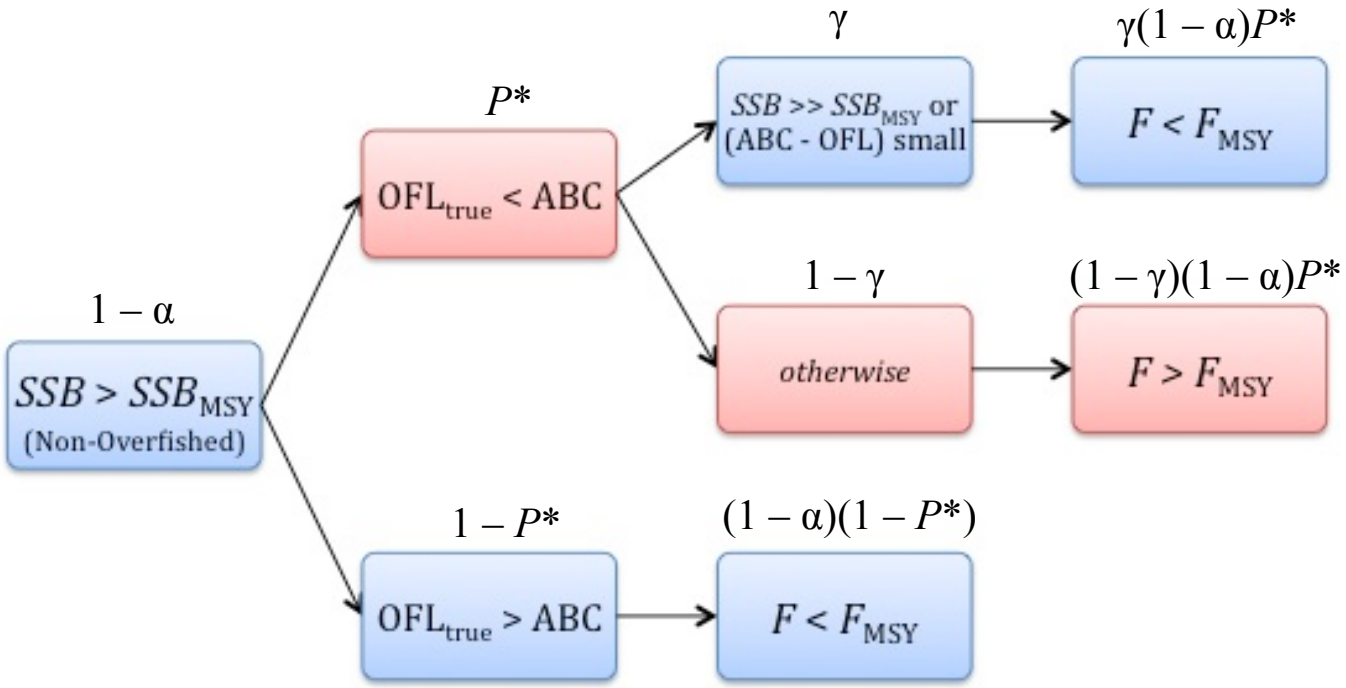

Figure 2.9. FLOW CHART 2B: Possible outcomes for populations already overfished (Eq. R4). (Pathways that lead to overfishing are highlighted in red.)

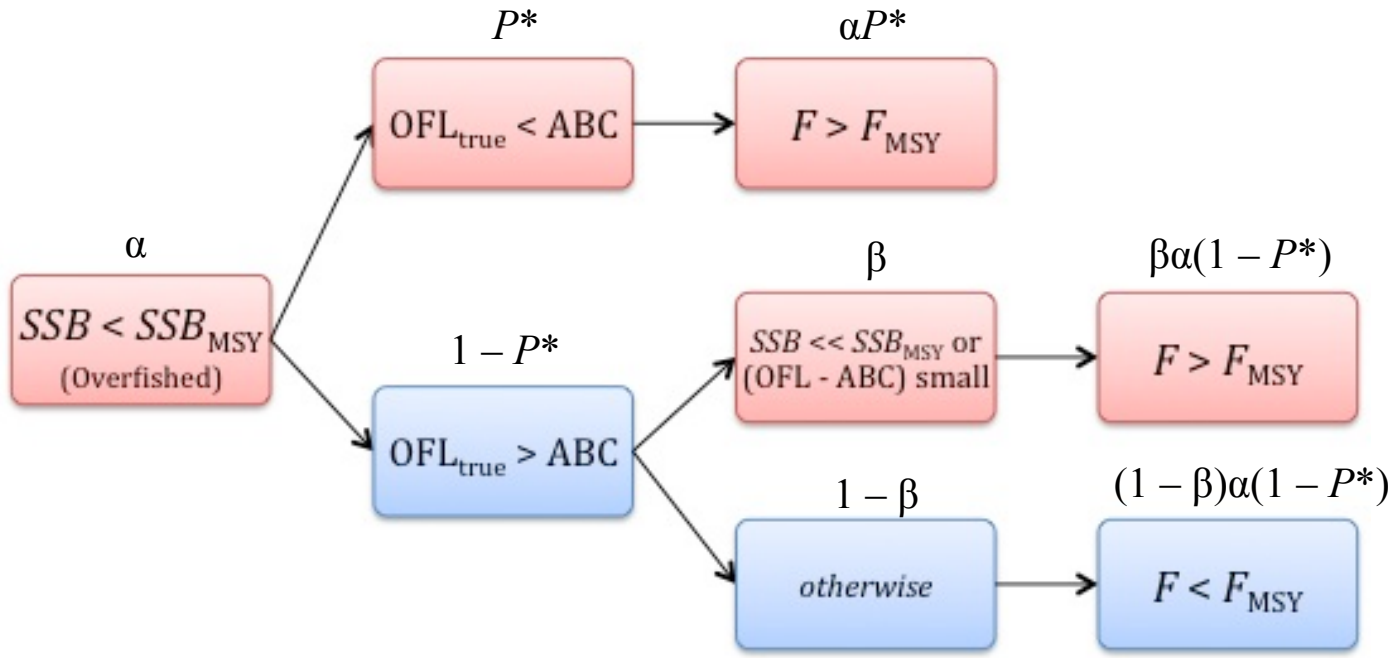

Figure 2.10. Current and cumulative percentages of vermilion snapper populations undergoing overfishing in each scenario. Scenarios are grouped by *P** level and colored according to level of uncertainty. Bold circles track yearly (or current) percentages, while light squares track cumulative percentages.

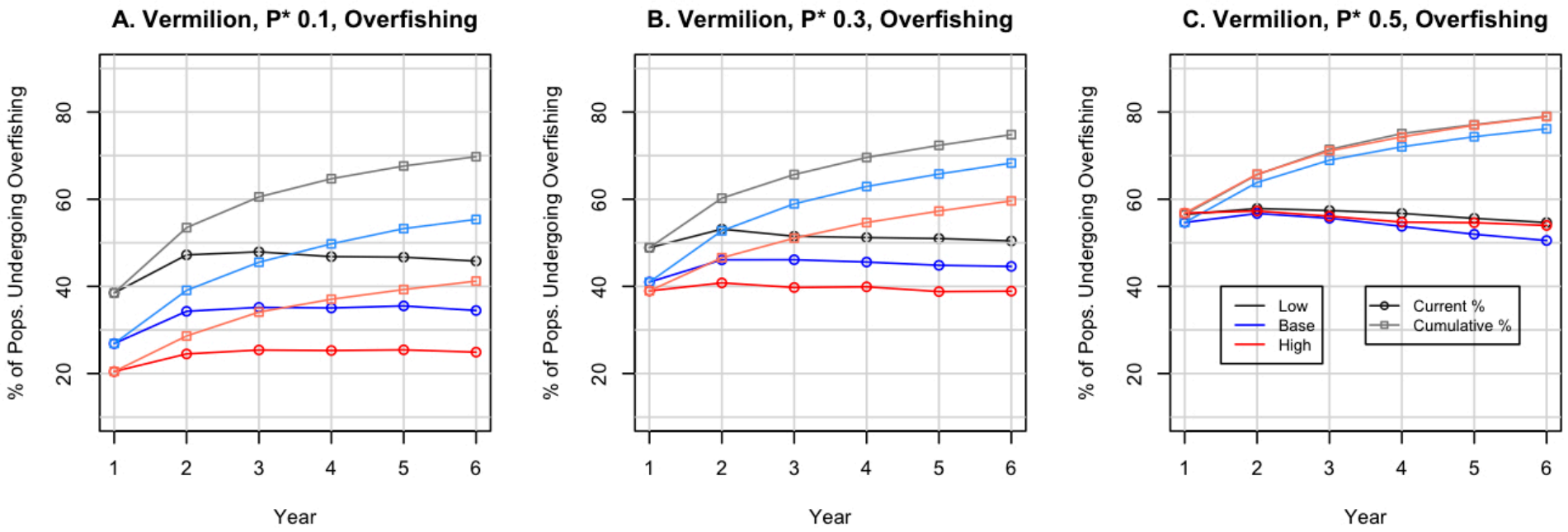

Figure 2.11. Current and cumulative percentages of sandbar shark populations undergoing overfishing in each scenario. Scenarios are grouped by *P** level and colored according to level of uncertainty. Bold circles track yearly (or current) percentages, while light squares track cumulative percentages.

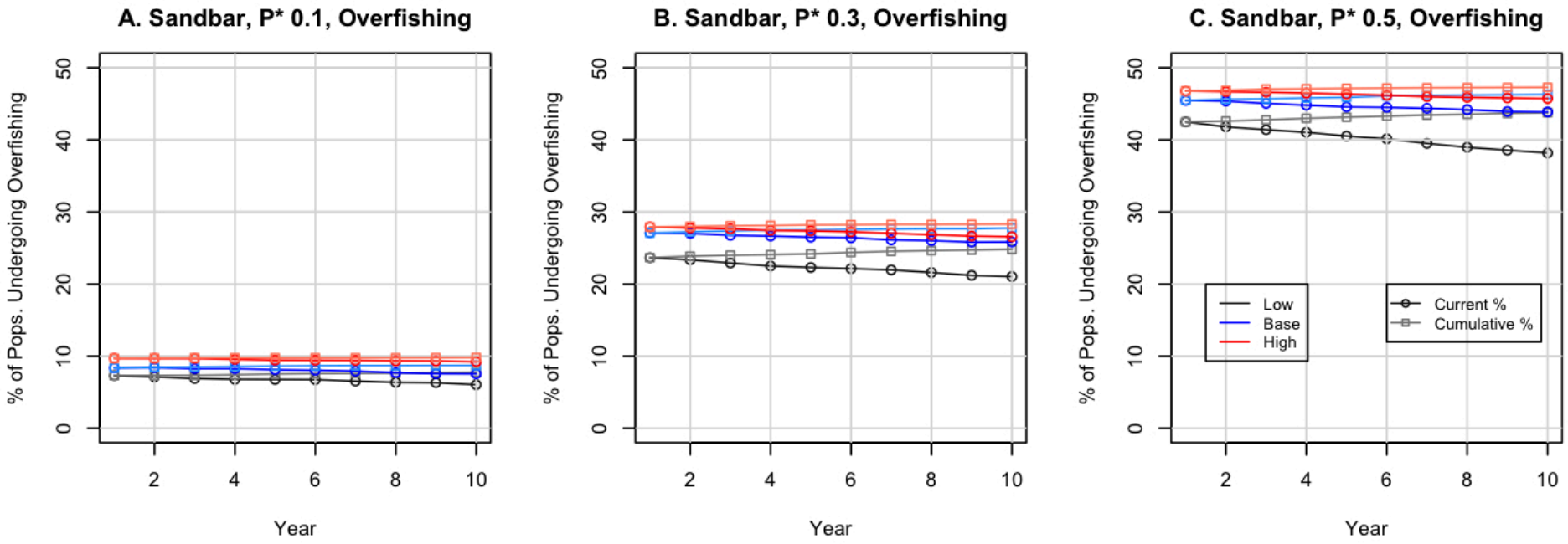

Figure 2.12. Current and cumulative percentages of gulf menhaden populations undergoing overfishing in each scenario. Scenarios are grouped by *P** level and colored according to level of uncertainty. Bold circles track yearly (or current) percentages, while light squares track cumulative percentages.

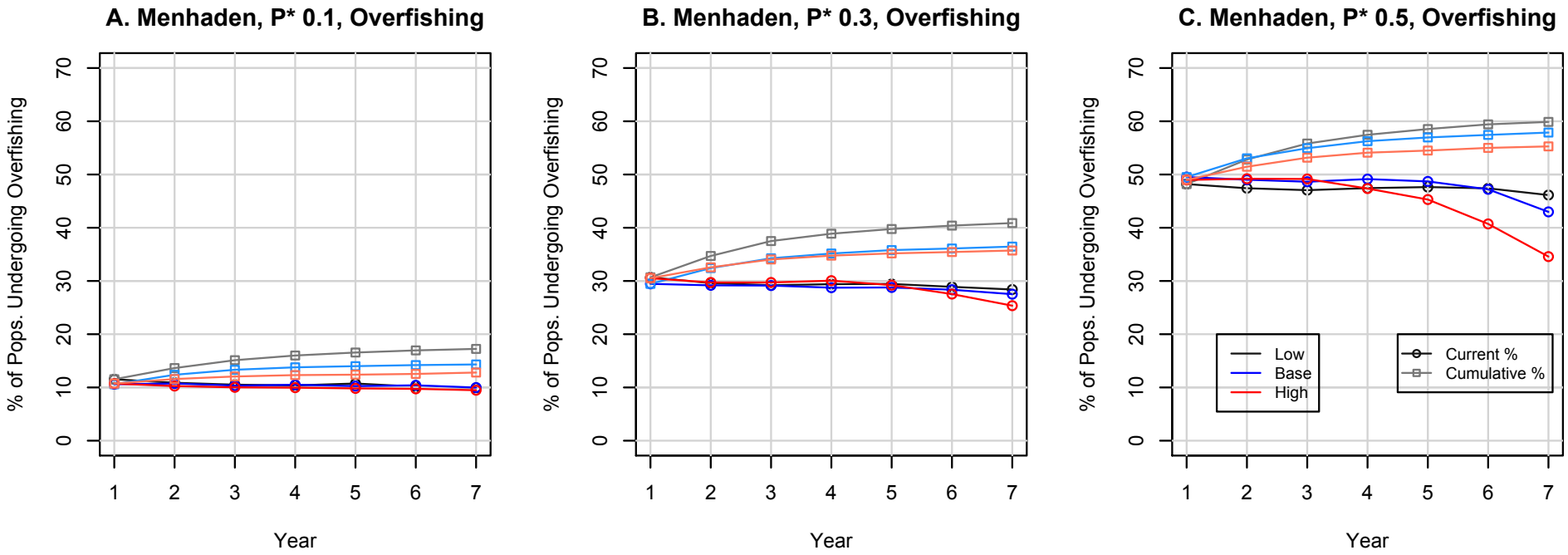

Figure 2.13. Increase in probabilistic risk of overfishing in the first four years following the control rules' implementation. Results are averaged across levels of uncertainty and grouped by P* level. Species are color-coded. The expected increases assuming independence of years are shown last, in gray.

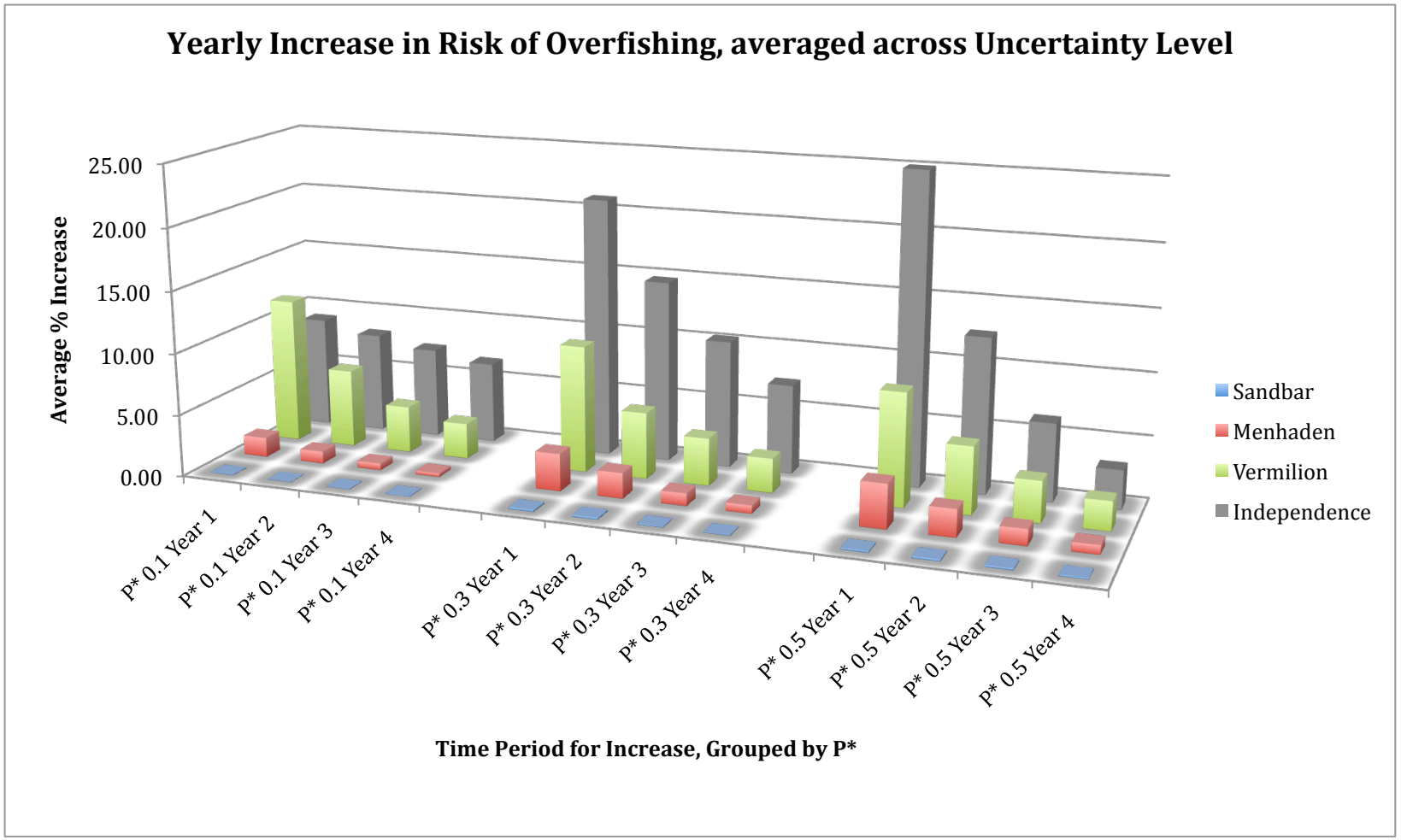

Figure 2.14. Current and cumulative percentages of vermilion snapper populations overfished in each scenario. Scenarios are grouped by *P** level and colored according to level of uncertainty. Bold circles track yearly (or current) percentages, while light squares track cumulative percentages. Note that year 1 describes the percentage overfished by the end of the initialization period, while year 2 marks the beginning of the experimental results.

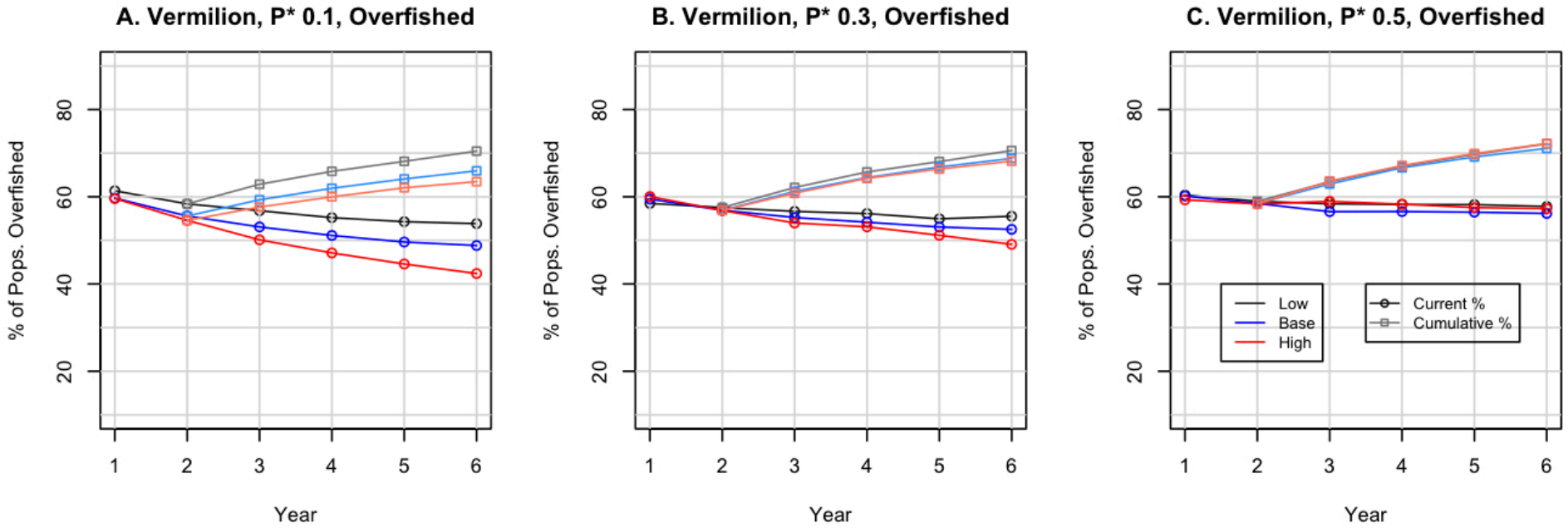

Figure 2.15. Current and cumulative percentages of sandbar shark populations overfished in each scenario. Scenarios are grouped by *P** level and colored according to level of uncertainty. Bold circles track yearly (or current) percentages, while light squares track cumulative percentages. Note that year 1 describes the percentage overfished by the end of the initialization period, while year 2 marks the beginning of the experimental results.

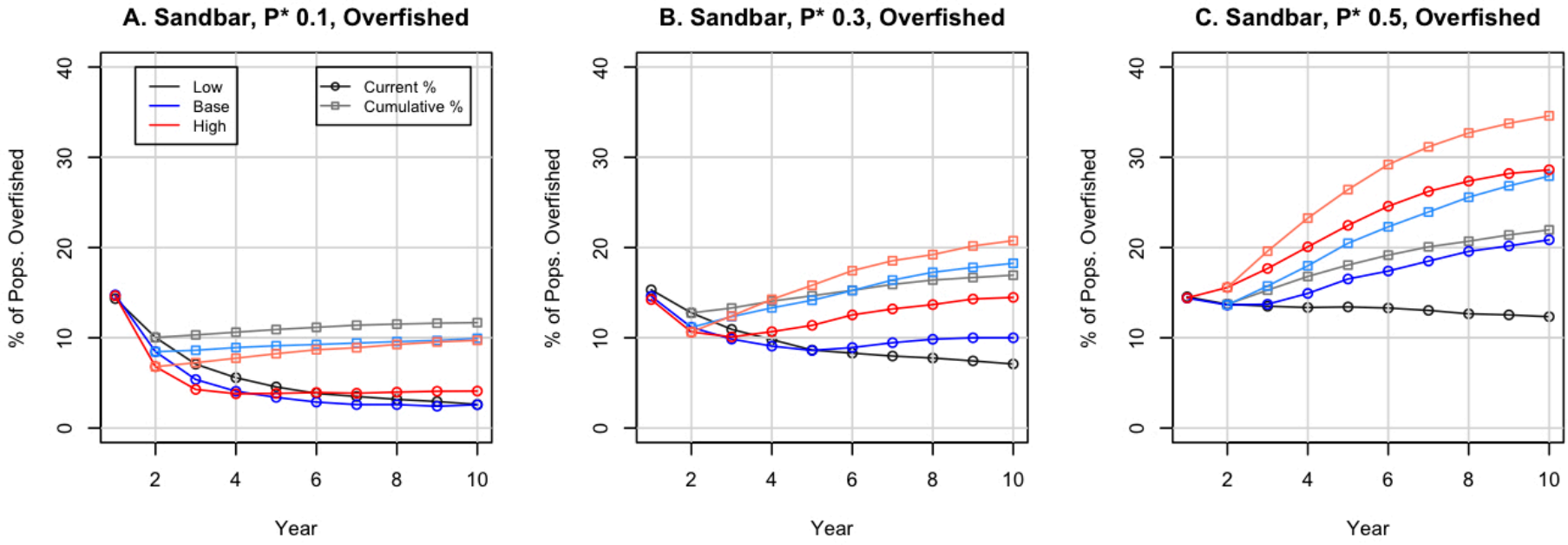

Figure 2.16. Current and cumulative percentages of gulf menhaden populations overfished in each scenario. Scenarios are grouped by *P** level and colored according to level of uncertainty. Bold circles track yearly (or current) percentages, while light squares track cumulative percentages. Note that year 1 describes the percentage overfished by the end of the initialization period, while year 2 marks the beginning of the experimental results.

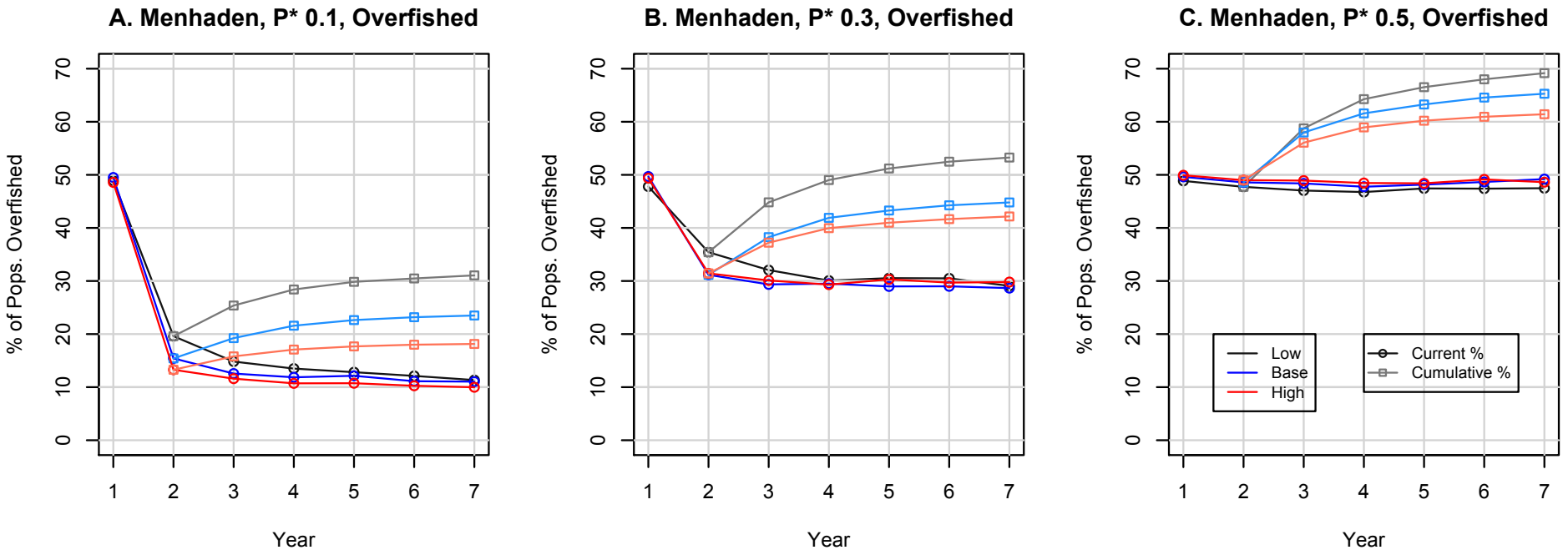

Figure 2.17. Percent of vermilion snapper populations crashing in the duration of the experiment. "Crashing" occurs when a population's *SSB* falls below ABC, such that catching ABC becomes impossible. Percentages are plotted against *P** level and colored according to level of uncertainty.

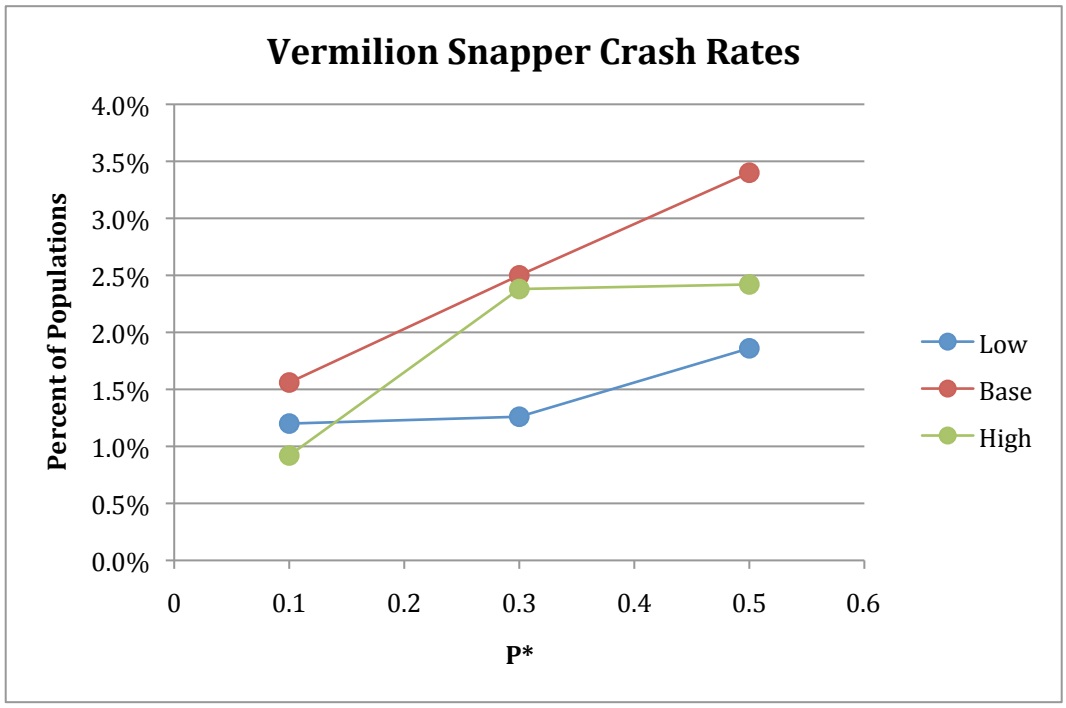

Figure 2.18. Percent of gulf menhaden populations crashing in the duration of the experiment. "Crashing" occurs when a population's total biomass B falls below ABC, such that catching ABC becomes impossible. Percentages are plotted against *P** level and colored according to level of uncertainty.

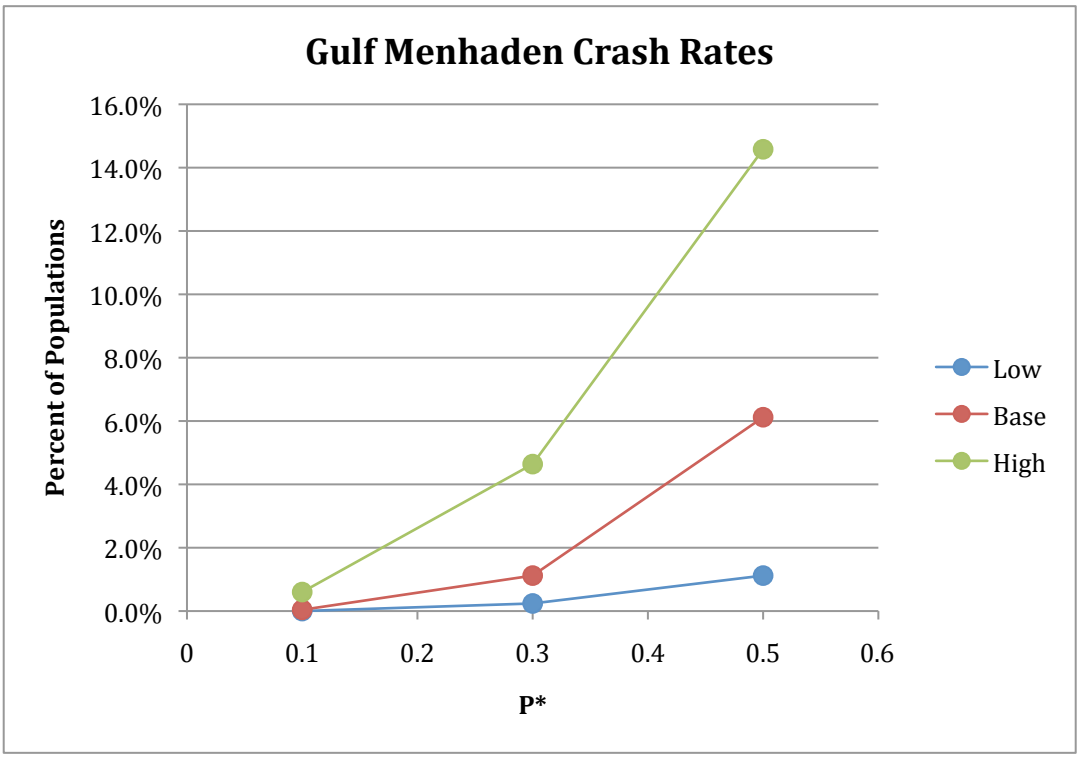

Figure 2.19. FLOW CHART 3: Ideal starting conditions lead to deterministic results (Eq. R8). (Pathways that lead to overfished status are highlighted in red.)

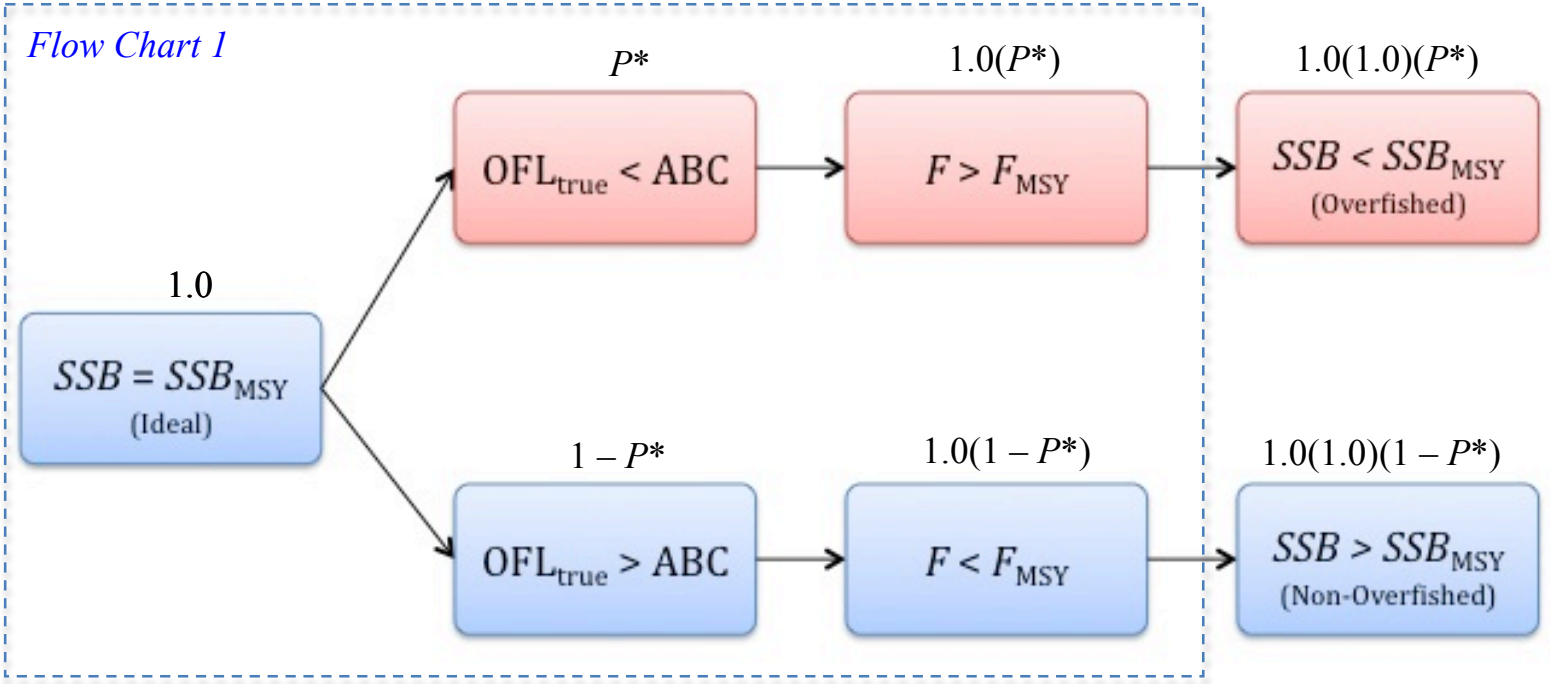

Figure 2.20. FLOW CHART 4A: There are three pathways by which non-overfished populations may become overfished (Eq. R11). (Pathways that lead to overfished status are highlighted in red.)

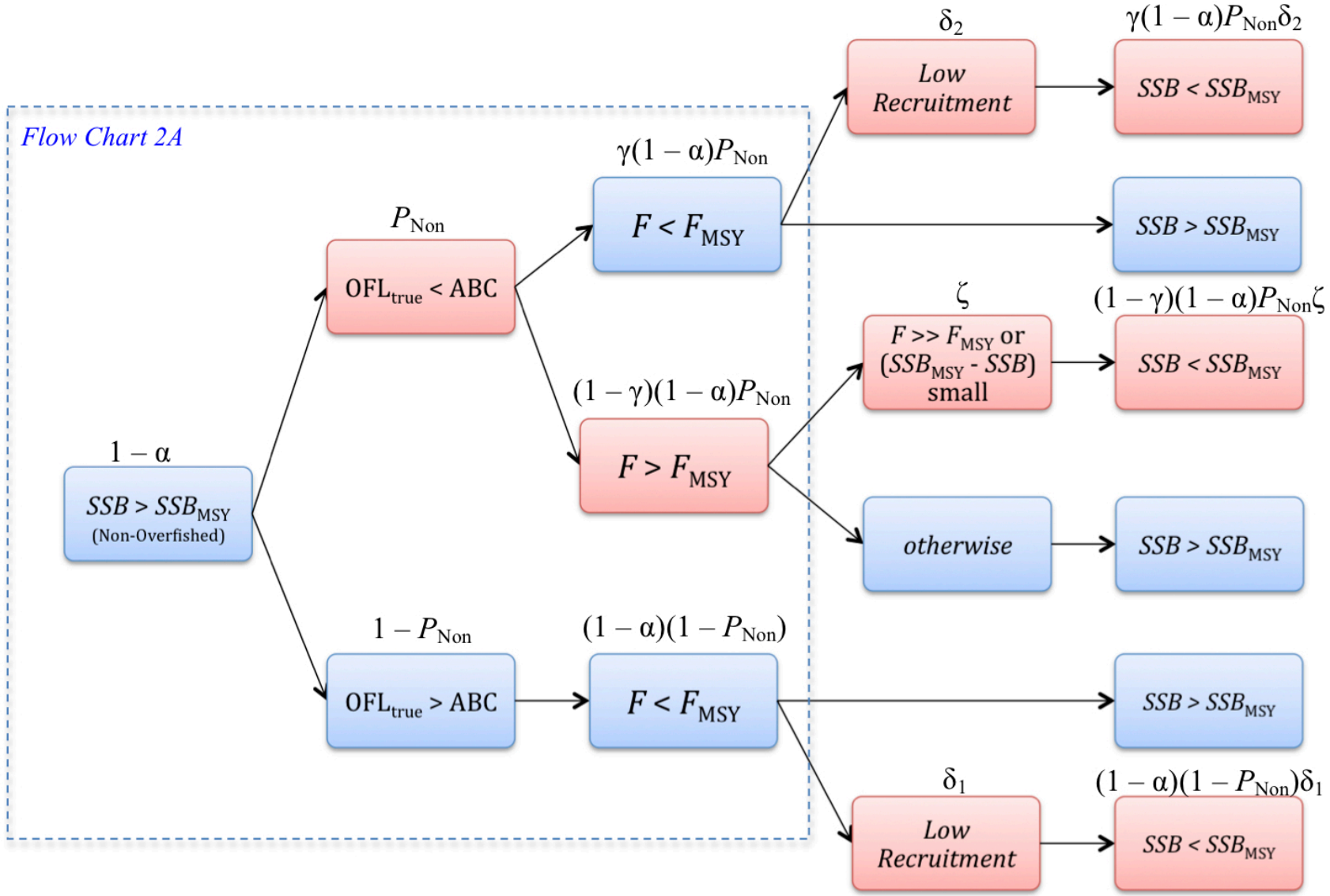

Figure 2.21. FLOW CHART 4B: There are three pathways by which overfished populations can recover (Eq. R14). (Pathways that lead to recovery are highlighted in blue.)